Supporting Information

Selective Vicinal Diiodination of Polycyclic Aromatic Hydrocarbons

Tanja Kaehler, Alexandra John, Tao Jin, Michael Bolte,
Hans-Wolfram Lerner, Matthias Wagner*

Table of contents:

1. General experimental procedures

If not stated otherwise, all reactions and manipulations were carried out under an atmosphere of dry nitrogen using Schlenk techniques. *n*-Hexane, toluene, and THF were distilled from Na/benzophenone. CH_3CN was used without drying. BBr_3 was stored over Hg. The starting materials 4,5-dichloro-1,2-bis(trimethylsilyl)benzene,[S1] $\mathbf{1}^{\mathbf{BMes}}$–$\mathbf{3}^{\mathbf{BMes}}$ and $\mathbf{5}^{\mathbf{BMes}}$–$\mathbf{7}^{\mathbf{BMes}}$,[S2] and 7,8-dibromo[5]helicene[S3] were prepared according to literature procedures. $Pd(PPh_3)_2Cl_2$ (*Heraeus*), $HN(i\text{-}Pr)_2$ (*abcr*; *i*-Pr = isopropyl), I_2 (*abcr*), and K_2CO_3 (*GRÜSSING*) were used as received.

NMR spectra were recorded at 298 K using the following spectrometers: Bruker DPX-250, Avance-300, Avance-400, Avance-500, or DRX-600. Chemical shift values are referenced to (residual) solvent signals ($^1H/^{13}C\{^1H\}$; $CDCl_3$: δ = 7.26/77.16 ppm, CD_3CN: δ = 1.94/1.32, 118.26 ppm) or external $BF_3{\cdot}Et_2O$ (^{11}B: 0.00 ppm). Abbreviations: s = singlet, d = doublet, dd = doublet of doublets, ddd = doublet of doublet of doublets, vt = virtual triplet, m = multiplet, br. = broad, n.o. = not observed. Resonances of carbon atoms attached to boron atoms were typically broadened and sometimes not observed due to the quadrupolar relaxation of the boron nuclei. Boron resonances of triarylborane compounds are typically very broad ($h_{1/2}$ > 1100 Hz) and were observed only in highly concentrated samples. Resonance assignments were aided by ^{H,H}COSY, ^{H,C}HSQC, and ^{H,C}HMBC spectra.

UV/Vis absorption spectra were recorded at room temperature using a *Varian* Cary 50 Scan or a *Varian* Cary 60 Scan UV/Vis spectrophotometer. Photoluminescence (PL) spectra were recorded at room temperature using a *Jasco* FP-8300 spectrofluorometer equipped with a calibrated *Jasco* ILF-835 100 mm diameter integrating sphere and analyzed using the *Jasco* FWQE-880 software. For PL quantum yield (Φ_{PL}) measurements, each sample was carefully degassed with argon using an injection needle and a septum-capped cuvette. Under these conditions the Φ_{PL} of the fluorescence standard 9,10-diphenylanthracene was determined as 97% (lit.: 97%).[S4,S5] For all Φ_{PL} measurements, at least three samples of different concentrations were used (range between 10^{-5} and 10^{-7} mol L^{-1}). Due to self-absorption, slightly lower Φ_{PL} values were observed at higher concentrations. This effect was corrected by applying a method reported by *Bardeen et al.*, which slightly improved the Φ_{PL} values (4% at most).[S6] Cyclic voltammetry (CV) measurements were performed in a glovebox at room temperature in a one-chamber, three-electrode cell using an *EG&G* Princeton Applied Research 263A potentiostat. A platinum disk electrode (2.00 mm diameter) was used as the working electrode with a platinum wire counter electrode and a silver wire reference electrode, which was coated with AgCl by immersion into HCl/HNO_3 (3:1). Prior to measurements, the solvent THF was dried with NaK, and degassed by three freeze-pump-thaw cycles. $[n\text{Bu}_4\text{N}][PF_6]$ (*Sigma Aldrich*; used as received) was employed as the supporting electrolyte (0.1 mol L^{-1}). All potential values were referenced against the FcH/FcH^+ redox couple (FcH = ferrocene; $E_{1/2}$ = 0 V). Scan rates were varied between 100 and 400 mV s^{-1}. High-resolution mass spectra were measured in positive mode using a *Thermo Fisher Scientific* MALDI LTQ Orbitrap XL spectrometer and 2,5-dihydroxybenzoic acid or α-cyano-4-hydroxycinnamic acid as the matrix.
Column chromatography was performed using silica gel 60 (*Macherey–Nagel*; 30 cm silica gel, diameter of column = 5 cm). Flash chromatography was performed on a *Biotage* ISOLERA ONE with an *Interchim* PF-25SIHC-JP-F0012 cartridge (flow rate = 10 mL/min).

2. Nomenclature

Assignment of NMR signals: The numbering schemes used for the *ortho*-diiodinated PAHs are given below. *Note*: The atom numbering deviates from the IUPAC nomenclature to ensure that the iodo substituents are always located at C2 and C3, which greatly facilitates a comparison of the individual spectra.

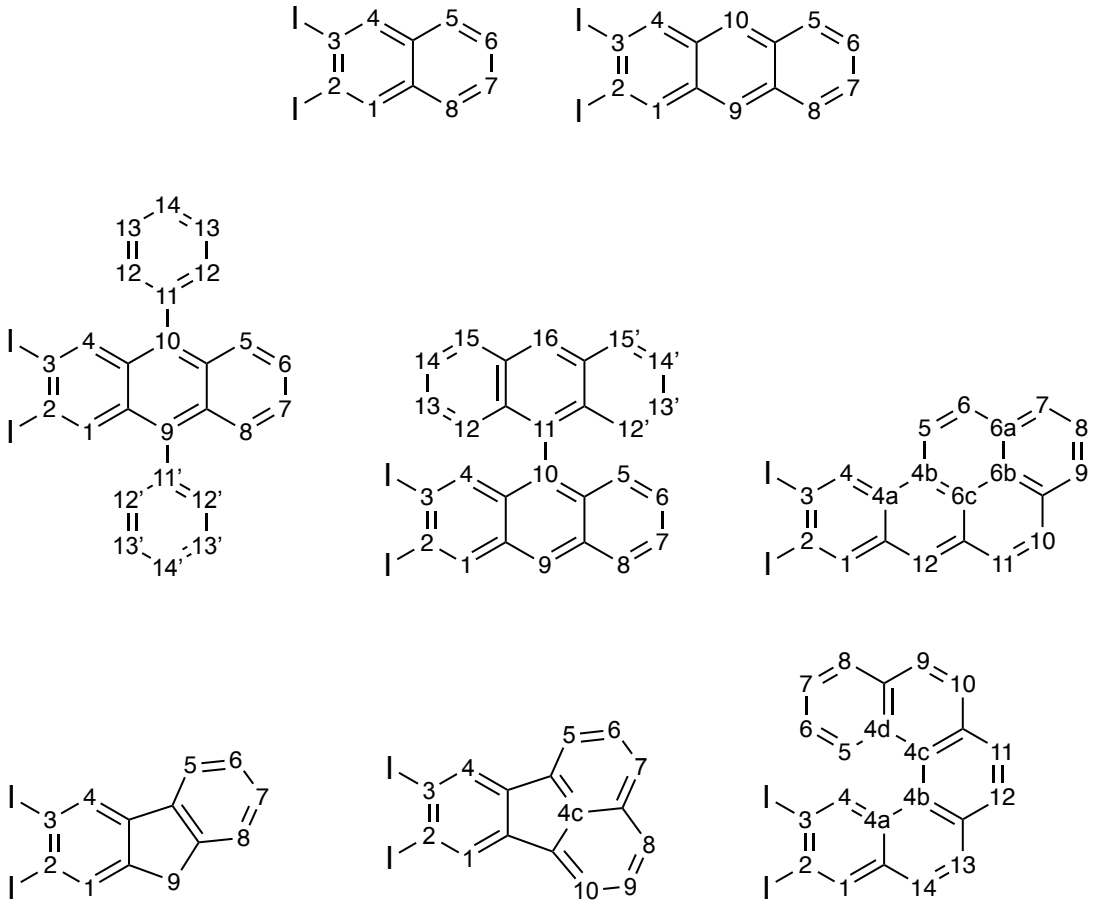

The boron-doped precursors are numbered in the same way as the corresponding *ortho*-diiodinated PAH; the chlorinated benzene ring is numbered as indicated below:

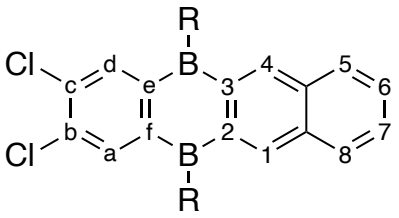

3. Syntheses, purification methods, and analytical data

3.1. General procedure for the preparation of *ortho*-diiodinated PAH derivatives

A microwave vial was charged with the respective *ortho*-diborylated PAH and K_2CO_3 and kept under a dynamic vacuum for 0.5 h to remove air. After the addition of excess I_2 and CH_3CN, the vial was closed with a septum cap under an N_2 atmosphere and heated to 80 °C for 17 h. The reaction mixture was cooled to room temperature. A saturated aqueous solution of $Na_2S_2O_5$ (20 mL) was added and the organic phase was separated by using a separation funnel. The aqueous phase was extracted with $CHCl_3$ (2 × 25 mL), the organic phases were combined, washed with H_2O (20 mL), dried over anhydrous $MgSO_4$, and filtered. All volatiles were removed from the filtrate under reduced pressure and the crude product was purified by column or flash chromatography.

2,3-Diiodonaphthalene $\mathbf{1^I}$

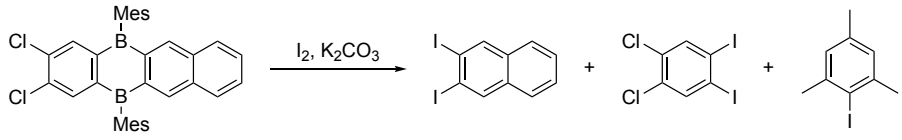

$\mathbf{1^{BMes}}$ $\mathbf{1^I}$

The synthesis was performed according to the general procedure described above using $\mathbf{1^{BMes}}$[S2] (0.076 g, 0.14 mmol), K_2CO_3 (0.24 g, 1.7 mmol), I_2 (0.44 g, 1.7 mmol), and CH_3CN (7 mL). The purification of the crude product by column chromatography (*c*-hexane, R_f = 0.61) afforded $\mathbf{1^I}$ as a colorless solid. Yield: 0.050 g (0.13 mmol, 93%). From this batch, we also isolated 1,2-dichloro-4,5-diiodobenzene[S7] (R_f = 0.83; yield: 0.051 g, 0.13 mmol, 93%) and 2-iodomesitylene[S8] (R_f = 0.77; 0.059 g (93% purity), which is equivalent to a yield of the pure compound of 0.055 g, 0.22 mmol, 79%). *Note*: To successfully separate the two spots belonging to the side products on a TLC plate, it is advisable to use *n*-hexane rather than *c*-hexane as the mobile phase. Single crystals of 1,2-dichloro-4,5-diiodobenzene were obtained by slow evaporation of a $CHCl_3$ solution.

^{1}H and ^{13}C{^{1}H} NMR spectra of $\mathbf{1^I}$ have already been published.[S9] Our own data and full signal assignments are given below.

^{1}H NMR (500.2 MHz, $CDCl_3$): δ = 8.40 (s, 2H; H-1,4), 7.68–7.65 (m, 2H; H-5,8), 7.51–7.47 ppm (m, 2H; H-6,7)
^{13}C{^{1}H} NMR (125.8 MHz, $CDCl_3$): δ = 138.5 (C-1,4), 133.9 (C-4a,8a), 127.3 (C-6,7), 126.8 (C-5,8), 104.2 ppm (C-2,3)

2,3-Diiodoanthacene 2^{I}

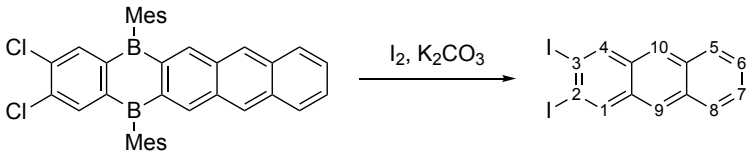

2^{BMes} **2^{I}**

The synthesis was performed according to the general procedure described above using **2^{BMes}**[S2] (0.059 g, 0.10 mmol), K_2CO_3 (0.16 g, 1.2 mmol), I_2 (0.29 g, 1.1 mmol), and CH_3CN (7 mL). The purification of the crude product by column chromatography (*c*-hexane, R_f = 0.50) afforded **2^{I}** as a colorless solid. Yield: 0.037 g (0.086 mmol, 86%).

^{1}H and $^{13}C\{^{1}H\}$ NMR spectra have already been published ([D_5]pyridine).[S10] Our own data and full signal assignments ($CDCl_3$) are given below.

^{1}H NMR (500.2 MHz, $CDCl_3$): δ = 8.62 (s, 2H; H-1,4), 8.26 (s, 2H; H-9,10), 8.00–7.96 (m, 2H; H-5,8), 7.52-7.48 ppm (m, 2H; H-6,7)
$^{13}C\{^{1}H\}$ NMR (125.8 MHz, $CDCl_3$): δ = 138.8 (C-1,4), 132.4 (C-8a, 10a), 131.8 (C-4a,9a), 128.5 (C-5,8), 126.5 (C-6,7), 125.5 (C-9,10), 103.5 ppm (C-2,3)

2,3-Diiodo-9,10-diphenylanthracene 3^{I}

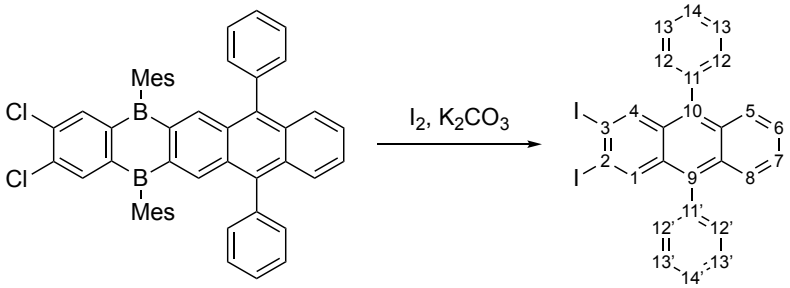

3^{BMes} **3^{I}**

The synthesis was performed according to the general procedure described above using **3^{BMes}**[S2] (0.069 g, 0.094 mmol), K_2CO_3 (0.16 g, 1.2 mmol), I_2 (0.29 g, 1.1 mmol), and CH_3CN (7 mL). The purification of the crude product by column chromatography (*c*-hexane, R_f = 0.47) afforded **3^{I}** as a yellow solid. Yield: 0.051 g (0.088 mmol, 94%). Single crystals were obtained by slow evaporation of a solution of **3^{I}** in $CHCl_3$.

^{1}H NMR (300.0 MHz, $CDCl_3$): δ = 8.25 (s, 2H; H-1,4), 7.68–7.58 (m, 8H; H-5,8,13,13',14,14'), 7.46–7.42 (m, 4H; H-12,12'), 7.38–7.32 ppm (m, 2H; H-6,7)
$^{13}C\{^{1}H\}$ NMR (75.4 MHz, $CDCl_3$): δ = 137.8 (C-11,11'), 137.8 (C-1,4), 136.6 (C-9,10), 131.3 (C-12,12'), 130.7 (C-8a,10a), 130.1 (C-4a,9a), 128.8 (C-13,13'), 128.1 (C-14,14'), 127.3 (C-5,8), 126.1 (C-6,7), 104.0 ppm (C-2,3)
HRMS: Calculated *m*/*z* for $[C_{26}H_{16}I_2]^+$: 581.93359, found: 581.93259
Melting point: 121 °C

2,3-Diiodo-10,11-bianthryl 4^{I}

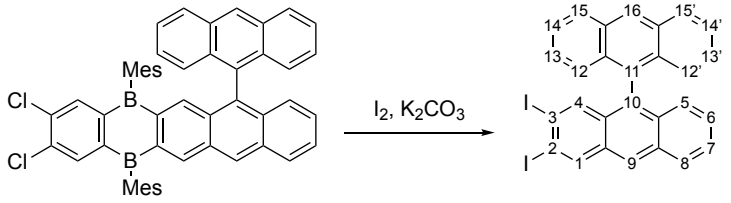

4^{BMes} **4^{I}**

The synthesis was performed according to the general procedure described above using **4^{BMes}** (0.030 g, 0.040 mmol), K_2CO_3 (0.069 g, 0.50 mmol), I_2 (0.12 g, 0.47 mmol), and CH_3CN (4 mL). The purification of the crude product by flash chromatography (silica gel, *c*-hexane, R_f = 0.29) afforded **4^{I}** as a colorless solid. Yield: 0.006 g (0.010 mmol, 25%). Single crystals were grown by layering a $CHCl_3$ solution of **4^{I}** with *n*-hexane at 8 °C.

^{1}H NMR (500.2 MHz, $CDCl_3$): δ = 8.76 (s, 1H; H-1), 8.71 (s, 1H; H-16), 8.50 (s, 1H; H-9), 8.17 (d, ^{3}J(H,H) = 8.5 Hz, 2H; H-15,15'), 8.11 (d, ^{3}J(H,H) = 8.5 Hz, 1H; H-8), 7.68 (s, 1H; H-4), 7.48–7.45 (m, 3H; H-7,14,14'), 7.19–7.13 (m, 3H; H-6,13,13'), 7.02–6.98 ppm (m, 3H; H-5,12,12')
^{13}C{^{1}H} NMR (125.8 MHz, $CDCl_3$): δ = 139.1 (C-1), 137.4 (C-4), 133.0 (C-10), 132.4 (C-8a/10a), 132.3 (C-8a/10a), 131.7 (C-4a/9a), 131.7 (C-4a/9a and 11a,11'a/15a,15'a), 131.6 (C-11a,11'a/15a,15'a), 131.6 (C-4a/9a/11a,11'a/15a,15'a), 131.4 (C-11), 128.8 (C-15,15'), 128.8 (C-8), 128.0 (C-16), 127.1 (C-5), 126.9 (C-6), 126.5 (C-12,12'), 126.5 (C-7/9), 126.4 (C-7/9), 126.4 (C-13,13'), 125.6 (C-14,14'), 104.7 (C-3), 104.1 ppm (C-2)
HRMS: Calculated *m*/*z* for $[C_{28}H_{16}I_2]^+$: 605.93359, found: 605.93267
Melting point: 294 °C

2,3-Diiodobenzo[a]pyrene 5^{I}

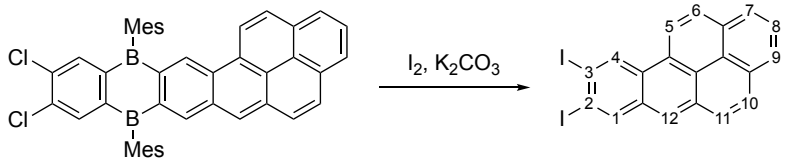

5^{BMes} **5^{I}**

The synthesis was performed according to the general procedure described above using **5^{BMes}**[S2] (0.016 g, 0.024 mmol), K_2CO_3 (0.040 g, 0.29 mmol), I_2 (0.074 g, 0.29 mmol), and CH_3CN (2 mL). The purification of the crude product by flash chromatography (silica gel, *c*-hexane, R_f = 0.34) afforded **5^{I}** as a colorless solid. Yield: 0.010 g (0.020 mmol, 83%). Single crystals of **5^{I}** were grown from a saturated $CHCl_3$ solution at 8 °C.

^{1}H NMR (500.2 MHz, $CDCl_3$): δ = 9.55 (s, 1H; H-4), 8.91 (d, ^{3}J(H,H) = 8.9 Hz, 1H; H-5), 8.82 (s, 1H; H-1), 8.35 (d, ^{3}J(H,H) = 8.9 Hz, 1H; H-6), 8.30 (s, 1H; H-12), 8.26 (d, ^{3}J(H,H) = 7.8 Hz, 1H; H-7), 8.12 (d, ^{3}J(H,H) = 7.4 Hz, 1H; H-9), 8.01 (vt, ^{3}J(H,H) = 7.8 Hz, ^{3}J(H,H) = 7.4 Hz, 1H; H-8), 7.96 ppm (n.r., 2H; H-10,11)
^{13}C{^{1}H} NMR (125.8 MHz, $CDCl_3$): δ = 139.1 (C-1), 134.3 (C-4), 131.8 (C-12a), 131.7 (C-q), 131.6 (C-q), 131.1 (C-q), 129.0 (C-10), 128.6 (C-4a), 128.5 (C-6), 128.0 (C-11), 126.8 (C-8), 126.3 (C-4b), 126.3 (C-7), 125.7 (C-9), 125.4 (C-6b), 124.2 (C-6c), 123.1 (C-12), 121.7 (C-5), 104.5 (C-2/3), 104.3 ppm (C-2/3). The three quaternary C atoms (C-q) correspond to C-6a, 9a, 11a. In these cases, extensively overlapping cross peaks in the 2D NMR spectra precluded unequivocal assignments.
HRMS: Calculated *m*/*z* for $[C_{20}H_{10}I_2]^+$: 503.88664, found: 503.88536
Melting point: 247 °C

2,3-Diiodofluorene 6^{I}

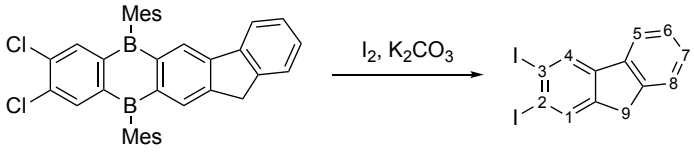

6^{BMes} **6^{I}**

The synthesis was performed according to the general procedure described above using **6^{BMes}**[S2] (0.040 g, 0.070 mmol), K_2CO_3 (0.12 mg, 0.87 mmol), I_2 (0.21 g, 0.83 mmol), and CH_3CN (7 mL). The purification of the crude product by flash chromatography (silica gel, *c*-hexane, R_f = 0.69) afforded **6^{I}** as a colorless solid. Yield: 0.010 g (0.024 mmol, 34%). Single crystals of **6^{I}** were grown from a saturated *n*-hexane solution at 8 °C.

^{1}H NMR (500.2 MHz, $CDCl_3$): δ = 8.29 (s, 1H; H-4), 8.07 (t, ^{4}J(H,H) = 0.9 Hz, 1H; H-1), 7.73–7.71 (dd, ^{3}J(H,H) = 6.7 Hz, ^{4}J(H,H) = 1.2 Hz, 1H; H-5), 7.54–7.52 (m, 1H; H-8), 7.40–7.34 (m, 2H; H-6,7) 3.79 ppm (n. r., 2H; CH_2-9)
^{13}C{^{1}H} NMR (125.8 MHz, $CDCl_3$): δ = 144.9 (C-9a), 143.9 (C-4a), 143.0 (C-8a), 139.6 (C-4b), 135.9 (C-1), 130.7 (C-4), 128.1 (C-7), 127.3 (C-6), 125.3 (C-8), 120.4 (C-5), 105.6 (C-3), 105.0 (C-2), 36.4 ppm (C-9)
HRMS: Calculated *m*/*z* for $[C_{13}H_8I_2]^+$: 417.87099, found: 417.87050
Melting point: 124 °C

2,3-Diiodofluoranthene 7^{I}

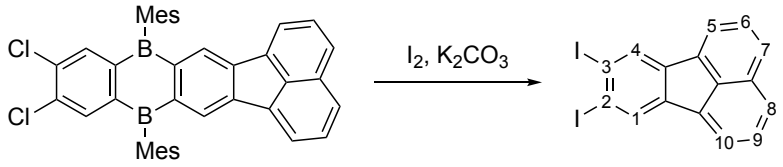

7^{BMes} **7^{I}**

The synthesis was performed according to the general procedure described above using **7^{BMes}**[S2] (0.060 g, 0.099 mmol), K_2CO_3 (0.16 mg, 1.2 mmol), I_2 (0.29 g, 1.1 mmol), and CH_3CN (7 mL). The purification of the crude product by column chromatography (*c*-hexane, R_f = 0.47) afforded **7^{I}** as a yellow solid. Yield: 0.038 g (0.084 mmol, 85%). The product **7^{I}** can be recrystallized from *n*-hexane to obtain single crystals.

^{1}H NMR (500.2 MHz, $CDCl_3$): δ = 8.39 (s, 2H; H-1,4), 7.92 (d, ^{3}J(H,H) = 8.2 Hz, 2H; H-7,8), 7.90 (d, ^{3}J(H,H) = 7.0 Hz, 2H; H-5,10) 7.64 ppm (dd, ^{3}J(H,H) = 8.2 Hz, ^{3}J(H,H) = 7.0 Hz, 2H; H-6,9)
^{13}C{^{1}H} NMR (125.8 MHz, $CDCl_3$): δ = 140.7 (C-4a,10b), 135.0 (C-4b,10a), 132.3 (C-4c), 132.1 (C-1,4), 130.1 (C-7a), 128.3 (C-6,9), 127.8 (C-7,8), 121.0 (C-5,10), 105.9 ppm (C-2,3)
HRMS: Calculated *m*/*z* for $[C_{16}H_8I_2]^+$: 453.87099, found: 453.87109
Melting point: 215 °C

2,3-Diiodo[5]helicene 8^{I}

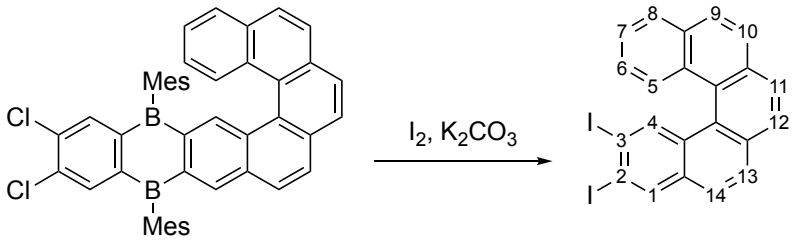

8^{BMes} 8^{I}

The synthesis was performed according to the general procedure described above using 8^{BMes} (0.032 g, 0.047 mmol), K_2CO_3 (0.12 g, 0.87 mmol), I_2 (0.22 g, 0.87 mmol), and CH_3CN (7 mL). The purification of the crude product by column chromatography (*c*-hexane, R_f = 0.34) afforded 8^{I} as a yellow solid. Yield: 0.022 g (0.041 mmol, 87%). Single crystals were obtained by slow evaporation of a solution of 8^{I} in $CHCl_3$.

^{1}H NMR (500.2 MHz, $CDCl_3$): δ = 9.06 (s, 1H; H-4), 8.53 (d, ^3J(H,H) = 8.5 Hz, 1H; H-5), 8.45 (s, 1H; H-1), 7.97 (d, ^3J(H,H) = 8.5 Hz, 1H; H-8), 7.94 (d, ^3J(H,H) = 8.5 Hz, 1H; H-9/10/11/12), 7.90 (d, ^3J(H,H) = 8.5 Hz, 1H; H-9/10/11/12), 7.87 (d, ^3J(H,H) = 8.5 Hz, 1H; H-13), 7.86 (d, ^3J(H,H) = 8.5 Hz, 1H; H-9/10/11/12), 7.83 (d, ^3J(H,H) = 8.5 Hz, 1H; H-9/10/11/12), 7.72 (d, ^3J(H,H) = 8.5 Hz, 1H; H-14), 7.58 (ddd, ^3J(H,H) = 8.5 Hz, ^3J(H,H) = 8.5 Hz, ^4J(H,H) = 1.2 Hz, 1H; H-7), 7.40 ppm (ddd, ^3J(H,H) = 8.5 Hz, ^3J(H,H) = 8.5 Hz, ^4J(H,H) = 1.2 Hz, 1H; H-6)
^{13}C{^{1}H} NMR (125.8 MHz, $CDCl_3$): δ = 139.5 (C-4), 138.0 (C-1), 133.3 (C-4b/14a), 133.0 (C-q), 132.8 (C-q), 132.7 (C-q), 131.6 (C-4a), 130.3 (C-q), 128.4 (C-5), 128.3 (CH), 128.2 (CH), 128.2 (2×CH), 127.2 (C-7), 127.0 (CH), 126.7 (C-q), 126.4 (CH), 125.9 (C-14), 125.7 (C-4b/14a), 125.0 (C-6), 104.2 (C-2), 102.6 ppm (C-3). The five quaternary C atoms (C-q) correspond to C-4c,4d,8a,10a,12a; the six H-bearing C atoms (CH) correspond to C-8,9,10,11,12,13. In all these cases, extensively overlapping cross peaks in the 2D NMR spectra precluded unequivocal assignments.
HRMS: Calculated *m/z* for $[C_{22}H_{12}I_2]^+$: 529.90299, found: 529.90138
Melting point: 194 °C

3.2. Synthesis of 7^{CCPh}

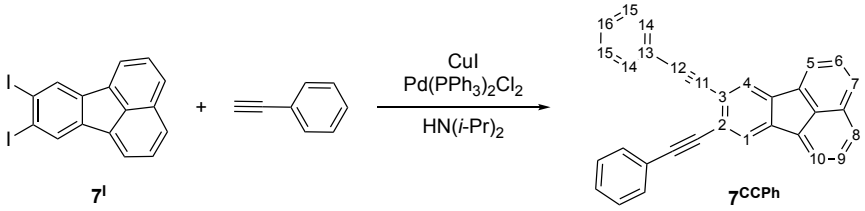

7^{I} 7^{CCPh}

A microwave vial was charged with 7^{I} (0.028 g, 0.062 mmol), CuI (0.002 g 0.01 mmol), $Pd(PPh_3)_2Cl_2$ (0.003 g, 0.004 mmol), and phenylacetylene (0.022 g, 0.22 mmol). The starting materials were dissolved in THF (2 mL) and $HN(i\text{-}Pr)_2$ (0.5 mL). The vial was closed with a septum cap under an N_2 atmosphere and heated to 90 °C for 5 h. The reaction mixture was allowed to cool to room temperature and filtered over a short plug of silica gel with THF as the eluent. All volatiles were removed from the filtrate under reduced pressure. The purification of the crude product by column chromatography (*c*-hexane:EtOAc = 20:1, R_f = 0.40) afforded 7^{CCPh} as a yellow solid. Yield: 0.023 g (0.057 mmol, 92%). Single crystals of 7^{CCPh} were grown from a saturated *c*-hexane solution at 8 °C.

^{1}H NMR (500.2 MHz, $CDCl_3$): δ = 8.12 (s, 2H; H-1,4), 7.98 (d, ^3J(H,H) = 7.0 Hz, 2H; H-5,10), 7.90 (d, ^3J(H,H) = 8.1 Hz, 2H; H-7,8) 7.69 (dd, ^3J(H,H) = 7.0 Hz, ^3J(H,H) = 8.1 Hz, 2H; H-6,9), 7.65–7.63 (m, 4H, H-14), 7.40–7.36 ppm (m, 6H, H-15,16)
^{13}C{^{1}H} NMR (125.8 MHz, $CDCl_3$): δ = 139.1 (C-4a,10b), 136.0 (C-4b,10a), 133.3 (C-4c), 131.8 (C-14), 130.2 (C-7a), 128.6 (C-15), 128.6 (C-16), 128.3 (C-6,9), 127.5 (C-7,8), 125.0 (C-1,4), 124.9 (C-2,3), 123.6 (C-13), 121.0 (C-5,10), 94.1 (C-12,12'), 89.4 ppm (C-11,11')
HRMS: Calculated *m/z* for $[C_{32}H_{18}]^+$: 402.14030, found: 402.14007
Melting point: 154 °C

4. Plots of ^{1}H and $^{13}C\{^{1}H\}$ spectra

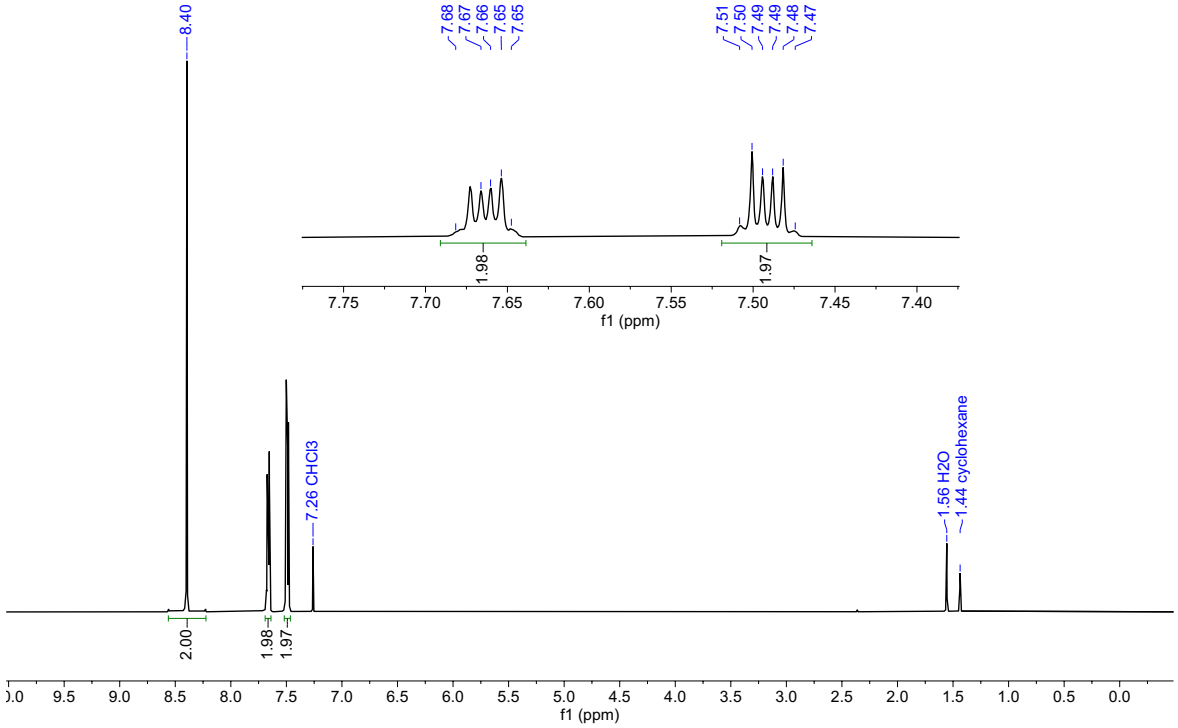

Figure S1: ^{1}H NMR spectrum of **1[I]** ($CDCl_3$, 500.2 MHz).

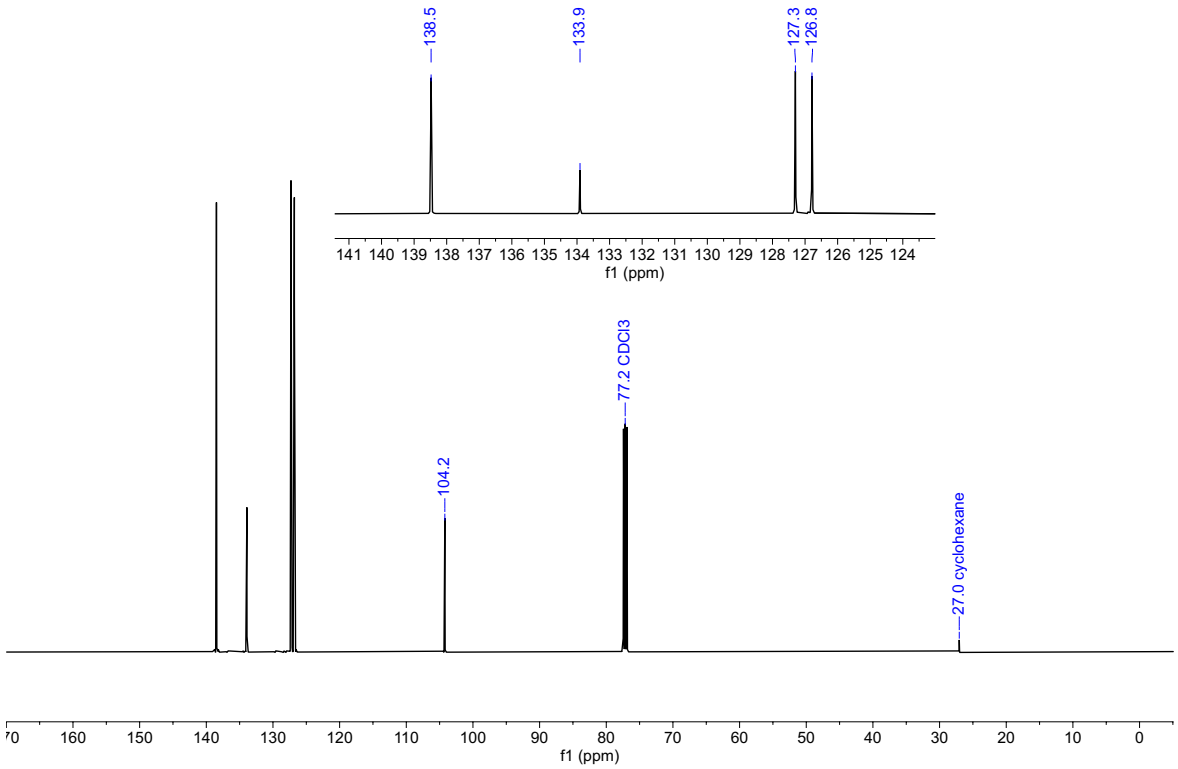

Figure S2: $^{13}C\{^{1}H\}$ NMR spectrum of **1[I]** ($CDCl_3$, 125.8 MHz).

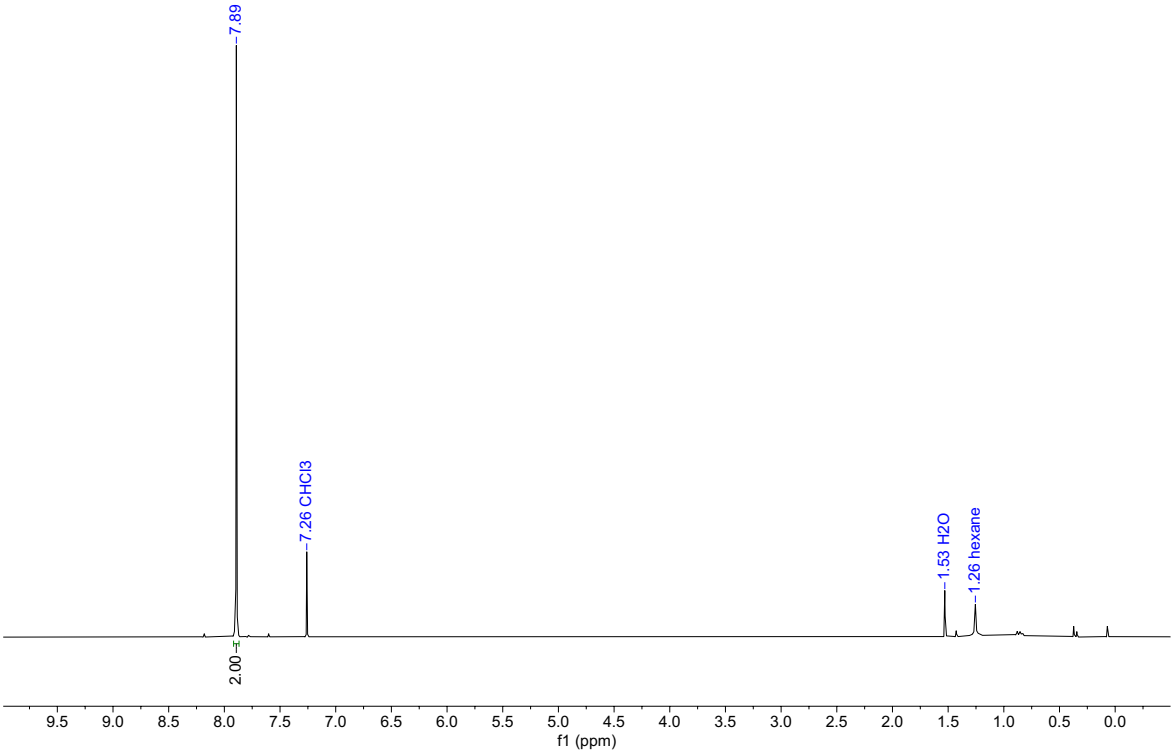

Figure S3: ^{1}H NMR spectrum of 1,2-dichloro-4,5-diiodobenzene ($CDCl_3$, 300.0 MHz).[S7]

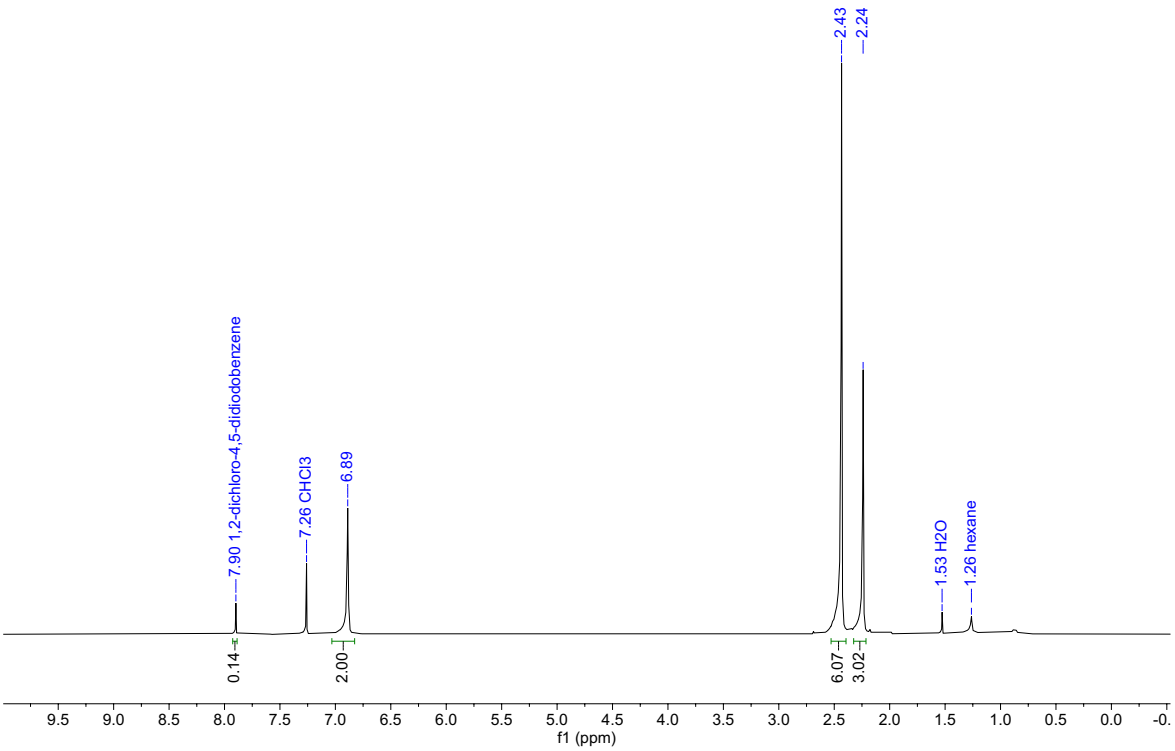

Figure S4: ^{1}H NMR spectrum of 2-iodomesitylene ($CDCl_3$, 250.1 MHz).[S8]

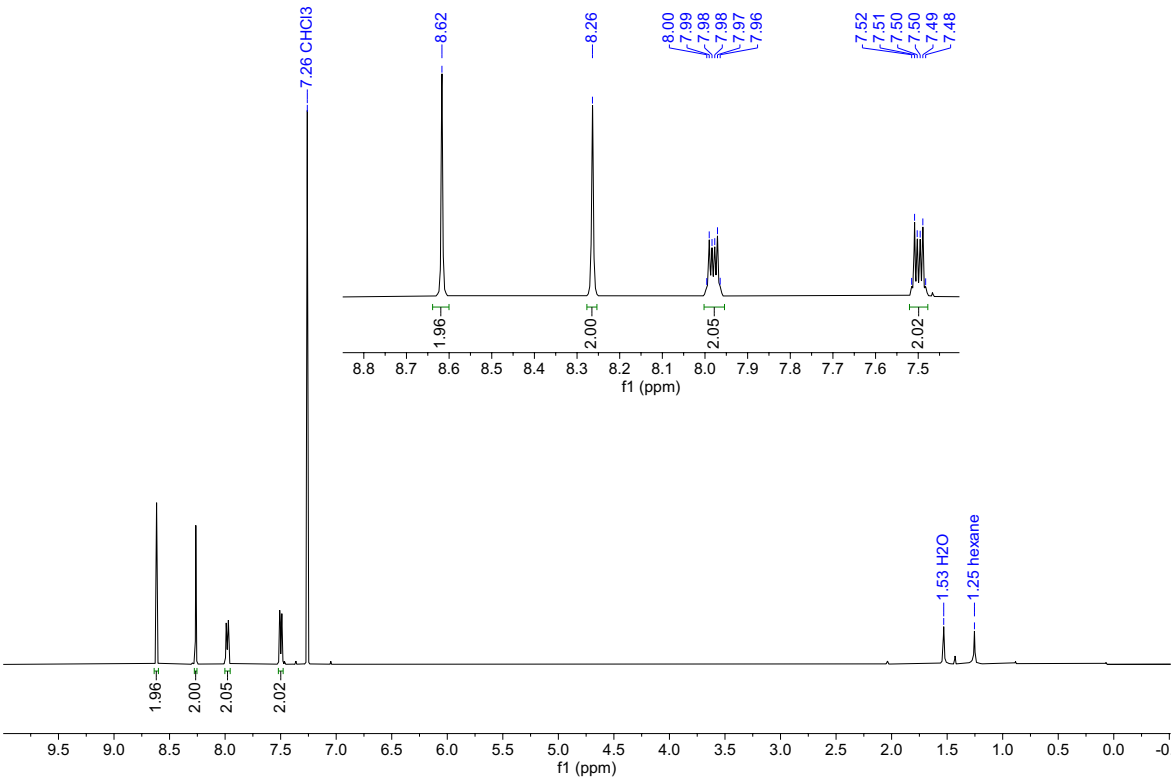

Figure S5: ^{1}H NMR spectrum of **2^{I}** ($CDCl_3$, 500.2 MHz).

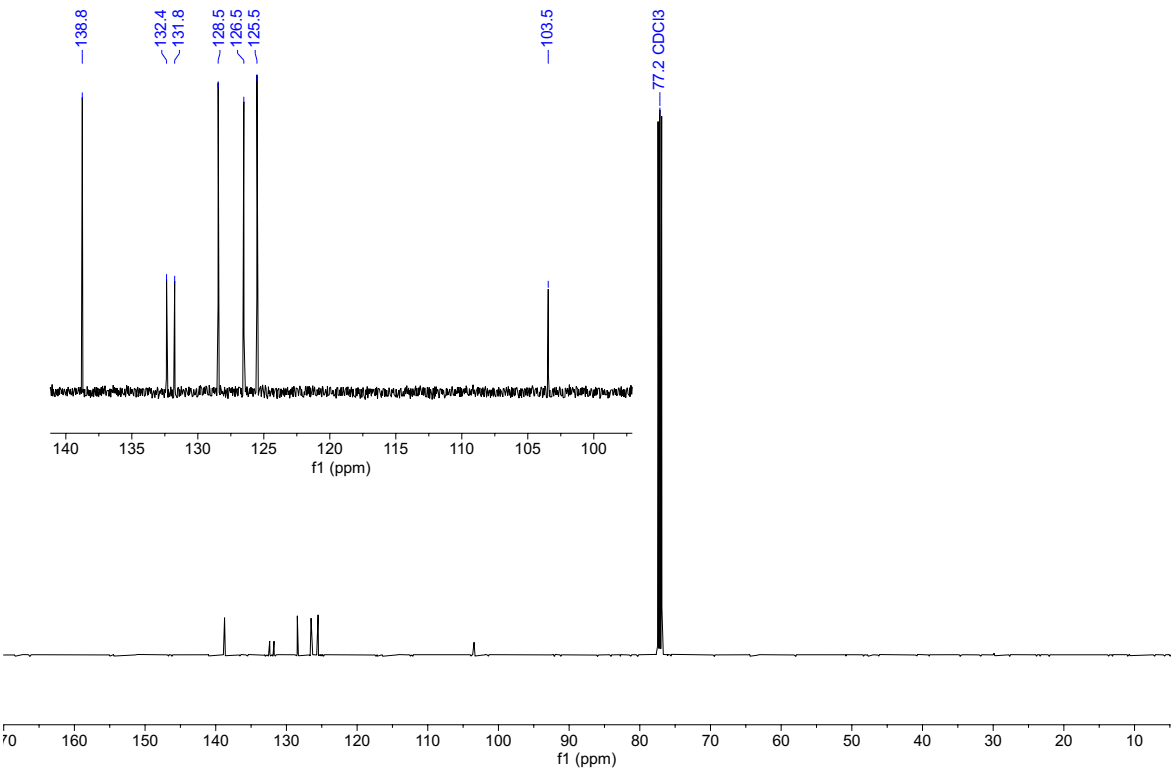

Figure S6: $^{13}C\{^{1}H\}$ NMR spectrum of **2^{I}** ($CDCl_3$, 125.8 MHz).

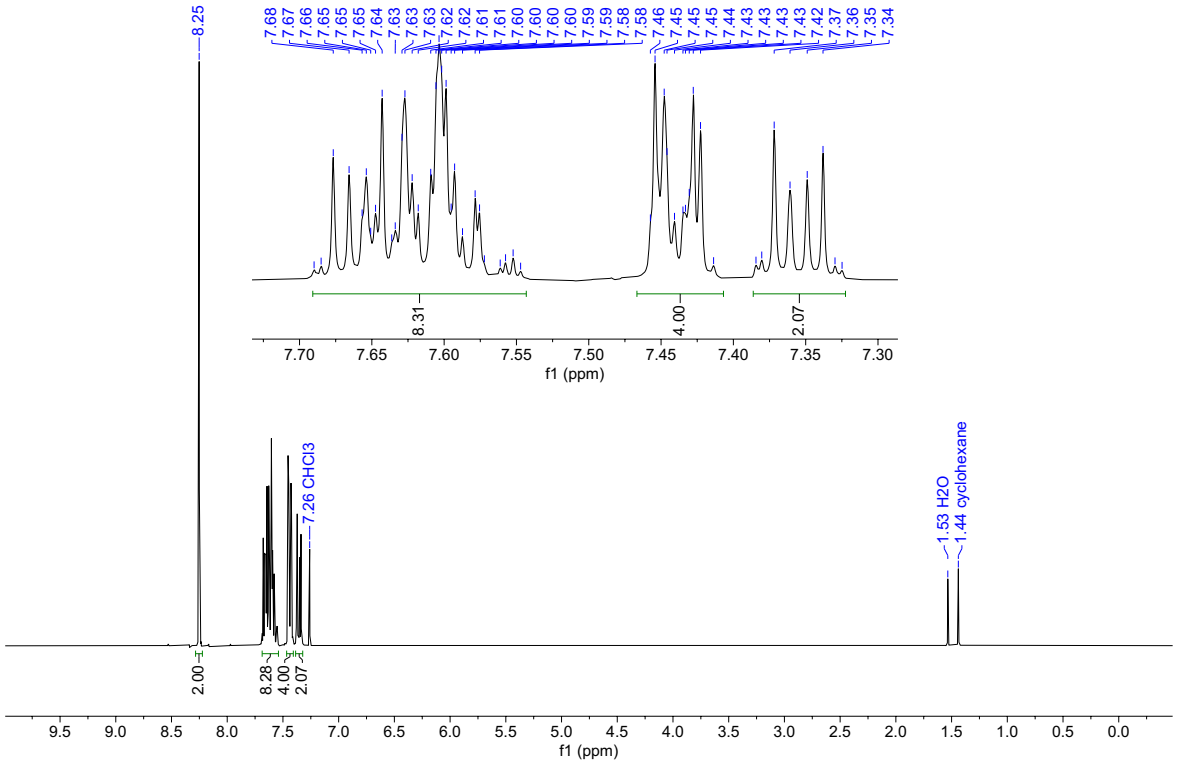

Figure S7: ^{1}H NMR spectrum of **3^{I}** ($CDCl_3$, 300.0 MHz).

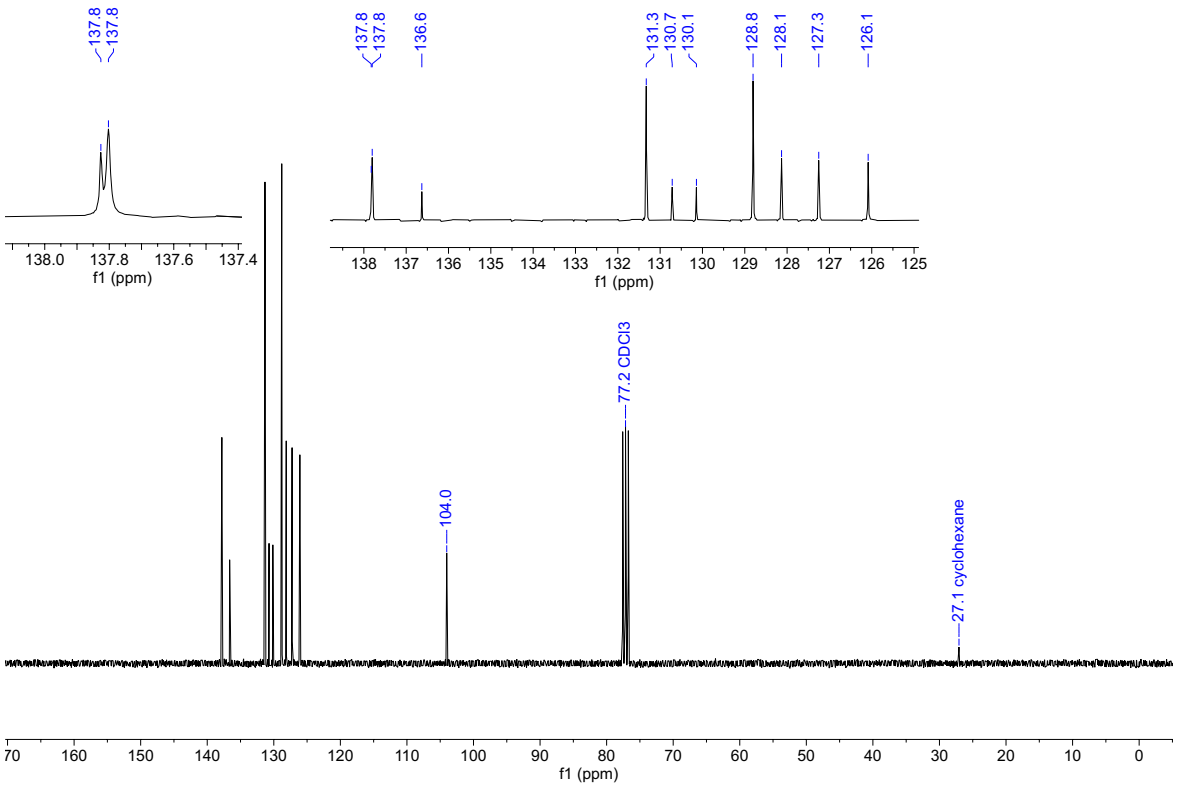

Figure S8: $^{13}C\{^{1}H\}$ NMR spectrum of **3^{I}** ($CDCl_3$, 75.4 MHz).

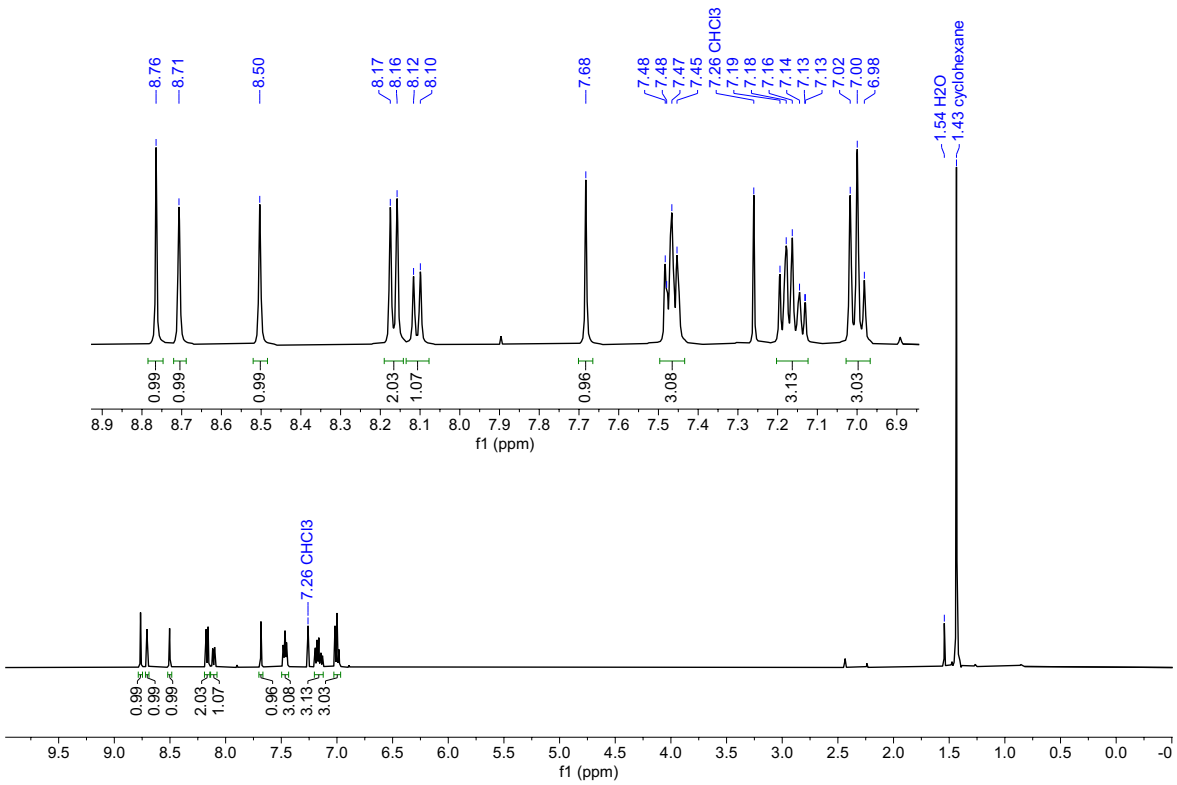

Figure S9: ^{1}H NMR spectrum of **4^{I}** ($CDCl_3$, 500.2 MHz).

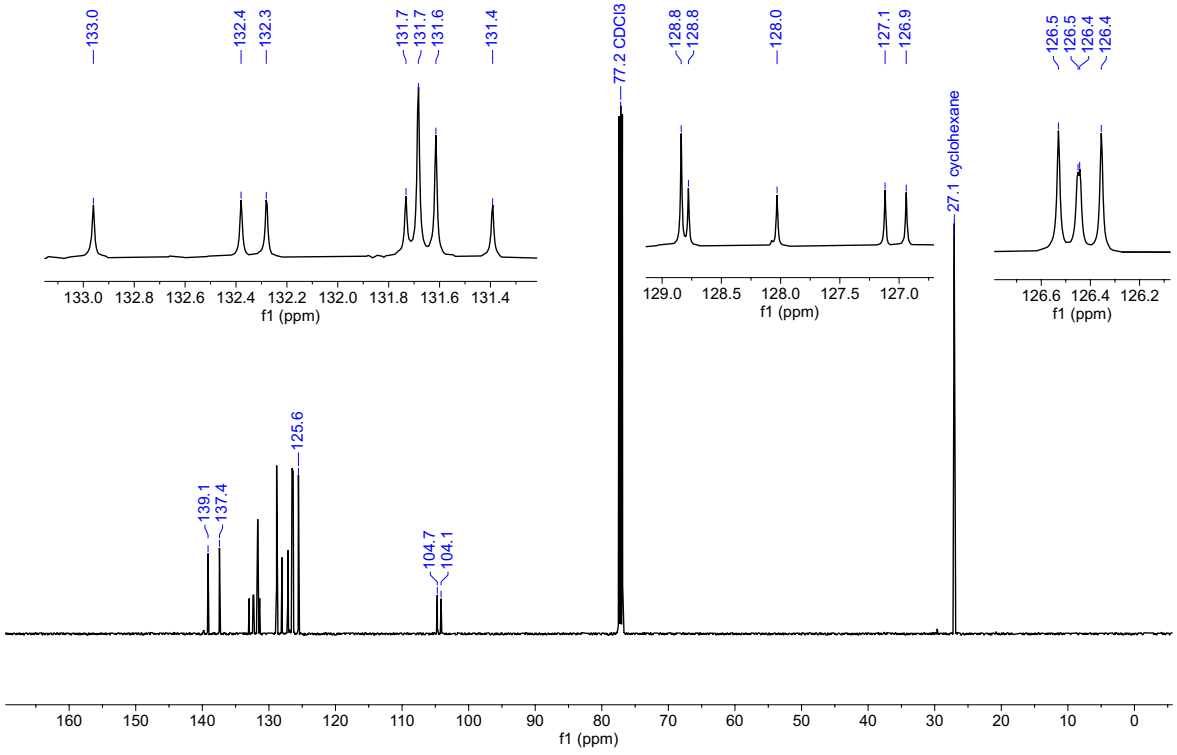

Figure S10: $^{13}C\{^{1}H\}$ NMR spectrum of **4^{I}** ($CDCl_3$, 125.8 MHz).

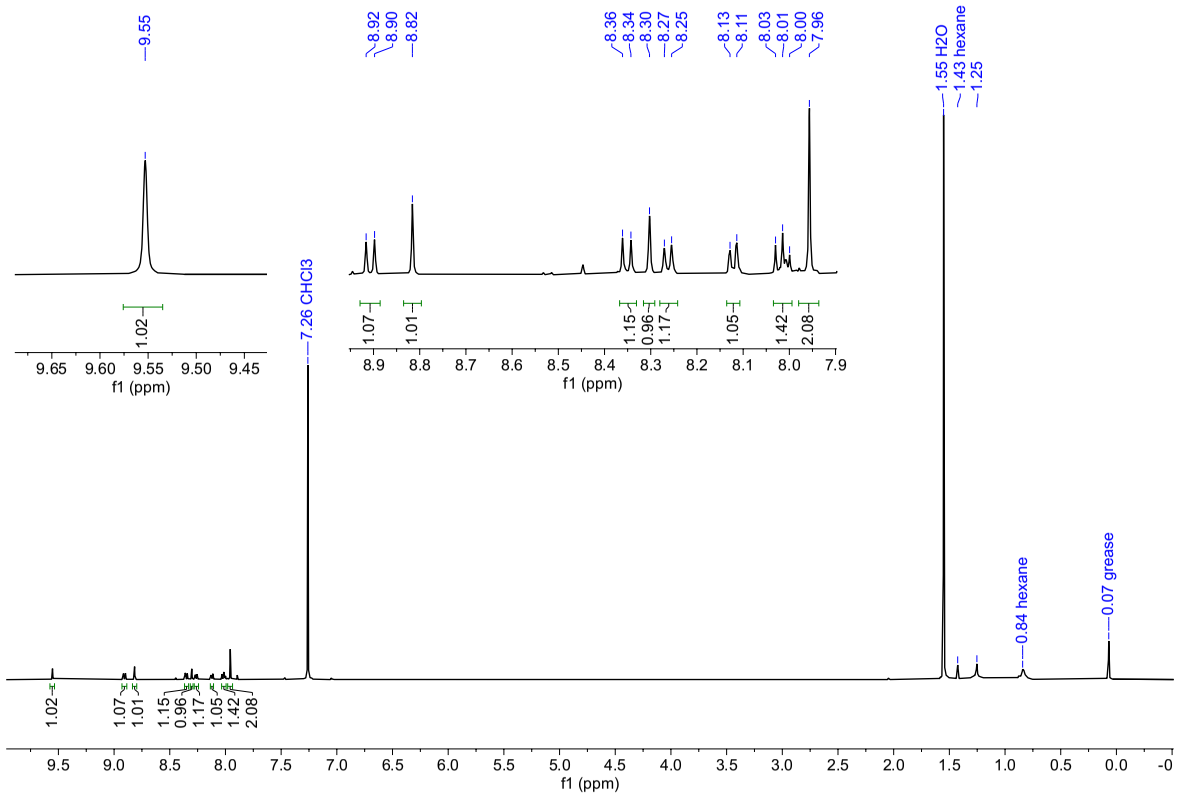

Figure S11: ^{1}H NMR spectrum of **5^{I}** ($CDCl_3$, 500.2 MHz).

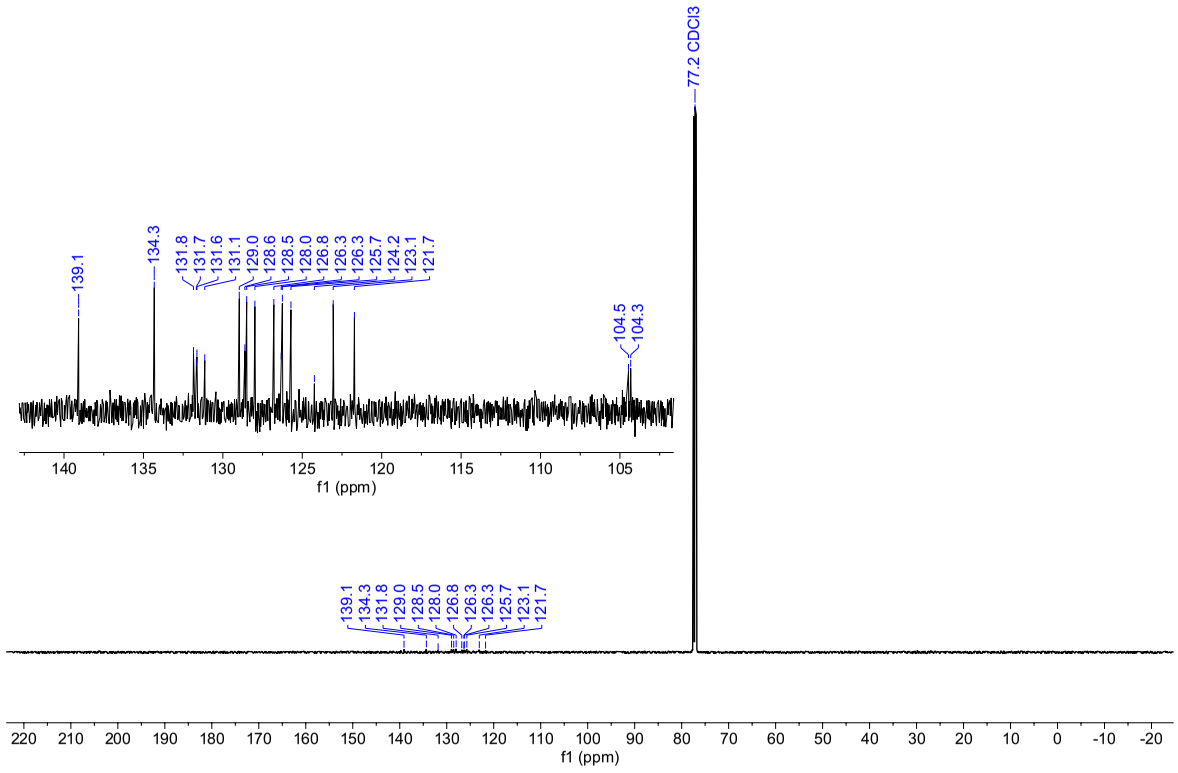

Figure S12: ^{13}C{^{1}H} NMR spectrum of **5^{I}** ($CDCl_3$, 125.8 MHz).

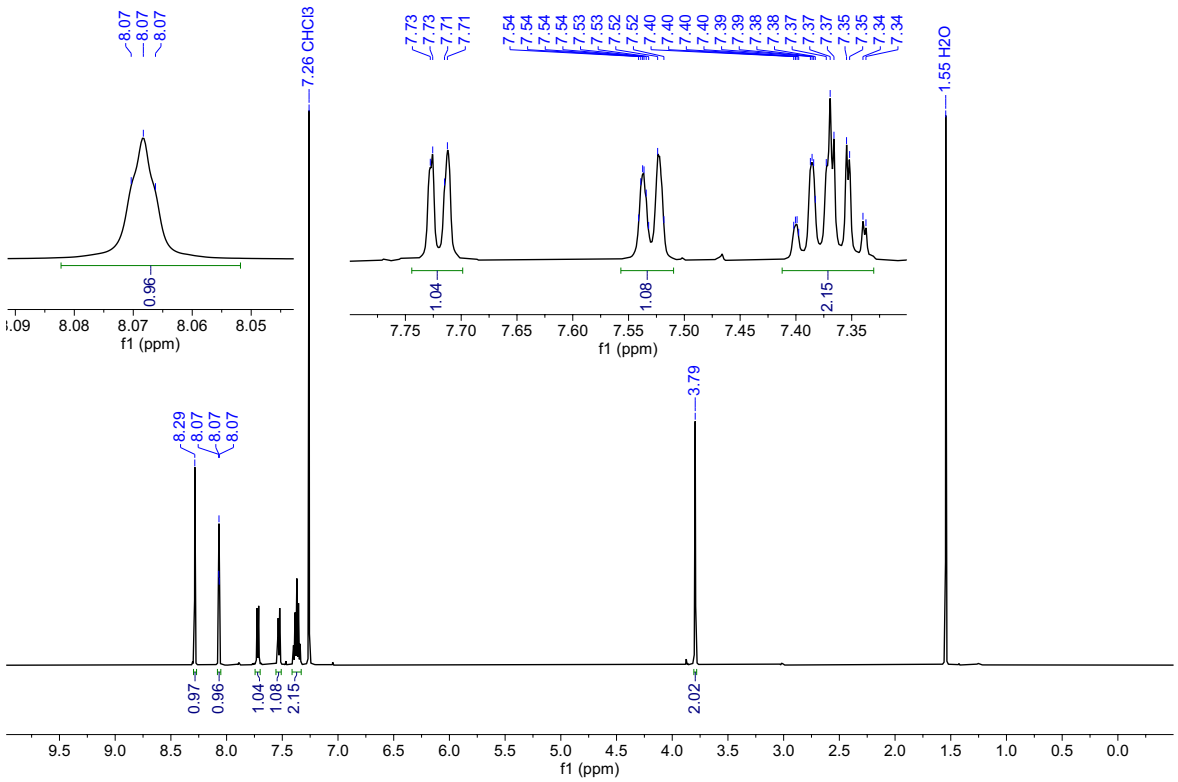

Figure S13: ^{1}H NMR spectrum of **6^{I}** ($CDCl_3$, 500.2 MHz).

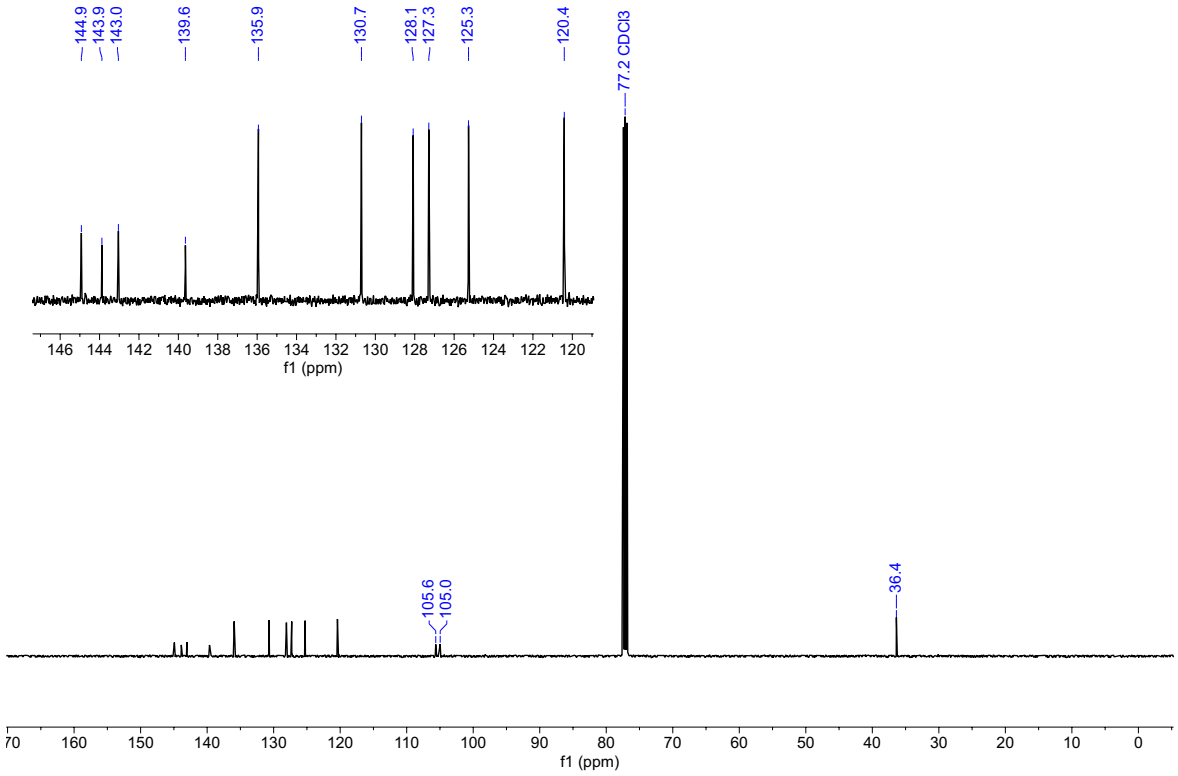

Figure S14: $^{13}C\{^{1}H\}$ NMR spectrum of **6^{I}** ($CDCl_3$, 125.8 MHz).

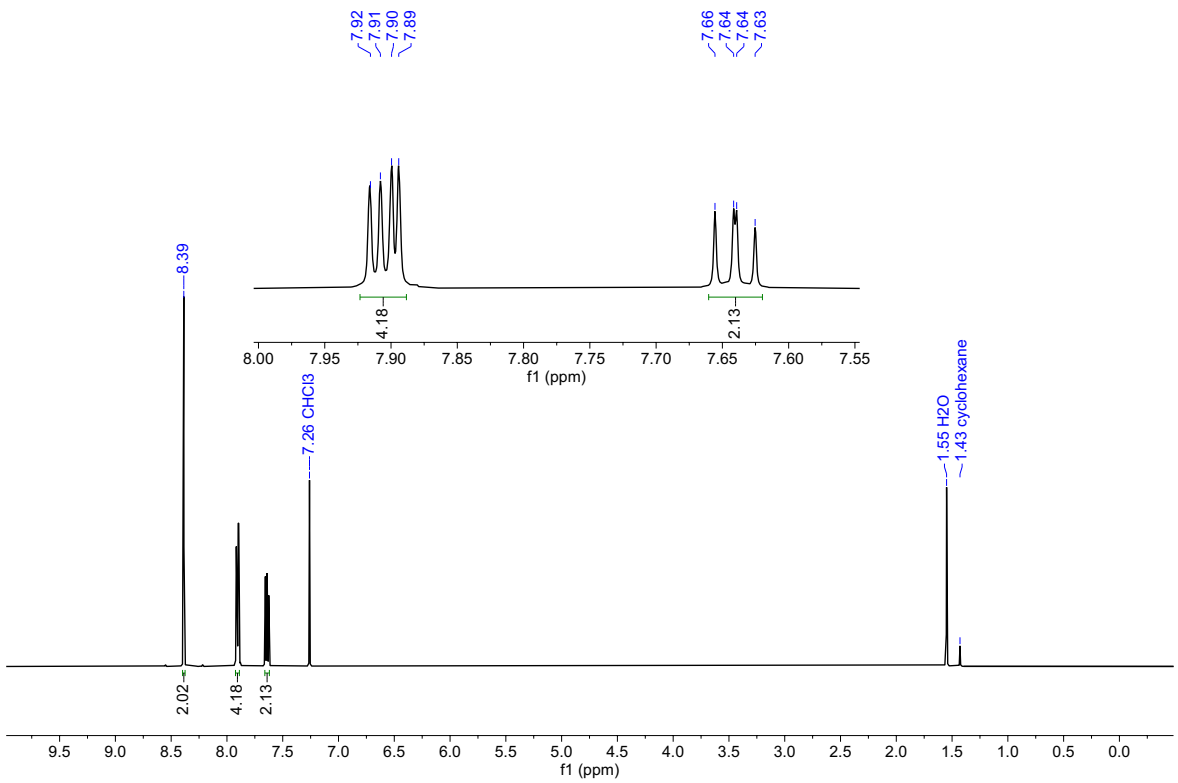

Figure S15: ^{1}H NMR spectrum of **7^{I}** ($CDCl_3$, 500.2 MHz).

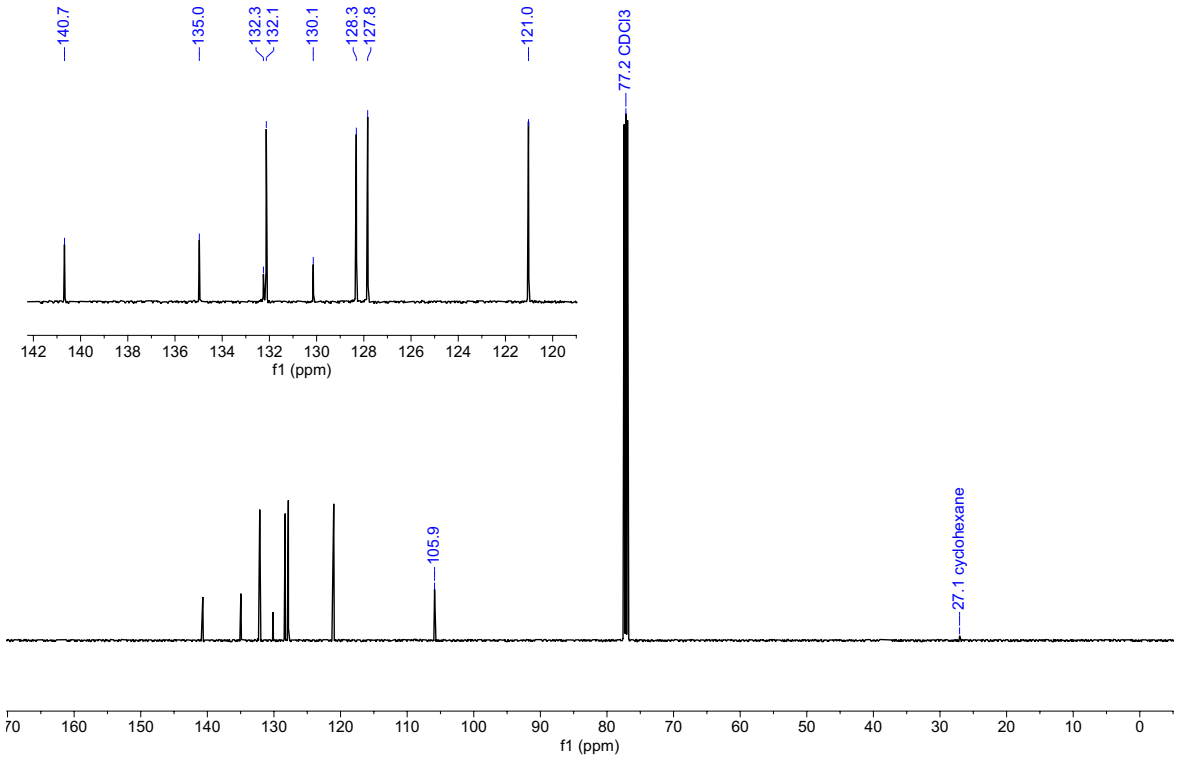

Figure S16: $^{13}C\{^{1}H\}$ NMR spectrum of **7^{I}** ($CDCl_3$, 125.8 MHz).

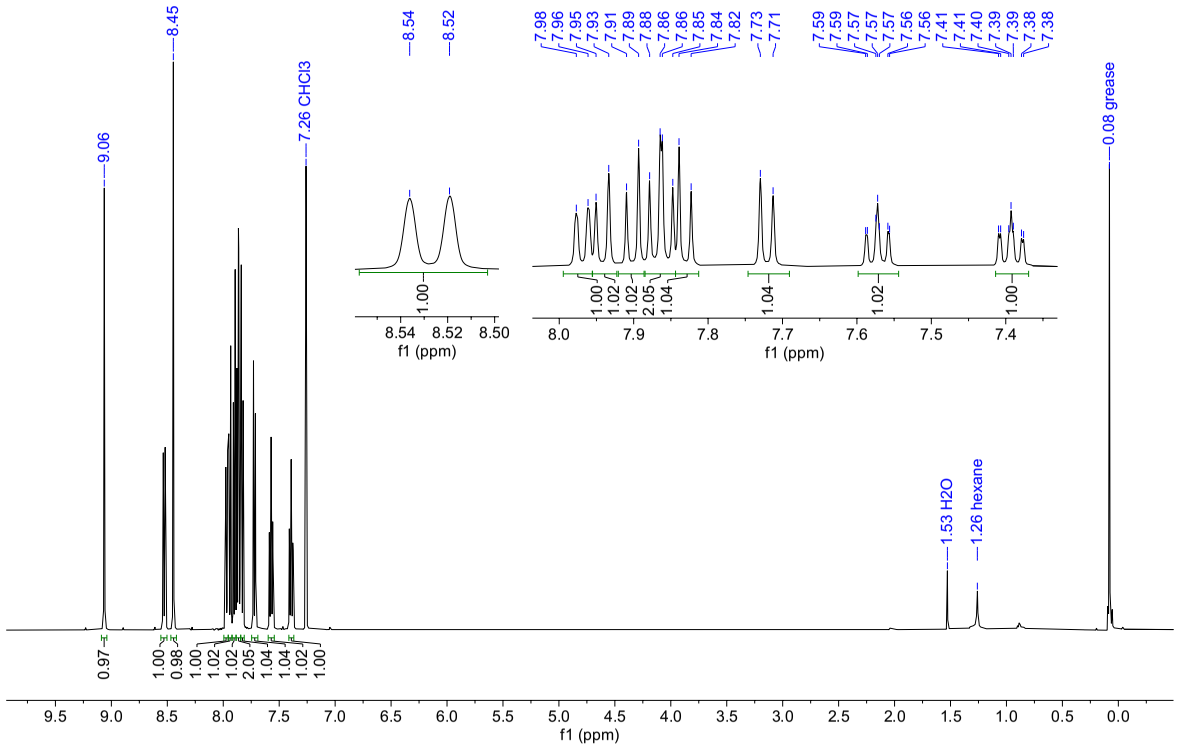

Figure S17: ^{1}H NMR spectrum of **8^{I}** ($CDCl_3$, 500.2 MHz).

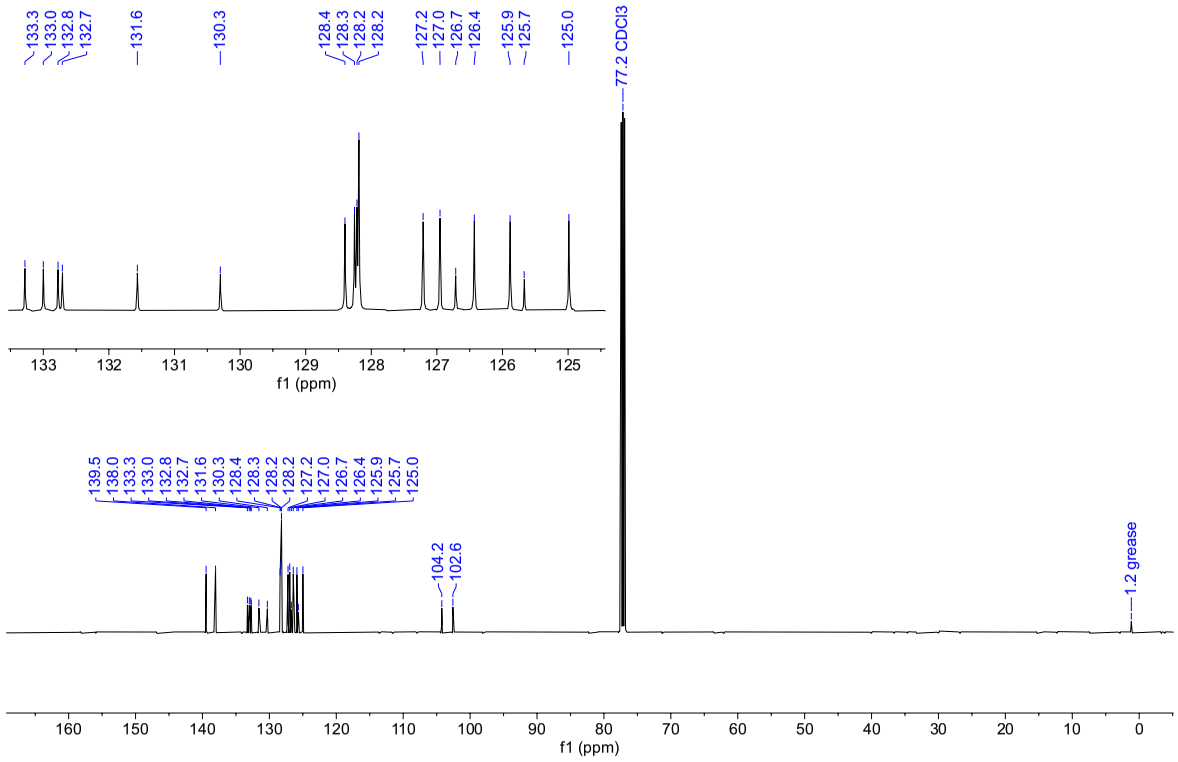

Figure S18: ^{13}C{^{1}H} NMR spectrum of **8^{I}** ($CDCl_3$, 125.8 MHz).

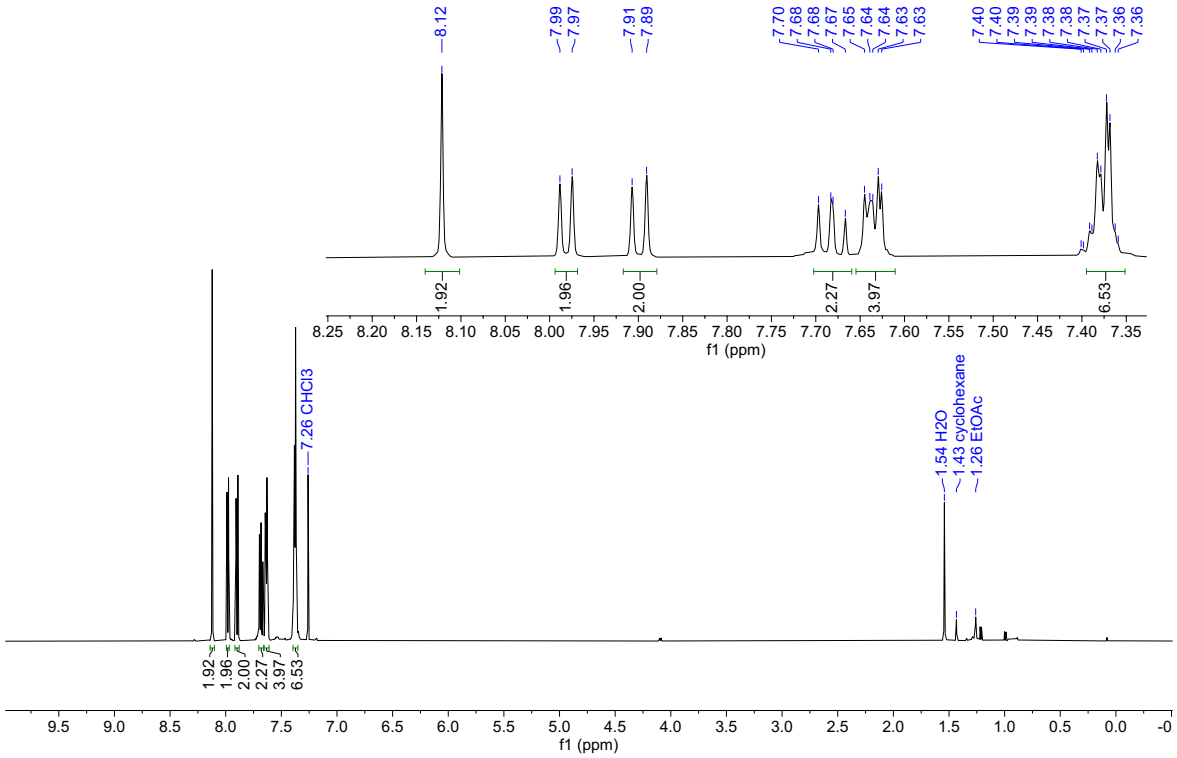

Figure S19: ^{1}H NMR spectrum of **7^{CCPh}** ($CDCl_3$, 500.2 MHz).

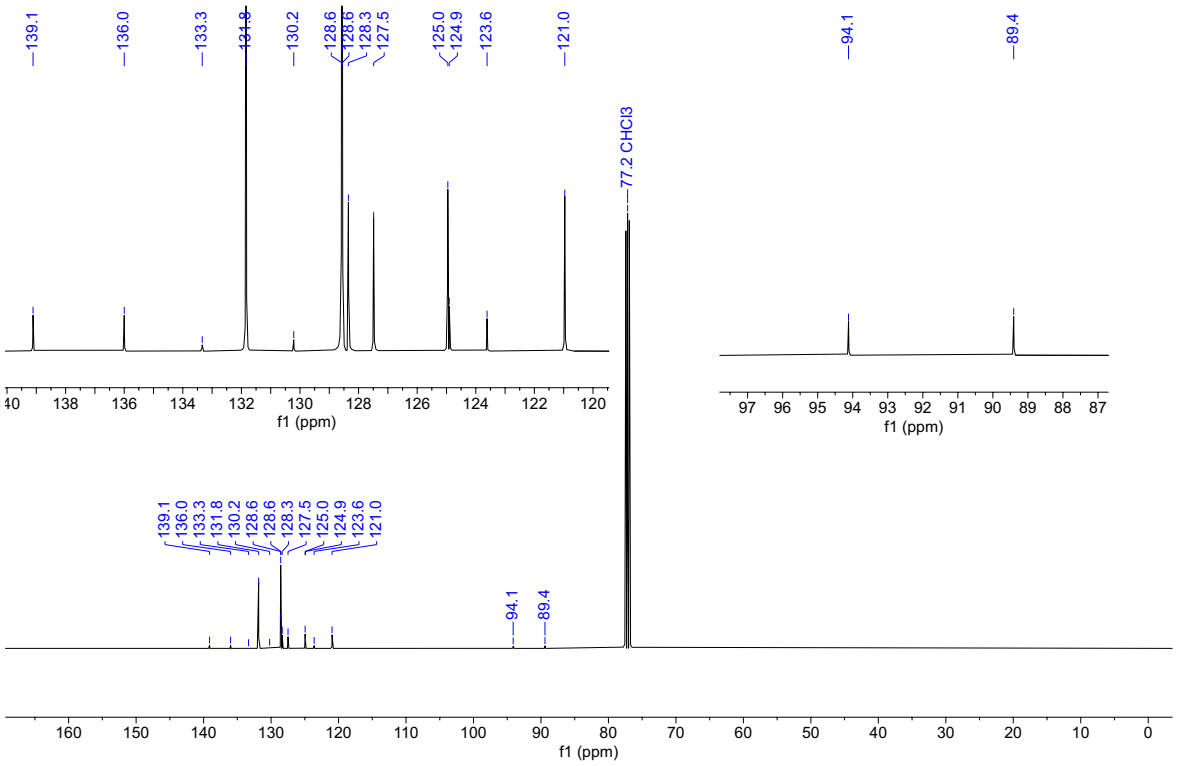

Figure S20: $^{13}C\{^{1}H\}$ NMR spectrum of **7^{CCPh}** ($CDCl_3$, 125.8 MHz).

5. Optimization of the reaction conditions for the *ortho*-diiodination of PAHs

The reaction was performed by following a modified literature protocol, using the least sophisticated, symmetric compound **9^{B}** as the model system.[S11,S12] A microwave vial was charged with **9^{B}** and K_2CO_3 and kept under a dynamic vacuum for 0.5 h to remove air. After the addition of I_2 and CH_3CN, the vial was closed with a septum cap under an N_2 atmosphere and heated to 80 °C. The reaction mixture was cooled to room temperature, all volatiles were removed under reduced pressure and a ^{1}H NMR spectrum of the respective sample was recorded (Figures S21 and S22). Published chemical shift values of **9^{I}** were used as references.[S13]

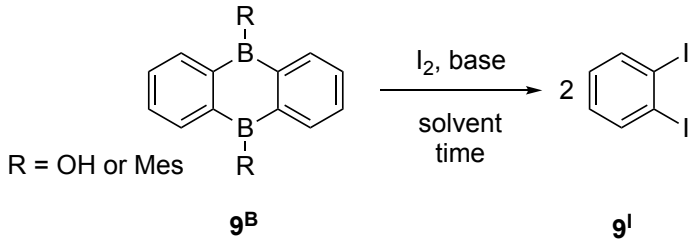

9^{B} **9^{I}**

Table 1: Optimization of the reaction conditions for the synthesis of 1,2-diiodobenzene (**9^{I}**).

Entry	Starting material	Solvent[a]	Time (h)	I_2 (equiv)	Base
1	**9^{BOH}**	CH_3CN	2.5	6	K_2CO_3[b]
2	**9^{BOH}**	CH_3CN	4	6	K_2CO_3[b]
3	**9^{BOH}**	CH_3CN	4	8	K_2CO_3[b]
4	**9^{BOH}**	CH_3CN	17	6	K_2CO_3[b]
5	**9^{BOH}**	CH_3CN	4	10	K_2CO_3[b]
6	**9^{BOH}**	CH_3CN	4	4.5	K_2CO_3[b]
7	**9^{BOH}**	CH_3CN	4	8	KOH[b]
8	**9^{BOH}**	EtOH	4	8	K_2CO_3[b]
9	**9^{BMes}**	CH_3CN	4	12	K_2CO_3[c]

[a] Reaction performed with 1 mL of solvent per 10 mg of **9^{B}**. [b] 8 equivalents. [c] 12 equivalents.

Reaction times and amount of I_2: After 2.5 h, some starting material **9^{BOH}** remained unconsumed (entry **1**); after 4 h, full conversion of **9^{BOH}** was achieved, but signals of side products (likely reaction intermediates) were still detectable when using 6 equiv I_2 and 8 equiv K_2CO_3 (entry **2**); the conversion of **9^{BOH}** to **9^{I}** was complete, even after 4 h, when 8 equiv of I_2 and 8 equiv K_2CO_3 were employed (entry **3**). Given that the lager PAHs lead to lower solubilities of both the boron precursors and the diiodinated products and may therefore require reaction times exceeding 4 h, we confirmed that a reaction time of 17 h does neither lead to iodine scrambling nor to multiple halogenations (entry **4**). The same was true when the amount of I_2 was increased to 10 equiv (entry **5**), whereas the use of only 4.5 equiv I_2 resulted in a complex reaction mixture (entry **6**).
Base and solvent: It is also possible to employ KOH (8 equiv) as the base (entry **7**); switching from CH_3CN to EtOH as the solvent results in a far less selective reaction (entry **8**).
Boron-bonded substituent: The introduction of mesityl substituents at the boron atoms helps to overcome the solubility issues and has no negative impact on the outcome of the diiodination reaction. However, the amounts of I_2 and K_2CO_3 have to be increased (12 equiv each) to account for the 2-iodomesitylene[S8] formed as a side product (entry **9**).

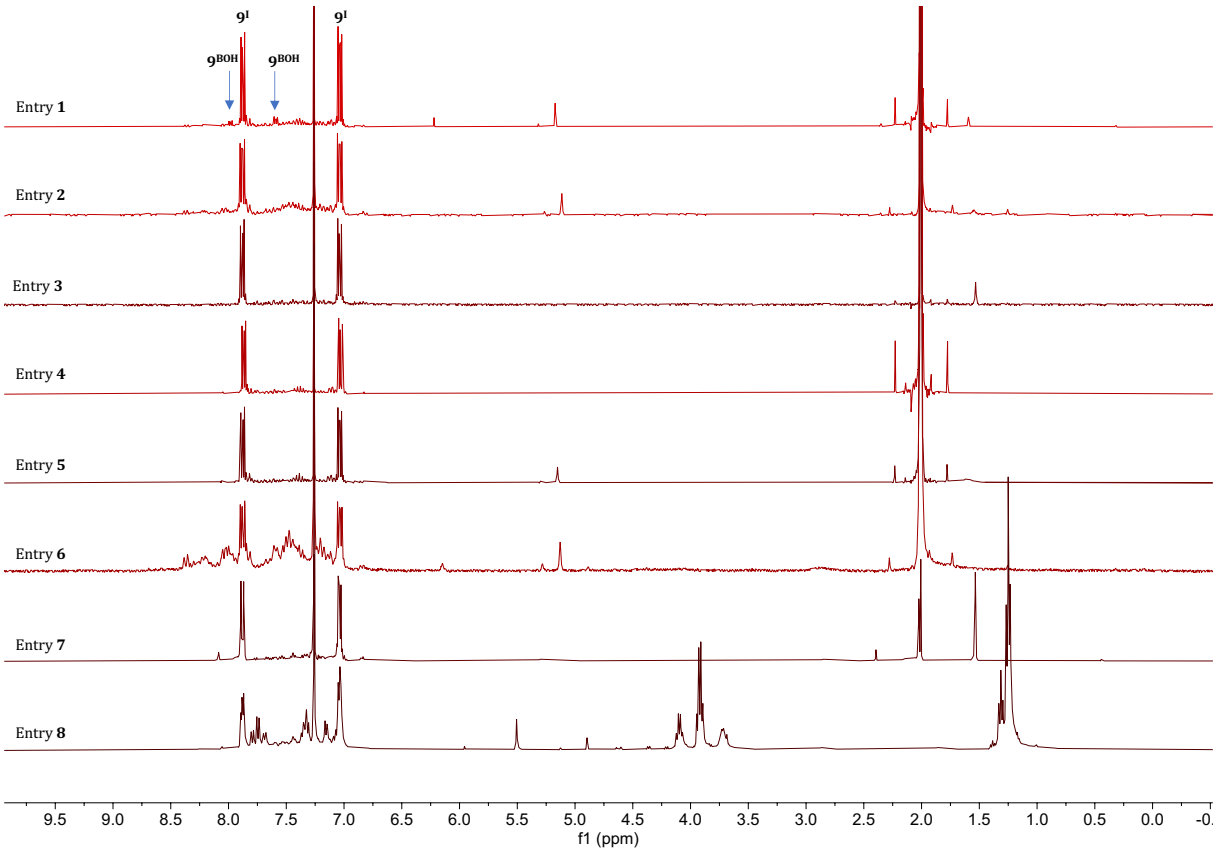

Figure S21: ^{1}H NMR spectra of the products of entry **1** – **8** ($CDCl_3$, 250.1 MHz).

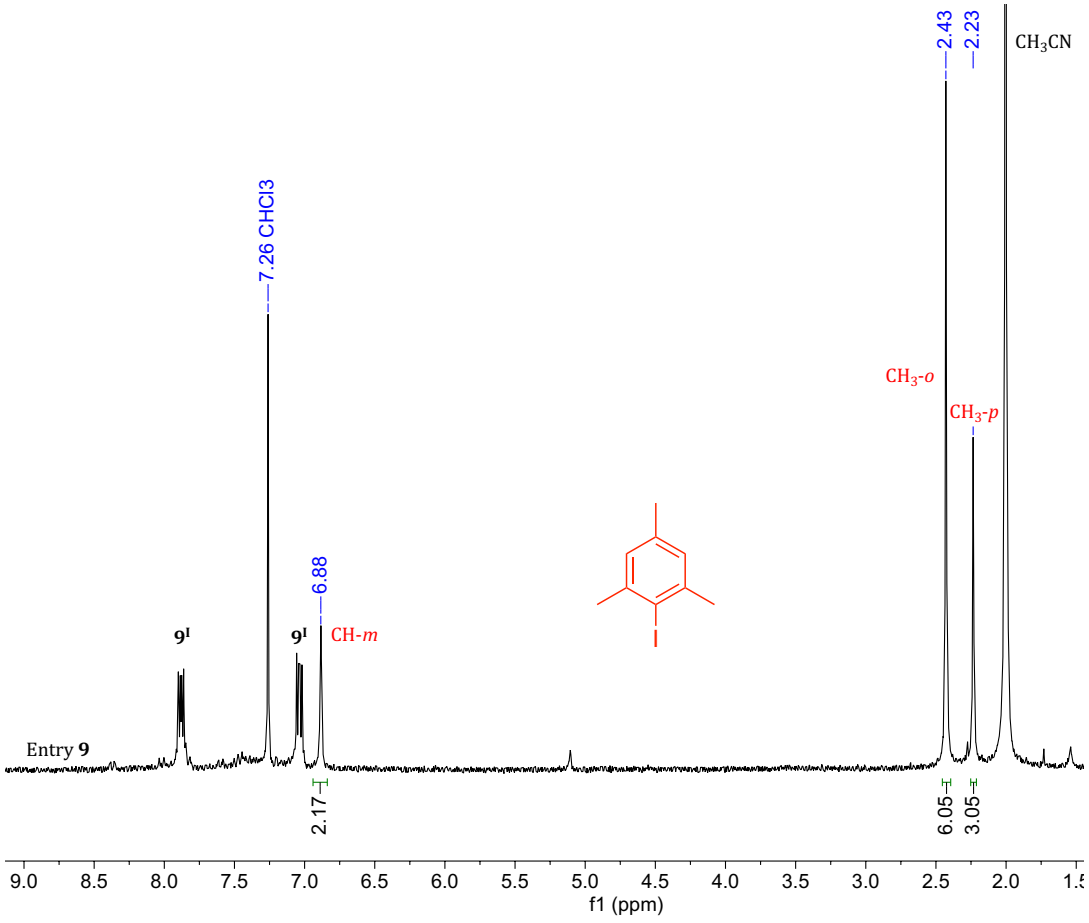

Figure S22: ^{1}H NMR spectrum of the products of entry **9** ($CDCl_3$, 250.1 MHz).

6. Further reactions

6.1. Synthesis of 1^{BOH}

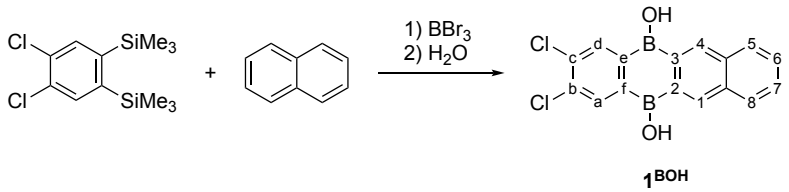

A thick-walled glass ampoule was charged with 4,5-dichloro-1,2-bis(trimethylsilyl)benzene (1.9 g, 6.5 mmol), naphthalene (1.9 g, 15 mmol), BBr_3 (2.0 mL, 5.3 g, 21 mmol), and *n*-hexane (10 mL) as the solvent. The ampoule was flame-sealed under vacuum and subsequently heated to 120 °C for 2.5 d. The dark solution obtained was cooled to room temperature, transferred to a Schlenk tube and evaporated to dryness under a dynamic vacuum. The solid residue was taken up in toluene (20 mL) and stirred at a reduced pressure of 25 torr for 1 h to remove residual BBr_3 (the volume of the solution decreases only slightly). H_2O (15 mL) was added dropwise with stirring over 2 min at 0 °C. The reaction mixture was allowed to warm to room temperature, whereupon the borinic acid precipitated. The precipitate was isolated by filtration and purified by washing with *c*-hexane (3 × 5 mL). **1^{BOH}** was obtained as a colorless solid. Yield: 0.63 g (1.9 mmol, 29%).

^{1}H NMR (600.3 MHz, CD_3CN): δ = 8.60 (s, 2H; H-1,4), 8.20 (s, 2H; H-a,d), 8.01–7.99 (m, 2H; H-5,8), 7.84 (br. s; OH), 7.63–7.61 ppm (m, 2H; H-6,7)
^{13}C{^{1}H} NMR (151.0 MHz, CD_3CN): δ = 145.4* (br.; C-e,f), 138.5* (br.; C-2,3), 135.9 (C-b,c), 135.5 (C-4a,8a), 135.2 (C-a,d), 134.5 (C-1,4), 129.9 (C-5,8), 128.7 ppm (C-6,7); *unequivocally detected only in the ^{H,C}HMBC spectrum

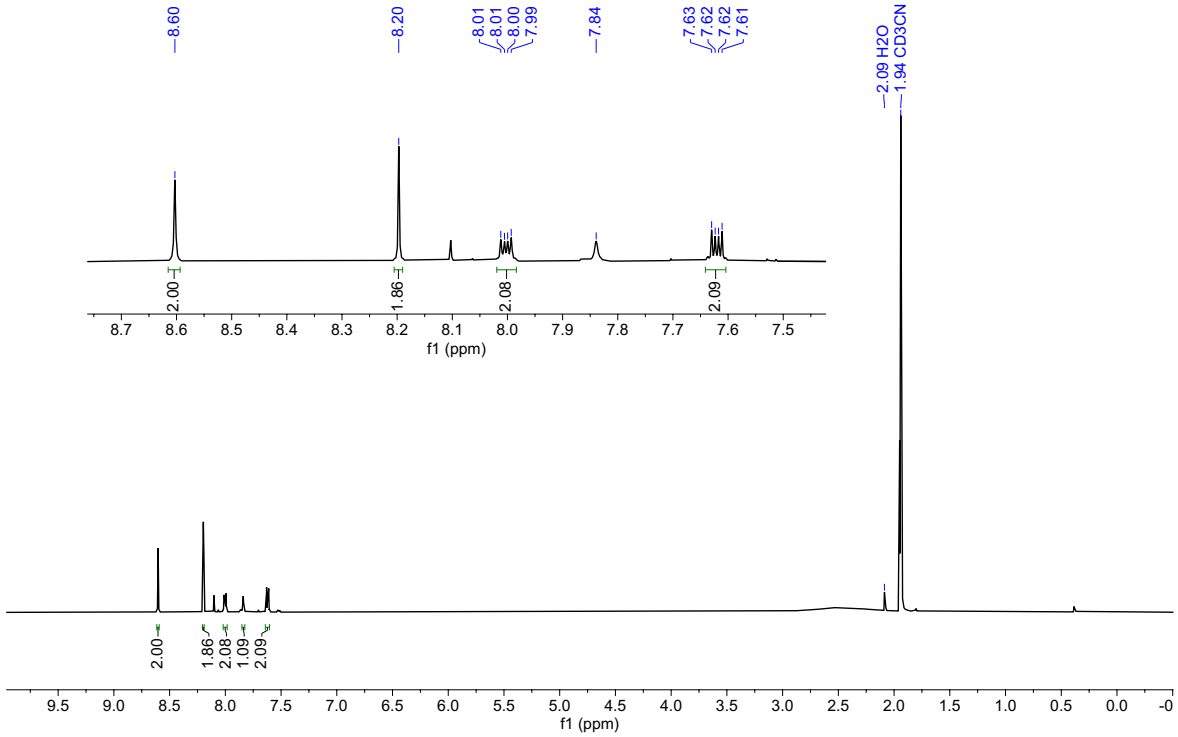

Figure S23: ^{1}H NMR spectrum of **1^{BOH}** (CD_3CN, 600.3 MHz).

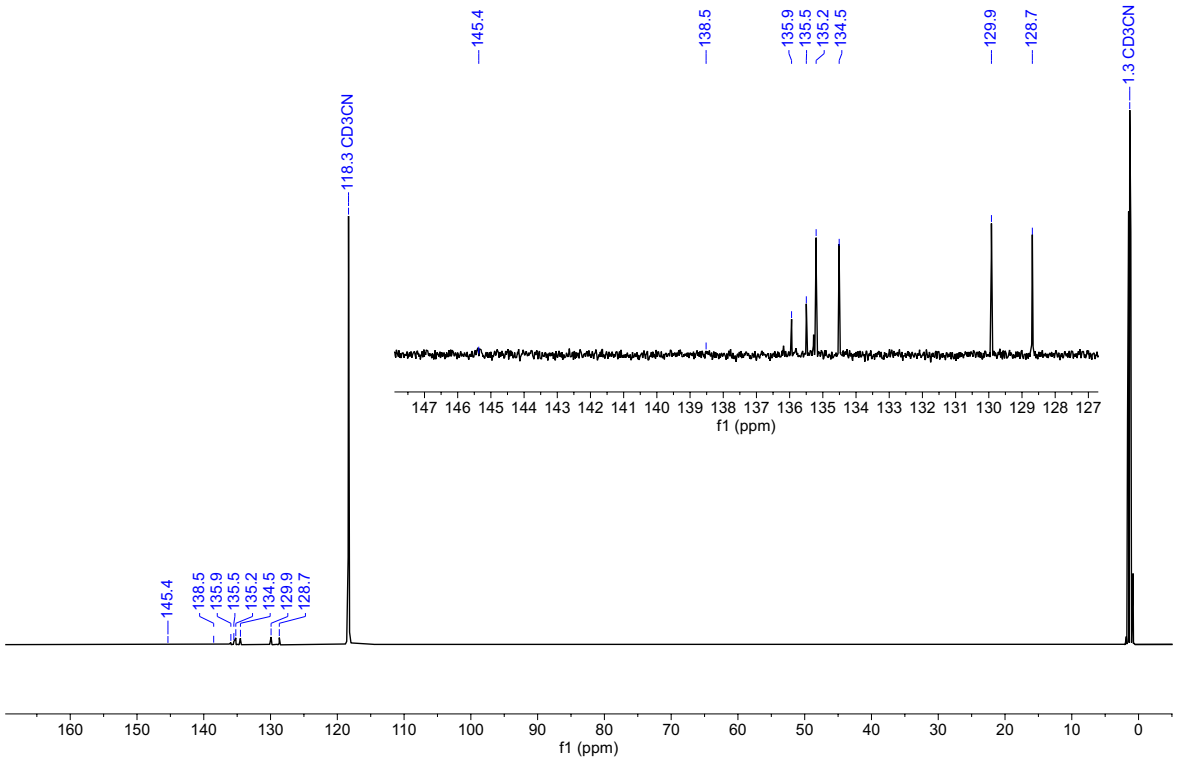

Figure S24: $^{13}C\{^{1}H\}$ NMR spectrum of $\mathbf{1^{BOH}}$ (CD_3CN, 151.0 MHz).

6.2. Iodination of $\mathbf{1}^{\mathbf{BOH}}$

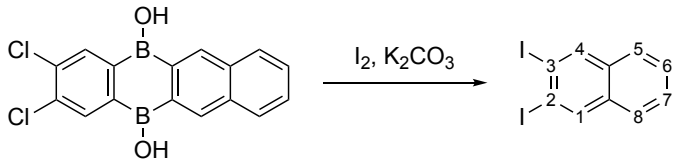

$\mathbf{1}^{\mathbf{BOH}}$ $\mathbf{1}^{\mathbf{I}}$

The synthesis was performed according to the general procedure for *ortho*-diiodinated PAHs (see paragraph 3.1), using $\mathbf{1}^{\mathbf{BOH}}$ (0.20 g, 0.62 mmol), K_2CO_3 (0.68 g, 4.9 mmol), I_2 (1.2 g, 4.7 mmol), and CH_3CN (10 mL). The purification of the crude product by flash chromatography (silica gel, *c*-hexane, R_f = 0.61) afforded $\mathbf{1}^{\mathbf{I}}$ as a colorless solid. Yield: 0.096 g (0.25 mmol, 40%).

The ^{1}H NMR spectrum is in accordance with the spectrum shown above (Figure S1 and S2).

6.3. Bromination of $\mathbf{1}^{\mathbf{BOH}}$

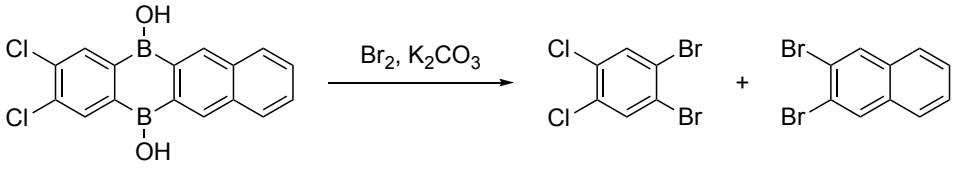

$\mathbf{1}^{\mathbf{BOH}}$ $\mathbf{1}^{\mathbf{Br}}$

A microwave vial was charged with $\mathbf{1}^{\mathbf{BOH}}$ (0.050 g, 0.15 mmol) and K_2CO_3 (0.17 g, 1.2 mmol) and kept under a dynamic vacuum for 0.5 h. After the addition of Br_2 (0.1 mL, 0.31 g, 1.9 mmol) and CH_3CN (7 mL), the vial was closed with a septum cap under an N_2 atmosphere and heated to 80 °C for 17 h. The reaction mixture was cooled to room temperature. A saturated aqueous solution of $Na_2S_2O_5$ (20 mL) was added and the organic phase was separated by using a separation funnel. The aqueous phase was extracted with $CHCl_3$ (2 × 25 mL), the organic phases were combined, washed with H_2O (20 mL), dried over anhydrous $MgSO_4$, and filtered. All volatiles were removed from the filtrate under reduced pressure and an ^{1}H NMR spectrum of the sample was recorded (Figures S25). Published chemical shift values of 1,2-dibromo-4,5-dichlorobenzene[S14] and $\mathbf{1}^{\mathbf{Br}}$[S15] were used as references.

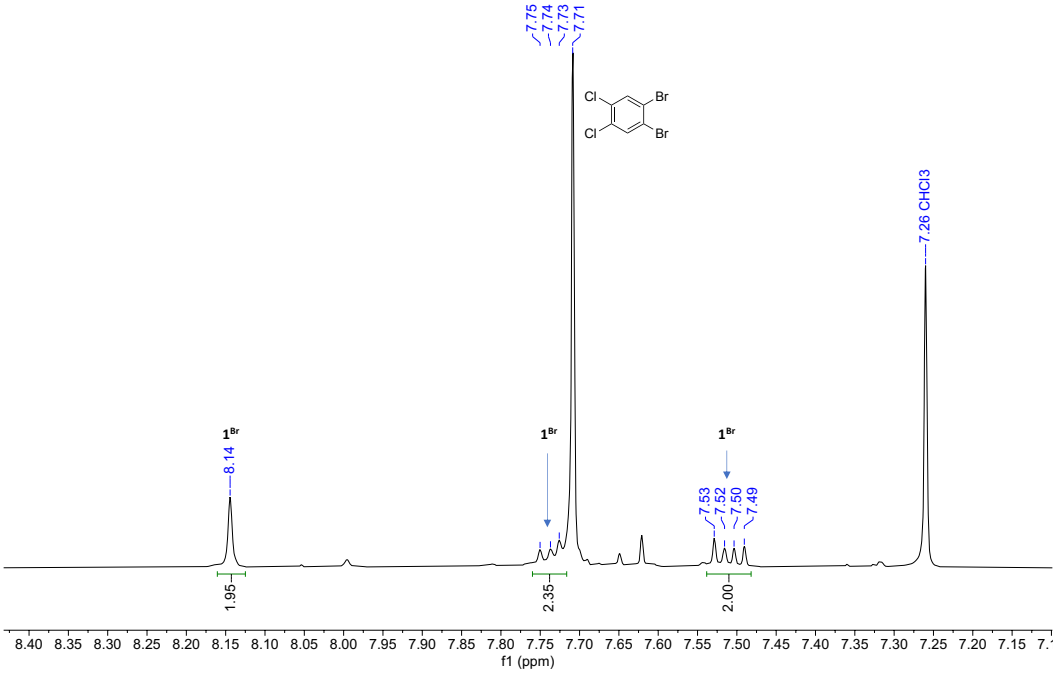

Figure S25: ^{1}H NMR spectrum of 1,2-dibromo-4,5-dichlorobenzene[S14] and $\mathbf{1}^{\mathbf{Br}}$[S15] (integrated) ($CDCl_3$, 250.1 MHz).

The ^{1}H NMR spectrum (Figure S26, top) proves the formation of **1^{Br}** and 1,2-dibromo-4,5-dichlorobenzene. The reaction becomes significantly less selective, when the amount of Br_2 is increased from 8 to 12 equiv (Figure S26, middle). To test whether overbromination is an issue, we exposed **1^{Br}** to 12 equiv Br_2 and 12 equiv K_2CO_3 in CH_3CN for 17 h at 80 °C. The products formed show similar ^{1}H NMR signals (Figure S26, bottom) as observed in Figure S26, middle. **1^{Br}** (after 16.29 min; Figure S28) and a triply brominated naphthalene (after 21.24 min; Figure S29) were detected by GC-MS analysis of the reaction mixture **1^{Br}**/Br_2.

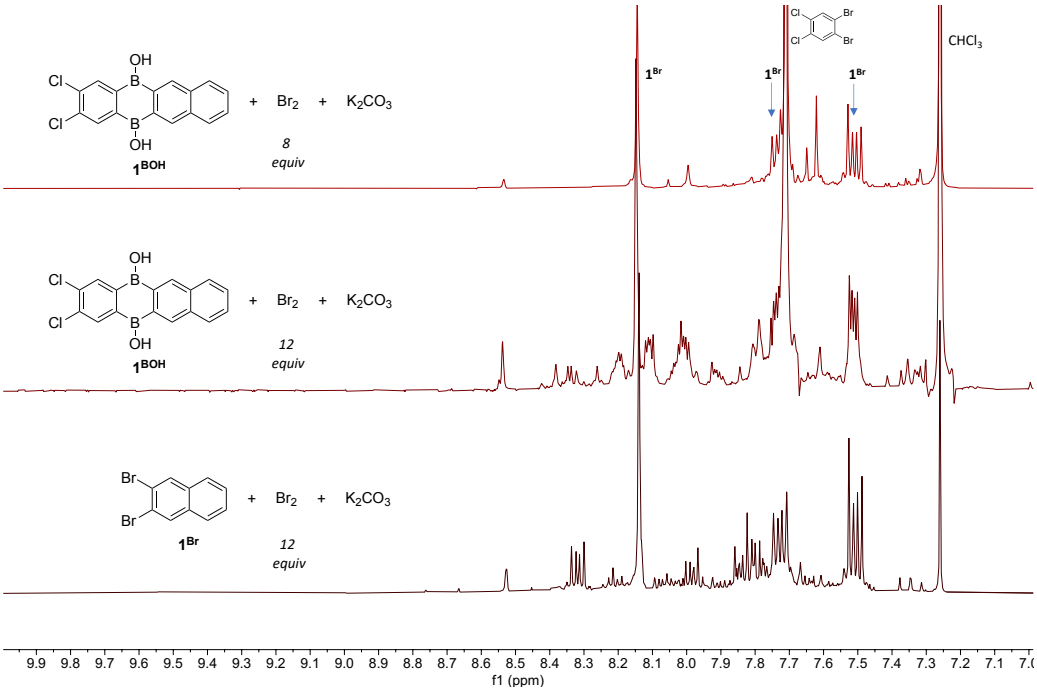

Figure S26: ^{1}H NMR spectra ($CDCl_3$, 250.1 MHz) recorded on the product mixtures obtained from **1^{BOH}** and 8 equiv Br_2 (top) or 12 equiv Br_2 (middle); ^{1}H NMR spectrum ($CDCl_3$, 250.1 MHz) recorded on the product mixture obtained from **1^{Br}**, Br_2 (12 equiv), and K_2CO_3 (8 equiv) in CH_3CN (bottom).

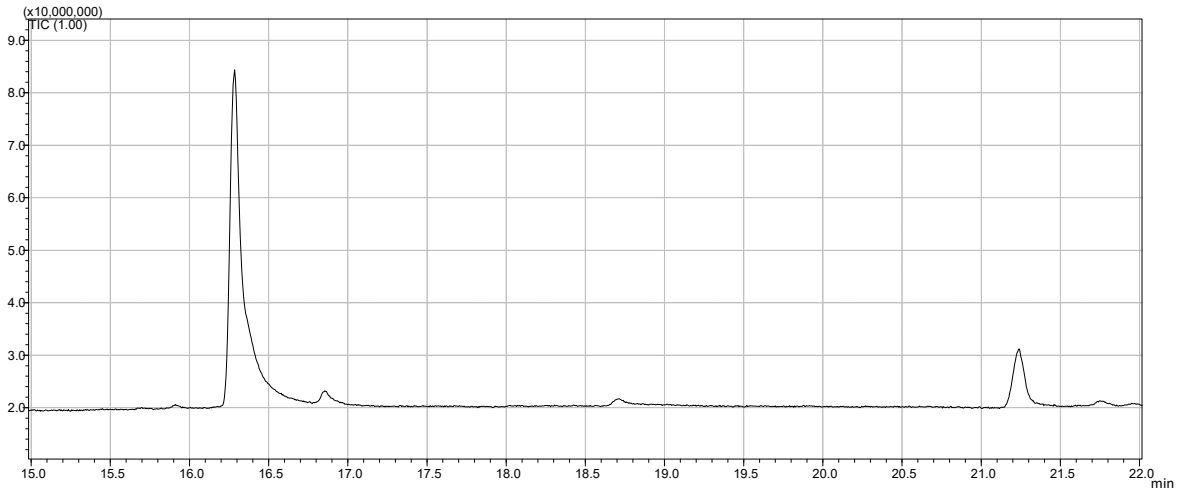

Figure S27: Gas chromatogram recorded on the product mixture obtained from **1^{Br}**, Br_2 (12 equiv), and K_2CO_3 (8 equiv) in CH_3CN.

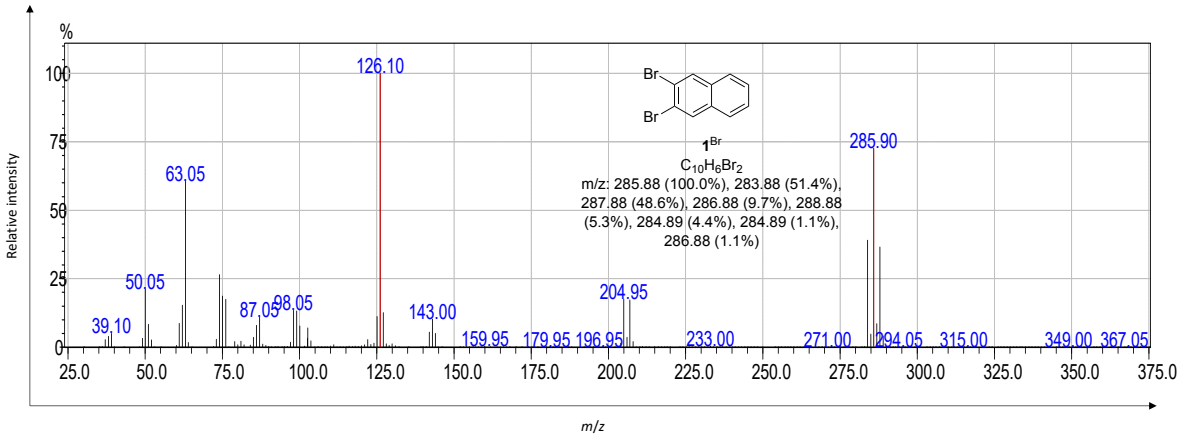

Figure S28: GC-MS spectrum of **1^{Br}** at a retention time of 16.29 min.

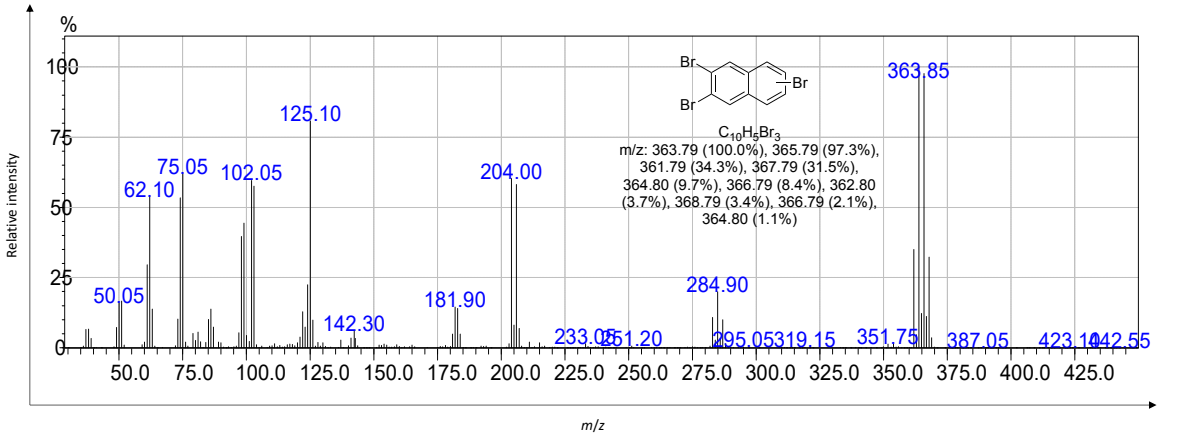

Figure S29: GC-MS spectrum of a triply brominated naphthalene at a retention time of 21.24 min.

6.4. Hydroxylation of $\mathbf{1^{BOH}}$

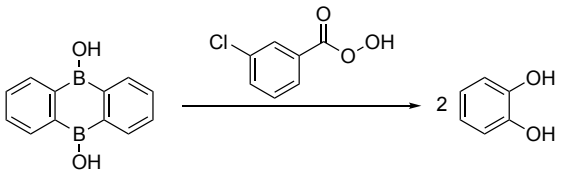

$\mathbf{9^{BOH}}$ $\mathbf{9^{OH}}$

A test reaction using $\mathbf{9^{BOH}}$ as the starting material was performed according to a modified literature procedure (for boronic acids as the starting materials).[S16] A flask was charged with $\mathbf{9^{BOH}}$ (0.032 g, 0.15 mmol) and a H_2O/EtOH (1:2) solution (1.5 mL). After cooling to 0 °C, *m*-CPBA (0.11 g, 0.62 mmol) was added. The reaction mixture was allowed to warm to room temperature within 6 h and quenched with saturated aqueous $NaHCO_3$ (3 mL). EtOAc (3 mL) was added, the organic phase was separated by using a separation funnel. The aqueous phase was extracted with EtOAc (2 × 3 mL). The organic phases were combined, washed with H_2O (3 mL) and saturated aqueous NaCl (3 mL), dried over anhydrous $MgSO_4$, and filtered. All volatiles were removed from the filtrate under reduced pressure to obtain the crude product as a yellow oil (0.019 g). An ^1H NMR spectrum ($CDCl_3$) was recorded to prove the formation of $\mathbf{9^{OH}}$ (see Figure S30).

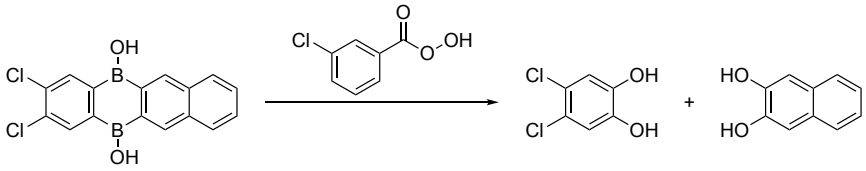

$\mathbf{1^{BOH}}$ $\mathbf{1^{OH}}$

The reaction was performed in a similar fashion as the test reaction using $\mathbf{1^{BOH}}$ (0.050 g, 0.15 mmol) and *m*-CPBA (0.11 g, 0.62 mmol). The crude product was filtered over a short plug of silica gel using *c*-hexane:EtOAc = 1:3 as the eluent. A product mixture (0.020 g) was obtained (see Figure S31). $\mathbf{1^{OH}}$ and 4,5-dichlorocatechol were separated from each other through fractional crystallization from $CHCl_3$.

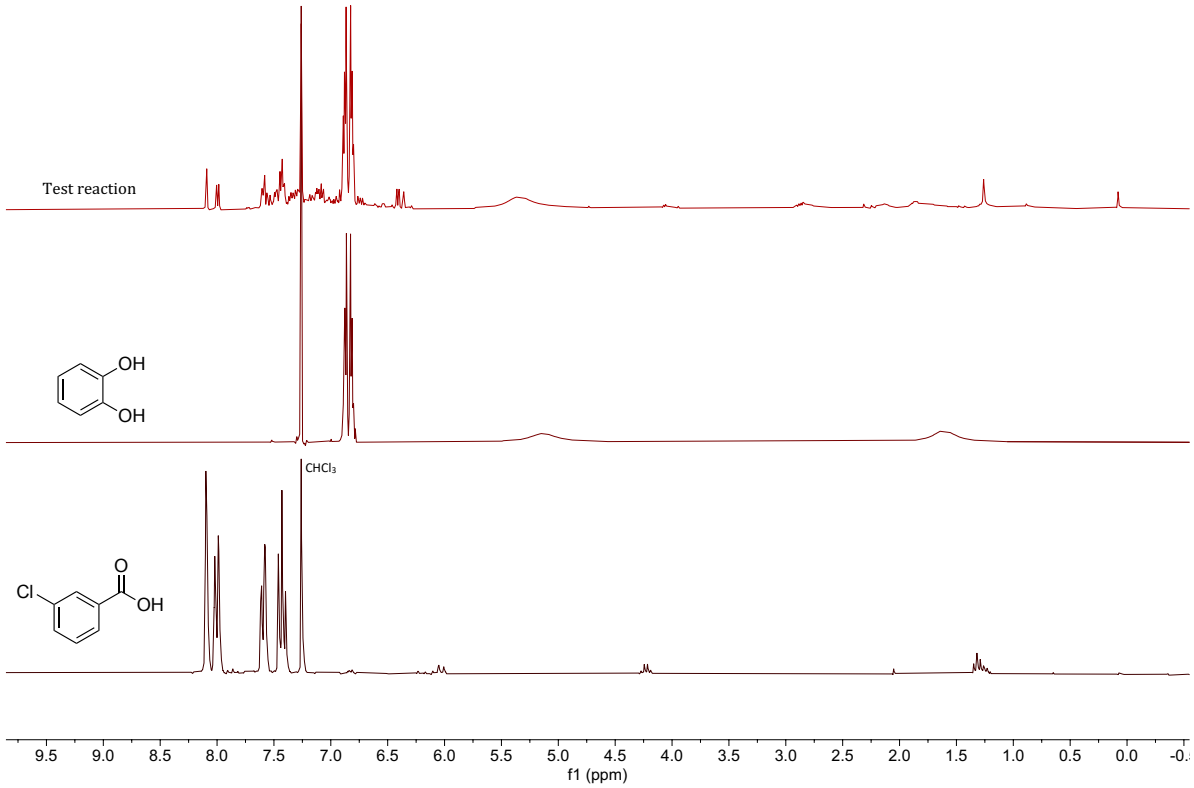

Figure S30: ^{1}H NMR spectrum of the product mixture obtained from the test reaction (top), catechol (middle, own measurement on a commercial sample), and *m*-chlorobenzoic acid (below, own measurement) ($CDCl_3$, 250.1 MHz).

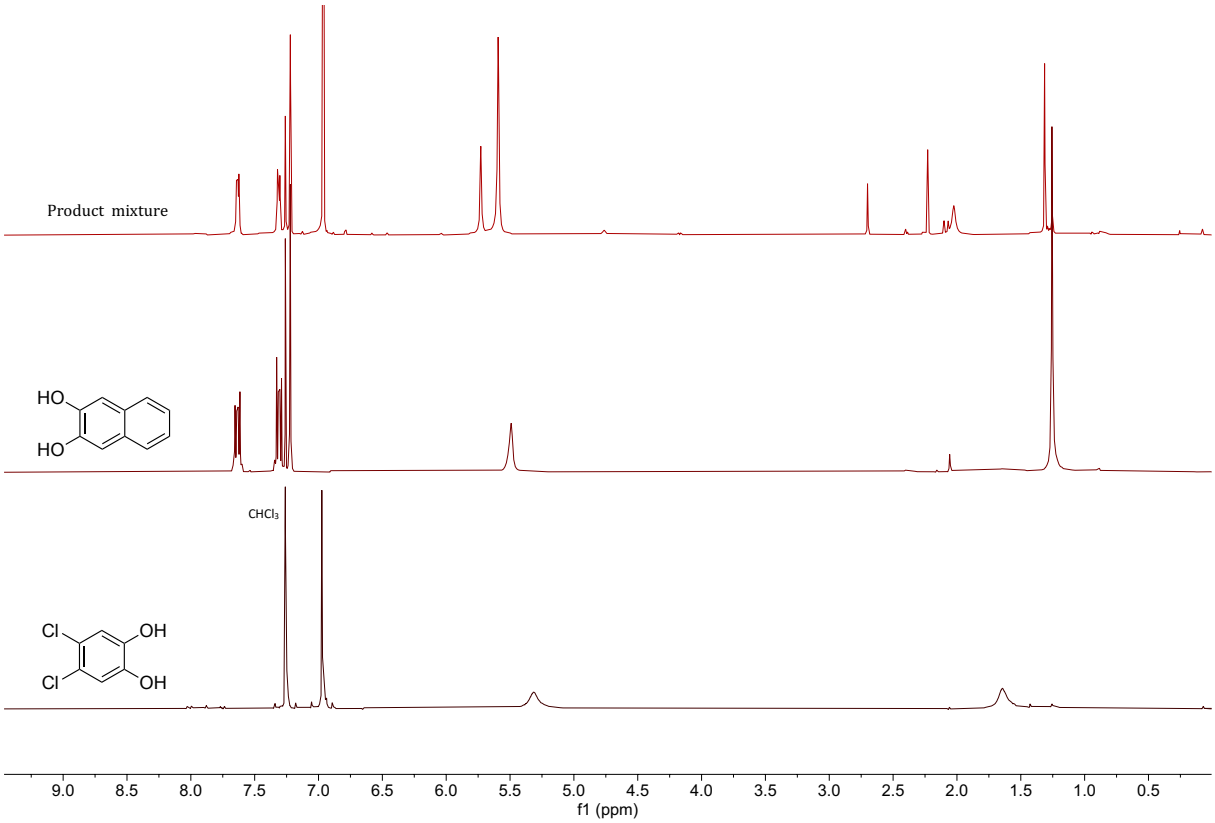

Figure S31: ^{1}H NMR spectrum of the product mixture obtained from the reaction (top), 1,2-dihydroxynapthalene (middle, own measurement on a commercial sample), and 1,2-dichloro-4,5-dihydroxybenzene (below, own measurement on a sample isolated from the reaction) ($CDCl_3$, 250.1 MHz).

7. Syntheses, purification methods, and analytical data for the *ortho*-diborylated PAH derivatives

7.1. General synthesis

A thick-walled glass ampoule was charged with 4,5-dichloro-1,2-bis(trimethylsilyl)benzene, the respective PAH, BBr_3, and *n*-hexane as the solvent. The ampoule was flame-sealed under vacuum and subsequently heated to 120 °C for 2.5 d. The dark solution obtained was cooled to room temperature, transferred to a Schlenk tube and evaporated to dryness under a dynamic vacuum. The solid residue was taken up in toluene (20 mL) and stirred at a reduced pressure of 25 torr for 1 h to remove residual BBr_3 (the volume of the solution decreases only slightly). A solution of MesMgBr in THF was added dropwise with stirring over 2 min at 0 °C. The reaction mixture was allowed to warm to room temperature overnight, quenched with saturated aqueous NH_4Cl (100 mL), and the organic phase was separated by using a separation funnel. The aqueous phase was extracted with $CHCl_3$ (2 × 25 mL). The organic phases were combined, washed with H_2O (20 mL), dried over anhydrous $MgSO_4$, and filtered. All volatiles were removed from the filtrate under reduced pressure and the crude product was purified by column or flash chromatography.

Synthesis of 4^{BMes}

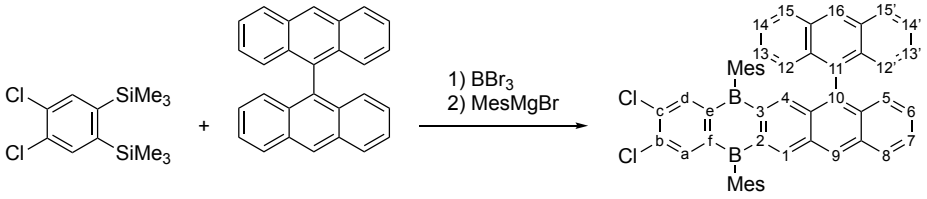

4^{BMes}

The synthesis was performed according to the general procedure described above using 4,5-dichloro-1,2-bis(trimethylsilyl)benzene (0.50 g, 1.7 mmol), 9,9'-bianthracene (0.30 g, 0.85 mmol), BBr_3 (1.0 mL, 2.6 g, 10 mmol), *n*-hexane (8 mL), and MesMgBr in THF (0.72 M, 9.5 mL, 6.8 mmol). The purification of the crude product by column chromatography (16 cm silica gel, d = 3 cm, *c*-hexane, R_f = 0.56) afforded **4^{BMes}** as an orange solid. Yield: 0.17 g (0.22 mmol, 26%). The BBr precursor **4^{BBr}** crystallized already in the reaction ampoule in the form of red plates, which were suitable for an X-ray crystal structure analysis.
Note: Contrary to most other syntheses,[S2] we used only 0.5 equiv of the PAH rather than a moderate excess, because we found that unreacted 9,9'-bianthracene was very hard to remove completely from the product **4^{BMes}**.

^{1}H NMR (500.2 MHz, $CDCl_3$): δ = 8.63 (s, 1H; H-9), 8.52 (s, 1H; H-16), 8.43 (s, 1H; H-1), 8.11–8.07 (m, 3H; H-8,15,15'), 7.70 (s, 1H; H-a/d), 7.69 (s, 1H; H-a/d), 7.52–7.48 (m, 1H; H-7), 7.44–7.40 (m, 2H; H-14,14'), 7.33 (d, ^3J(H,H) = 8.5 Hz, 1H; H-5), 7.26–7.24 (m, 1H; H-6), 7.11–7.07 (m, 2H; H-13,13'), 7.02 (s, 2H; Mes-CH-*m*), 6.97 (d, ^3J(H,H) = 8.5 Hz, 2H; H-12,12'), 6.91 (s, 1H; H-4), 6.23 (s, 2H; Mes-CH-*m*), 2.48 (s, 3H; Mes-CH_3-*p*), 2.29 (s, 3H; Mes-CH_3-*p*), 2.11 (s, 6H; Mes-CH_3-*o*), 1.41 ppm (s, 6H; Mes-CH_3-*o*)
^{13}C{^{1}H} NMR (125.8 MHz, $CDCl_3$): δ = 146.4 (br.; C-e/f), 146.2 (br.; C-e/f), 143.7 (C-1), 143.1 (C-4), 140.5 (C-a/d), 140.4 (C-a/d), 140.1 (br.; Mes-C-*i*), 139.3 (br.; C-3), 139.0 (br.; C-2), 138.9 (br.; Mes-C-*i*), 138.5 (Mes-C-*o*), 137.9 (C-b/c), 137.9 (C-b/c), 137.5 (Mes-C-*o*), 137.3 (Mes-C-*p*), 137.2 (C-10), 136.2 (Mes-C-*p*), 133.5 (C-8a/10a), 133.3 (C-8a/10a), 133.1 (C-4a/9a), 133.0 (C-4a/9a), 131.6 (C-11a,11a'), 131.6 (C-11), 131.3 (C-15a,15a'), 130.2 (C-9), 129.3 (C-8), 128.5 (C-15,15'), 127.6 (C-5), 127.4 (C-6/16), 127.4 (C-6/16), 127.3 (Mes-CH-*m*), 126.9 (C-7), 126.6 (C-12,12'), 126.2 (Mes-CH-*m*), 125.8 (C-13,13'), 125.1 (C-14,14'), 23.1 (Mes-CH_3-*o*), 22.4 (Mes-CH_3-*o*), 21.5 (Mes-CH_3-*p*), 21.3 ppm (Mes-CH_3-*p*)
^{11}B NMR (96.3 MHz, $CDCl_3$): δ = n. d.
HRMS: Calculated *m*/*z* for $[C_{52}H_{40}B_2Cl_2]^+$: 756.26877, found: 756.26883
UV/Vis (*c*-hexane): λ_{max} (ε) = 367 (12249), 389 (11128), 419 (10243), 445 (17953), 474 nm (28222 $mol^{-1}dm^3cm^{-1}$)
Fluorescence (*c*-hexane, λ_{ex} = 419 nm): λ_{max} = 479, 510, 549 nm (vibrational fine structure); Φ_{PL} = 89%
Cyclic voltammetry (THF, [*n*-Bu_4N][PF_6] 0.1 M, 200 mV s^{-1}, vs. FcH/FcH$^+$): $E_{1/2}$ = −1.75 V

Synthesis of [5]helicene

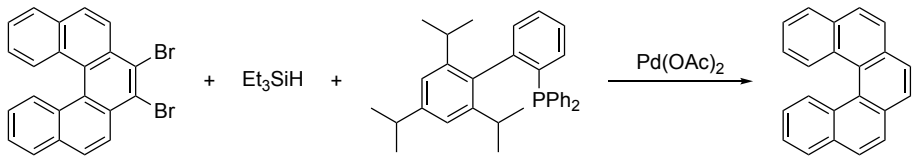

A Schlenk tube was charged with 7,8-dibromo[5]helicene (1.2 g, 2.8 mmol), 2-(2‘,4‘,6‘-triisopropylbiphenyl)diphenylphosphine (0.58 g, 1.2 mmol), and $Pd(OAc)_2$ (0.093 mg, 0.41 mmol) and kept under a dynamic vacuum for 0.5 h. The solids were dissolved in toluene (40 mL; three freeze-pump-thaw cycles) and Et_3SiH (1.2 mL, 7.5 mmol) was added. The reaction mixture was heated to 80 °C for 21 h. After cooling to room temperature, all volatiles were removed from the reaction mixture under reduced pressure and the crude product was purified by flash chromatography (silica gel, *c*-hexane, R_f = 0.76) to give [5]helicene as a pale yellow solid. Yield: 0.686 g (2.46 mmol, 89%). Single crystals were obtained by slow evaporation of a solution of [5]helicene in $CHCl_3$.

The ^{1}H chemical shifts are in agreement with published values.[S17]

Synthesis of 8^{BMes}

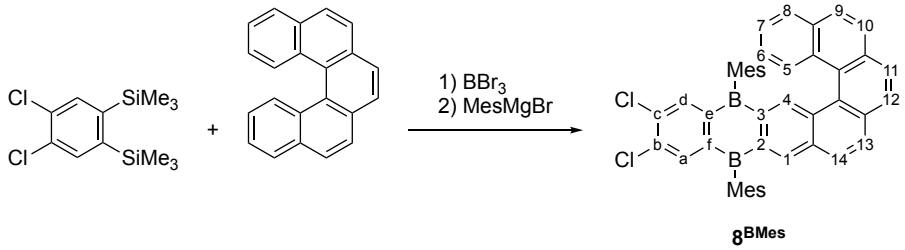

8^{BMes}

The synthesis was performed according to the general procedure described above using 4,5-dichloro-1,2-bis(trimethylsilyl)benzene (0.30 g, 1.0 mmol), [5]helicene (0.56 g, 2.0 mmol), BBr_3 (0.35 mL, 0.92 g, 3.7 mmol), *n*-hexane (6.5 mL), and MesMgBr in THF (0.79 M, 2.8 mL, 2.2 mmol). The purification of the crude product by flash chromatography (*c*-hexane to *c*-hexane:EtOAc = 92:8, R_f = 0.29) afforded $\mathbf{8^{BMes}}$ as an orange solid. Yield: 0.20 g (0.29 mmol, 29%). Single crystals were obtained by slow evaporation of a solution of $\mathbf{8^{BMes}}$ in toluene.

^{1}H NMR (600.3 MHz, $CDCl_3$): δ = 8.69 (s, 1H; H-1/4), 8.36 (d, ^3J(H,H) = 8.5 Hz, 1H; H-5/8), 8.24 (s, 1H; H-1/4), 7.92 (d, ^3J(H,H) = 8.5 Hz, 1H), 7.88 (d, ^3J(H,H) = 8.5 Hz, 1H), *7.86* (d, ^3J(H,H) = 8.0 Hz, 1H), **7.84** (d, ^3J(H,H) = 8.0 Hz, 1H), *7.81* (d, ^3J(H,H) = 8.0 Hz, 1H), 7.80 (d, ^3J(H,H) = 8.0 Hz, 1H, H-5/8), **7.78** (d, ^3J(H,H) = 8.0 Hz, 1H), 7.68 (s, 1H; H-a/d), 7.64 (s, 1H; H-a/d), 7.39 (ddd, ^3J(H,H) = 6.8 Hz, ^3J(H,H) = 8.4 Hz, ^4J(H,H) = 1.2 Hz, 1H; H-6/7), 7.15 (ddd, ^3J(H,H) = 6.8 Hz, ^3J(H,H) = 8.4 Hz, ^4J(H,H) = 1.2 Hz, 1H; H-6/7), 7.04 (s, 1H; Mes-CH-*m*), 7.01 (s, 1H; Mes-CH-*m*), 6.67 (s, 1H; Mes-CH-*m*), 6.46 (s, 1H; Mes-CH-*m*), 2.48 (s, 3H; Mes-CH_3-*p*), 2.27 (s, 3H; Mes-CH_3-*p*), 2.25 (s, 3H; Mes-CH_3-*o*), 2.12 (s, 3H; Mes-CH_3-*o*), 2.04 (s, 3H; Mes-CH_3-*o*), 1.56 ppm (s, 3H; Mes-CH_3-*o*)

^{13}C{^{1}H} NMR (151.0 MHz, $CDCl_3$): δ = 146.2* (br.; C-e/f), 145.8* (br.; C-e/f), 141.8 (C-1/4), 141.7 (C-1/4), 140.8* (br.; C-2/3), 140.3 (C-a/d), 140.2 (C-a/d), 140.1* (br.; Mes-C-*i*), 139.5* (br.; C-Mes-C-*i*), 139.5* (br.; C-2/3), 138.4 (Mes-C-*o*), 138.4 (Mes-C-*o*), 138.1 (C-b/c), 137.9 (C-b/c), 137.4 (Mes-C-*o*), 137.3 (Mes-C-*o*), 137.3, 136.5 (Mes-C-*p*), 135.5, 134.4, 133.7, 132.5, 132.4, 130.9, 129.1, 128.6, 128.5, 128.4, 128.3, 128.2, 127.8 (C-5/8), 127.5, 127.4, 127.3, 127.2, 127.0 (C-5/8), 126.7 (C-6/7), 126.5 (Mes-CH-*m*), 125.8, 125.3 (C-6/7), 23.7 (Mes-CH_3-*o*), 23.1 (Mes-CH_3-*o*), 22.9 (Mes-CH_3-*o*), 22.5 (Mes-CH_3-*o*), 21.5 (Mes-CH_3-*p*), 21.3 ppm (Mes-CH_3-*p*); *unequivocally detected only in the ^{H,C}HMBC spectrum

The six ^{1}H signals marked in orange correspond to H-9–H-14; individual pairs have been formatted in the same way (i.e., plain, boldface, italic); the one ^{13}C signal marked in orange corresponds to one of the C atoms C-9–C-14. The four ^{13}C signals marked in green correspond to Mes-C-*p*, Mes-CH-*m* (2×), Mes-CH-*m*. In all these cases, extensively overlapping cross peaks in the 2D NMR spectra precluded unequivocal assignments.

Note: There is no free rotation about the B–C(Mes) bonds. The following connectivity applies for the terminal phenylene ring: 8.36(127.8)–7.15(125.3)–7.39(126.7)–7.80(127.0).

^{11}B NMR (160.5 MHz, $CDCl_3$): δ = 73 ppm ($h_{1/2} \approx 2400$ Hz)
HRMS: Calculated m/z for $[C_{46}H_{36}B_2Cl_2]^+$: 680.23747, found: 680.23759
UV/Vis (*c*-hexane): λ_{max} (ε) = 376 (11977), 404 (5262), 427 (7236), 452 nm (11056 $mol^{-1}dm^3cm^{-1}$)
Fluorescence (*c*-hexane, λ_{ex} = 376 nm): λ_{max} = 461, 489, 521 nm (vibrational fine structure); Φ_{PL} = 46%
Cyclic voltammetry (THF, [*n*-Bu_4N][PF_6] 0.1 M, 200 mV s^{-1}, vs. FcH/FcH^+): $E_{1/2}$ = −1.92 V

8. Plots of ^{1}H, $^{13}C\{^{1}H\}$, and ^{11}B spectra for the *ortho*-diborylated PAH derivatives

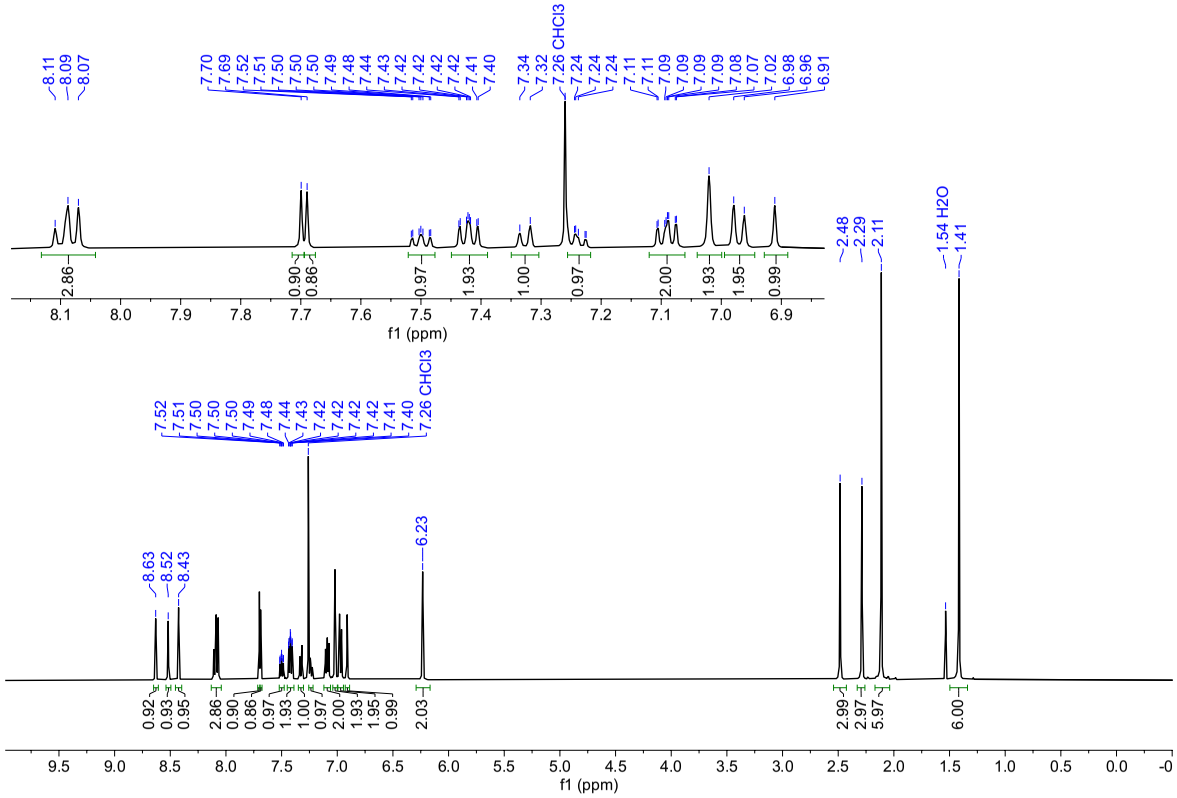

Figure S32: ^{1}H NMR spectrum of $\mathbf{4^{BMes}}$ ($CDCl_3$, 500.2 MHz).

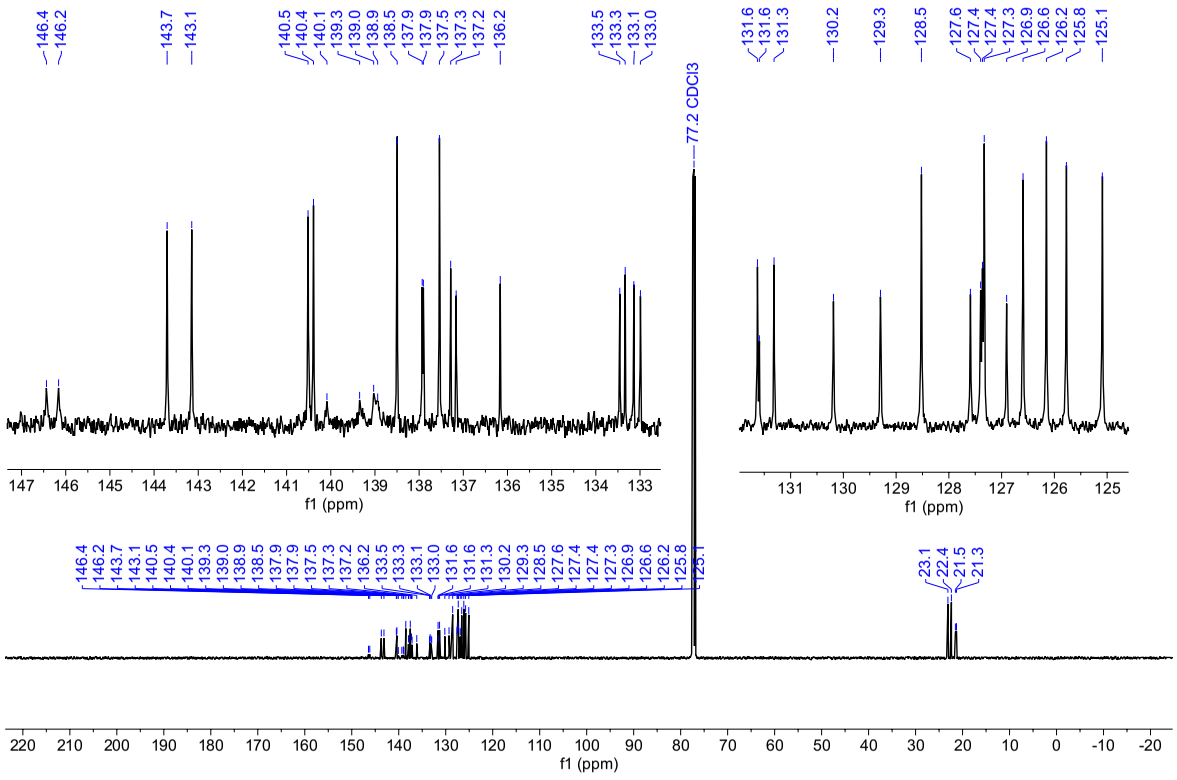

Figure S33: $^{13}C\{^{1}H\}$ NMR spectrum of $\mathbf{4^{BMes}}$ ($CDCl_3$, 125.8 MHz).

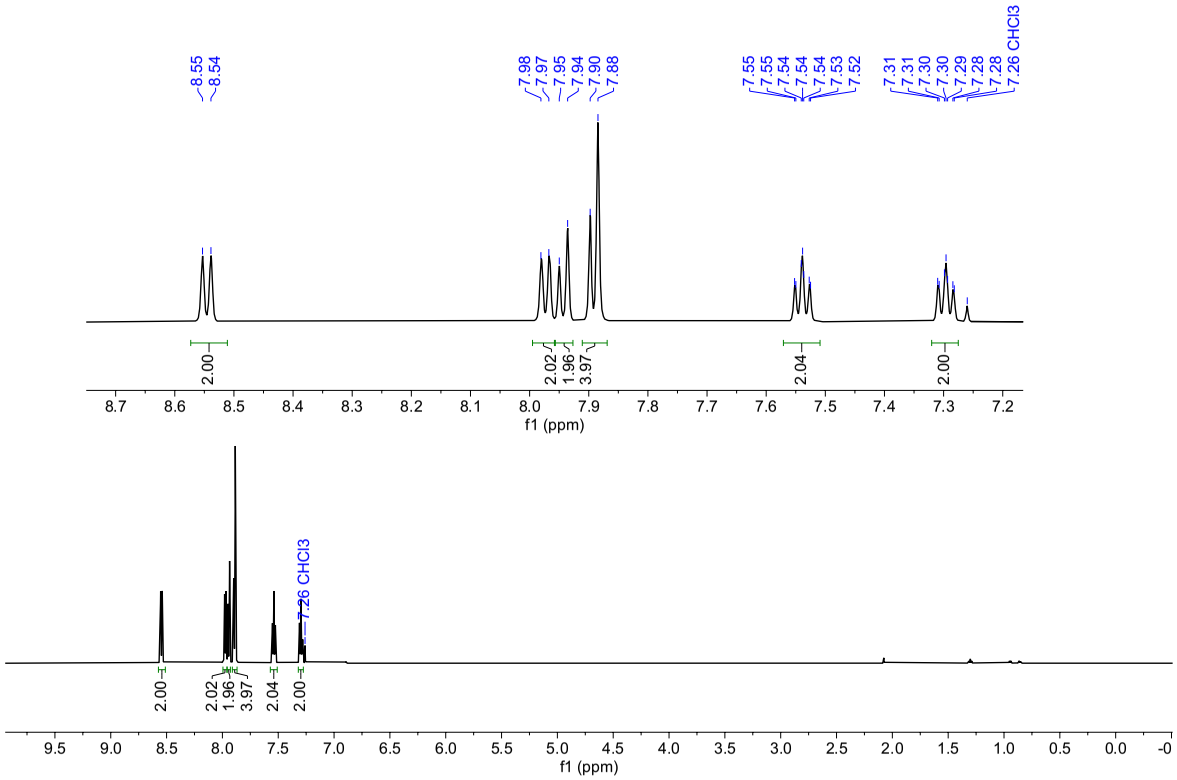

Figure S34: ^{1}H NMR spectrum of [5]helicene ($CDCl_3$, 600.3 MHz).

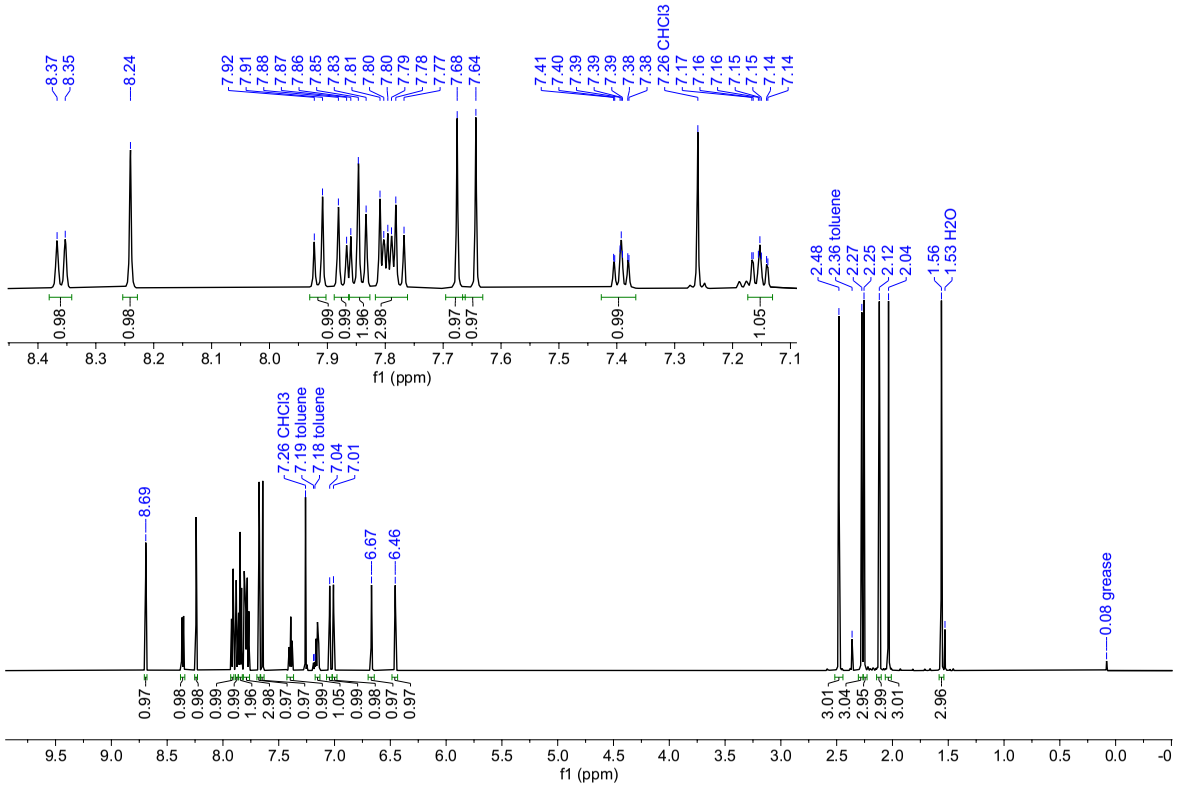

Figure S35: ^{1}H NMR spectrum of **8**$^{\mathbf{BMes}}$ ($CDCl_3$, 600.3 MHz).

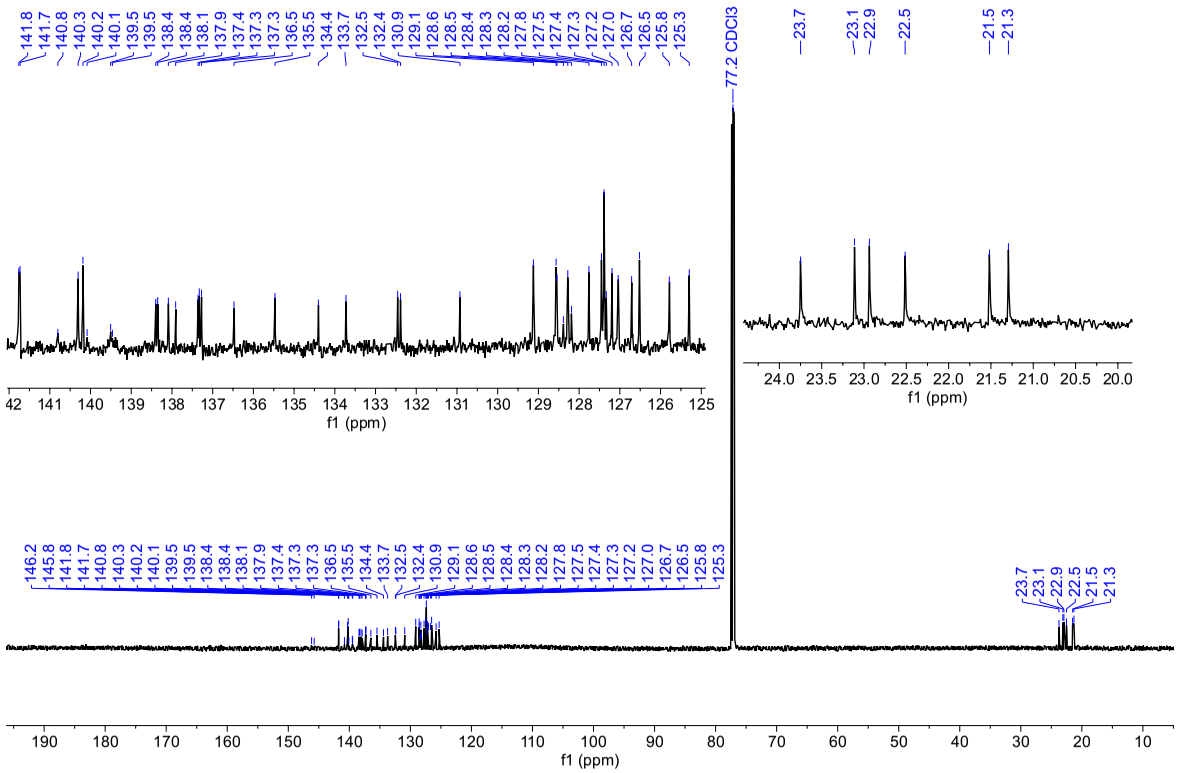

Figure S36: $^{13}C\{^{1}H\}$ NMR spectrum of **8^{BMes}** ($CDCl_3$, 151.0 MHz).

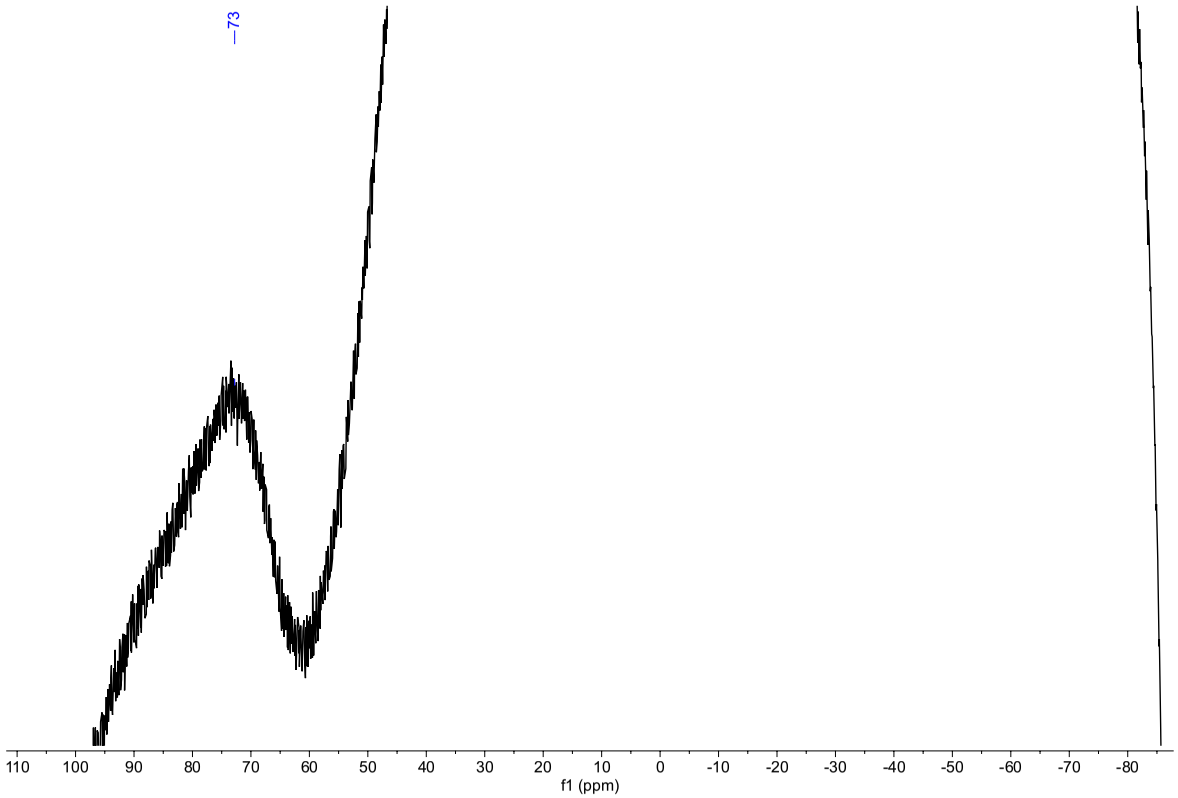

Figure S37: ^{11}B NMR spectrum of **8^{BMes}** ($CDCl_3$, 160.5 MHz).

9. Photophysical and electrochemical data for the *ortho*-diborylated PAH dervatives

Table S2: Photophysical and electrochemical data of the compounds **4**$^{\mathbf{BMes}}$ and **8**$^{\mathbf{BMes}}$. Optical measurements were performed in *c*-hexane, and electrochemical measurements were performed in THF.

	λ_{abs} [nm][a] (ε [M^{-1} cm^{-1}])	λ_{onset} [nm][b]	λ_{ex} [nm]	λ_{em} [nm][a]	Φ_{PL} [%][c]	Stokes shift [cm^{-1}][d]	E_{HOMO}/ E_{LUMO} [eV][e]	$E_{1/2}$ [V]	E_G^{opt} [eV][f]
4$^{\mathbf{BMes}}$	367 (12249) 389 (11128) 419 (10243) 445 (17953) 474 (28222)	482	419	479 510 549	89	220	–3.05/ –5.62	–1.75	2.57
8$^{\mathbf{BMes}}$	376 (11977) 404 (5262) 427 (7236) 452 (11056)	462	376	461 489 521	46	432	–2.88/ –5.56	–1.92	2.68

[a] Resolved vibrational fine structure. [b] Each onset wavelength (λ_{onset}) was determined by constructing a tangent on the point of inflection of the bathochromic slope of the most red-shifted absorption maximum. [c] Quantum yields were determined by using a calibrated integrating sphere. [d] Stokes shifts represent the difference between each longest-wavelength absorption maximum and the corresponding shortest-wavelength emission maximum. [e] $E_{HOMO} = E_{LUMO} - E_G^{opt}$, $E_{LUMO} = -4.8\ eV - E_{1/2}^{Red1}$ ($FcH/FcH^+ = -4.8$ eV vs vacuum level). [f] Optical band gap $E_G^{opt} = 1240/\lambda_{onset}$.

9.1. UV/Vis absorption and emission spectra

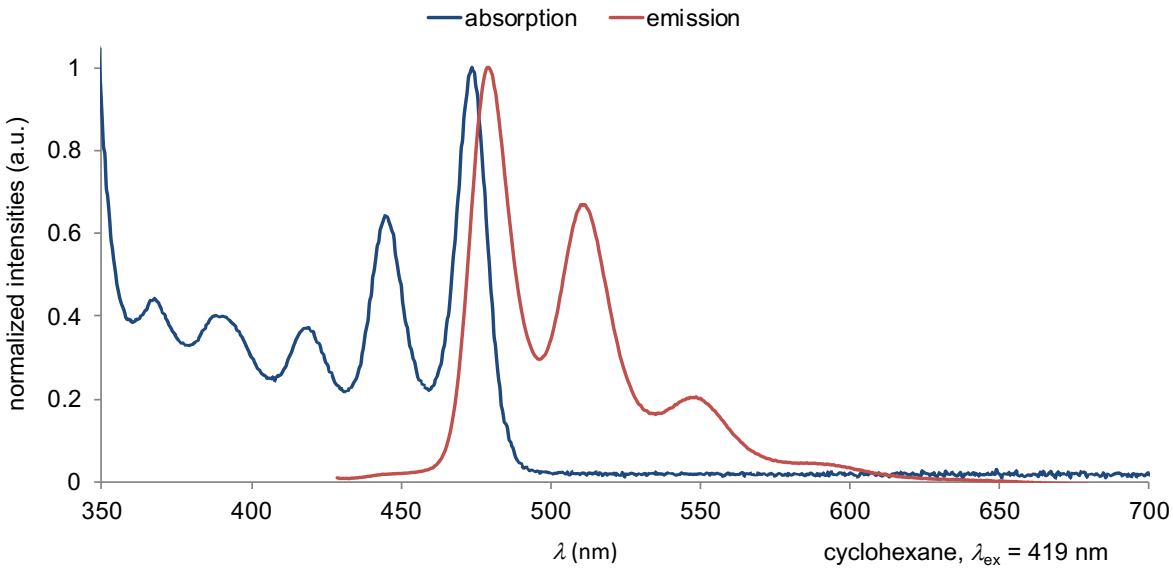

Figure S38: Normalized UV/Vis absorption and emission spectra of $\mathbf{4}^{\mathbf{BMes}}$.

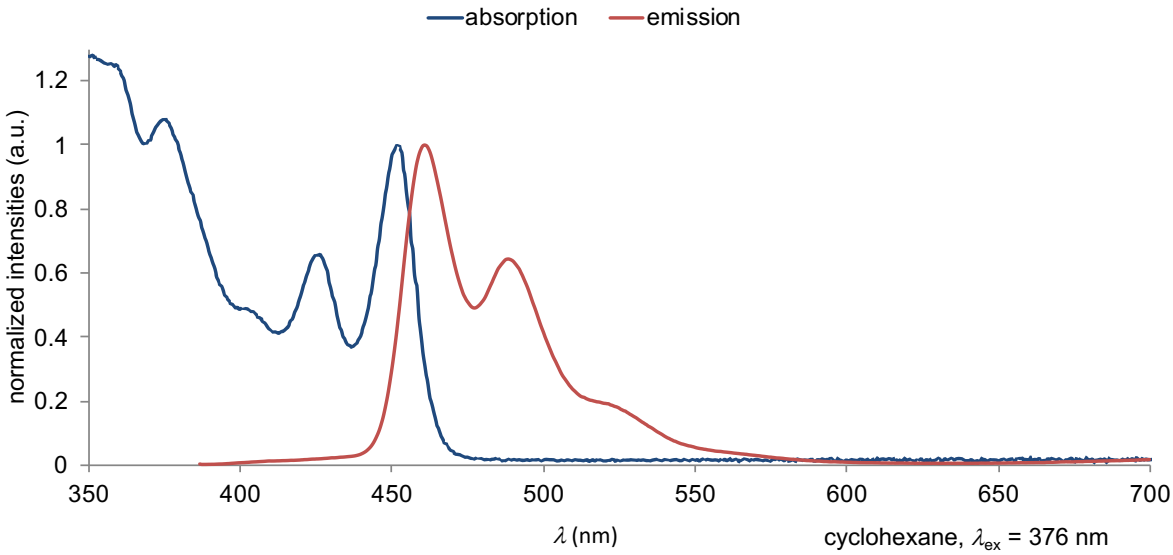

Figure S39: Normalized UV/Vis absorption and emission spectra of $\mathbf{8}^{\mathbf{BMes}}$.

9.2. Plots of cyclic voltammograms

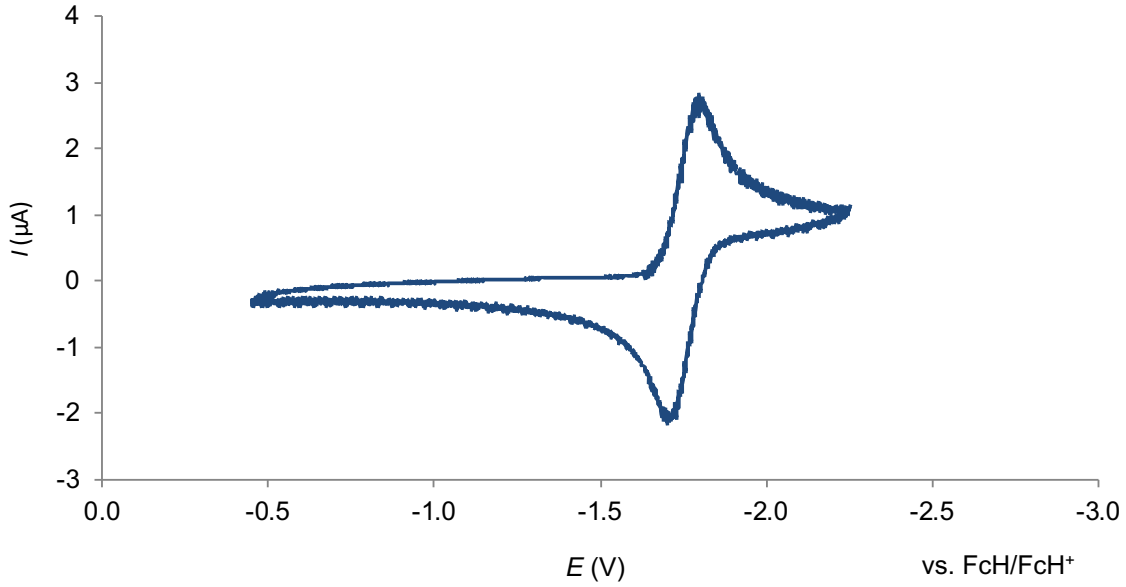

Figure S40: Cyclic voltammogram of **4**^{BMes} in THF (room temperature, supporting electrolyte: [*n*-Bu_4N][PF_6] (0.1 M), scan rate 200 mV s^{-1}.

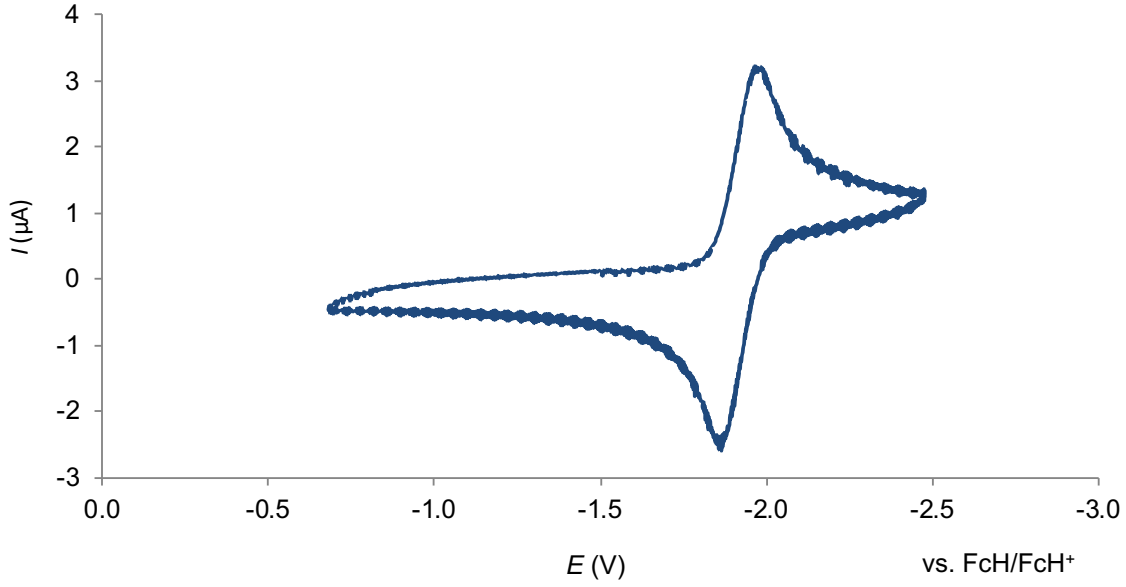

Figure S41: Cyclic voltammogram of **8**^{BMes} in THF (room temperature, supporting electrolyte: [*n*-Bu_4N][PF_6] (0.1 M), scan rate 200 mV s^{-1}.

10. X-ray crystal structure analyses

Data for all structures were collected on a STOE IPDS II two-circle diffractometer with a Genix Microfocus tube with mirror optics using MoK_α radiation (λ = 0.71073 Å) and scaled using the frame-scaling procedure in the *X-AREA*[S18] program system. The structures were solved by direct methods using the program *SHELXS*[S19] and refined against F^2 with full-matrix least-squares techniques using the program *SHELXL-97*.[S19]

1,2-dichloro-4,5-diiodobenzene (CCDC 2007111) is twinned with a fractional contribution of 0.1016(5) of the minor domain. It crystallizes with two crystallographically independent, albeit almost identical, molecules, 1,2-dichloro-4,5-diiodobenzene$^{\mathbf{A}}$ and 1,2-dichloro-4,5-diiodobenzene$^{\mathbf{B}}$, in the asymmetric unit (only 1,2-dichloro-4,5-diiodobenzene$_{\mathbf{A}}$ is shown in Figure S42).

3$^{\mathbf{I}}$ (CCDC 2007112) crystallizes with one molecule of $CHCl_3$ in the asymmetric unit.

The compound **4$^{\mathbf{I}}$** (CCDC 2007113) requires no special comments.

For **5$^{\mathbf{I}}$** (CCDC 2007114), the absolute structure was determined. The Flack-x-parameter refined to 0.09(5).

6$^{\mathbf{I}}$ (CCDC 2007115) is twinned with a fractional contribution of 0.4649(14) of the minor domain.

The compound **7$^{\mathbf{I}}$** (CCDC 2007116) requires no special comments.

8$^{\mathbf{I}}$ (CCDC 2007117) is twinned with a fractional contribution of 0.179(3) of the minor domain. It crystallizes with four almost identical molecules in the asymmetric unit (**8$^{\mathbf{I}}_{\mathbf{A}}$** – **8$^{\mathbf{I}}_{\mathbf{D}}$**; only **8$^{\mathbf{I}}_{\mathbf{A}}$** is shown in Figure S48). Bond lengths and angles of the four molecules were restrained to be equal. The displacement ellipsoids of the C atoms were restrained to an isotropic behavior.

The compound **7$^{\mathbf{CCPh}}$** (CCDC 2007118) requires no special comments.

4,5-dichlorocatechol (CCDC 2007119) is twinned with a fractional contribution of 0.454(2) of the minor domain. It crystallizes with three almost identical molecules in the asymmetric unit which differ only in the torsion angles about the C–O bonds (4,5-dichlorocatechol$^{\mathbf{A}}$ – 4,5-dichlorocatechol$^{\mathbf{C}}$; only 4,5-dichlorocatechol$^{\mathbf{A}}$ is shown in Figure S50). The coordinates of the hydroxyl H atoms were refined with the O–H distances restrained to 0.84(1) Å. The U(H) values were set to 1.5 Ueq(O).
Two of the three molecules in the asymmetric unit form centrosymmetric dimers (4,5-dichlorocatechol$^{\mathbf{A}}$ and 4,5-dichlorocatechol$^{\mathbf{B}}$) whereas the third one connects these dimers to a three-dimensional network. The dimers show π-stacking with centroid-to-centroid distances of 3.709 Å and 3.741 Å.

1$^{\mathbf{OH}}$ (CCDC 2007120) crystallizes with two almost identical molecules in the asymmetric unit which differ only in the torsion angles about the C–O bonds (**1$^{\mathbf{OH}}_{\mathbf{A}}$** and **1$^{\mathbf{OH}}_{\mathbf{B}}$**; only **1$^{\mathbf{OH}}_{\mathbf{A}}$** is shown in Figure S51). The hydroxyl H atoms were freely refined. The H atoms of two hydroxyl groups are disordered over two equally occupied positions.
The two molecules in the asymmetric unit form dimers which are connected by O–H···O and O–H···π contacts to double chains running along the b axis. There is no π-stacking in the structure.
The orthorhombic polymorph of **1$^{\mathbf{OH}}$**[S20], shows a very similar crystal packing. There are dimers of symmetry-equivalent molecules forming double chains connected by O–H···O and O-H···π contacts running along the a axis.

The compound **4$^{\mathbf{BBr}}$** (CCDC 2007121) requires no special comments.

The molecules of [5]helicene (CCDC 2007122) are located on a two-fold rotation axis.

8^{BMes} (CCDC 2007123) is twinned with a fractional contribution of 0.3967(17) of the minor domain.

CCDC files 1,2-dichloro-4,5-diiodobenzene–**8**^{BMes} (CCDC 2007111–CCDC 2007123) contain the supplementary crystallographic data for this paper and can be obtained free of charge from The Cambridge Crystallographic Data Centre via www.ccdc.cam.ac.uk/data_request/cif.

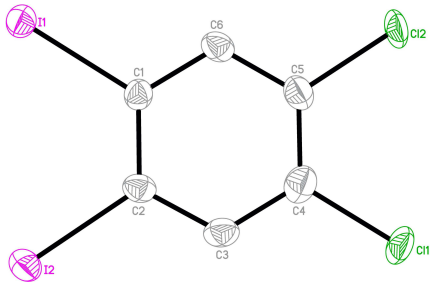

Figure S42 (CCDC 2007111): Molecular structure of 1,2-dichloro-4,5-diiodobenzene[A] in the solid state. Displacement ellipsoids are drawn at the 50% probability level; hydrogen atoms are omitted for clarity. Selected bond lengths (Å), bond angles (°), and torsion angles (°): I1–C1 = 2.085(5), I2–C2 = 2.077(6), Cl1–C4 = 1.765(6), Cl2–C5 = 1.758(6); I1–C1–C2 = 122.7(4), I1–C1–C6 = 117.1(4), C2–C1–C6 = 120.2(5), I2–C2–C1 = 123.2(4), I2–C2–C3 = 117.8(4), C1–C2–C3 = 119.0; I1–C1–C2–I2 = 0-7(7), Cl1–C4–C5–Cl2 = –0.8(8).

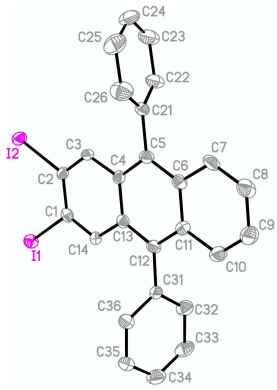

Figure S43 (CCDC 2007112): Molecular structure of **3**[I] in the solid state. Displacement ellipsoids are drawn at the 50% probability level; hydrogen atoms and $CHCl_3$ are omitted for clarity. Selected bond lengths (Å), bond angles (°), and torsion angles (°): I1–C1 = 2.095(5), I2–C2 = 2.093(5), C5–C21 = 1.494(7), C12–C31 = 1.491(7); I1–C1–C2 = 120.9(4), I1–C1–C14 = 119.3(4), C2–C1–C14 = 119.7(4), I2–C2–C1 = 122.0(4), I2–C2–C3 = 117.8(4), C1–C2–C3 = 120.2(5), C4–C5–C6 = 119.3(5), C11–C12–C13 = 119.4(5); I1–C1–C2–I2 = 0.7(6), C4–C5–C21–C22 = –72.8(7), C13–C12–C31–C32 = 101.6(6).

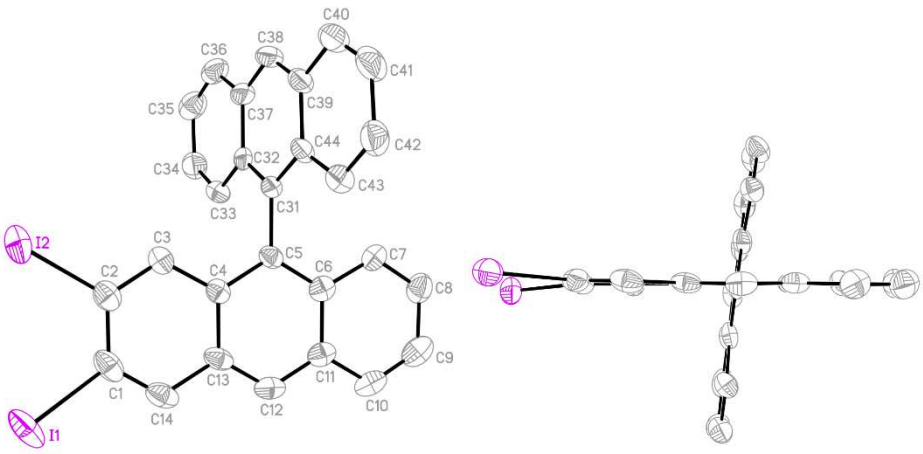

Figure S44 (CCDC 2007113): Molecular structure of **4**[I] in the solid state. Displacement ellipsoids are drawn at the 50% probability level; hydrogen atoms are omitted for clarity. Selected bond lengths (Å), bond angles (°), and torsion angles (°): I1–C1 = 2.103(6), I2–C2 = 2.104(7), C5–C31 = 1.504(8); I1–C1–C2 = 122.8(5), I1–C1–C14 = 116.7(5), C2–C1–C14 = 120.5(6), I2–C2–C1 = 121.3(5), I2–C2–C3 = 118.2(5), C1–C2–C3 = 120.4(6); I1–C1–C2–I2 = –7.4(7), C4–C5–C31–C32 = –81.8(7).

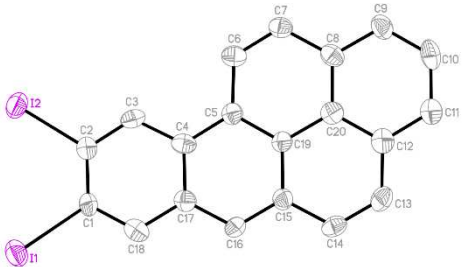

Figure S45 (CCDC 2007114): Molecular structure of **5^{I}** in the solid state. Displacement ellipsoids are drawn at the 50% probability level; hydrogen atoms are omitted for clarity. Selected bond lengths (Å), bond angles (°), and torsion angles (°): I1–C1 = 2.109(11), I2–C2 = 2.109(12); I1–C1–C2 = 122.3(9), I1–C1–C18 = 117.4(9), C2–C1–C18 = 120.2(11), I2–C2–C1 = 123.3(8), I2–C2–C3 = 116.4(9), C1–C2–C3 = 120.2(11); I1–C1–C2–I2 = –9.7(14).

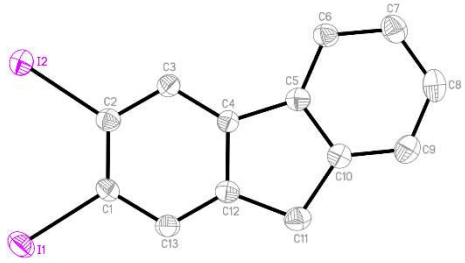

Figure S46 (CCDC 2007115): Molecular structure of **6^{I}** in the solid state. Displacement ellipsoids are drawn at the 50% probability level; hydrogen atoms are omitted for clarity. Selected bond lengths (Å), bond angles (°), and torsion angles (°): I1–C1 = 2.091(4), I2–C2 = 2.094(5); I1–C1–C2 = 123.0(3), I1–C1–C13 = 116.9(3), C2–C1–C13 = 120.1(4), I2–C2–C1 = 122.7(3), I2–C2–C3 = 117.0(3), C1–C2–C3 = 120.3(4), C10–C11–C12 = 103.0(4); I1–C1–C2–I2 = 1.2(5).

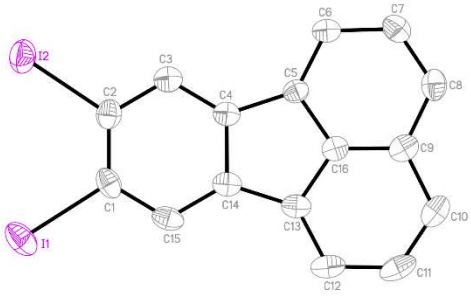

Figure S47 (CCDC 2007116): Molecular structure of **7^{I}** in the solid state. Displacement ellipsoids are drawn at the 50% probability level; hydrogen atoms are omitted for clarity. Selected bond lengths (Å), bond angles (°), and torsion angles (°): I1–C1 = 2.102(4), I2–C2 = 2.102(4); I1–C1–C2 = 122.5(3), I1–C1–C15 = 116.3(3), C2–C1–C15 = 121.1(3), I2–C2–C1 = 123.9(3), I2–C2–C3 = 115.7(3), C1–C2–C3 = 120.5(4), C5–C16–C13 = 111.4(3); I1–C1–C2–I2 = –0.6(5).

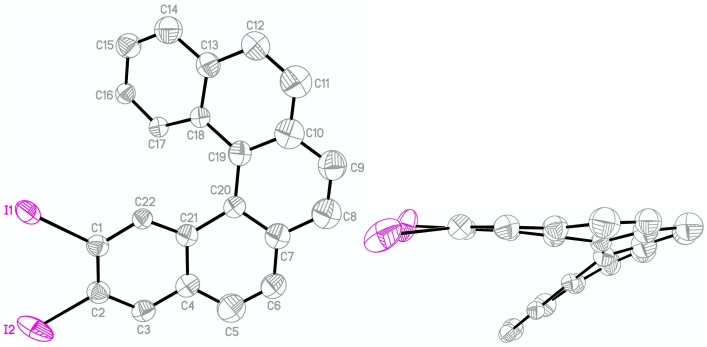

Figure S48 (CCDC 2007117): Molecular structure of $\mathbf{8^{I}_{A}}$ in the solid state. Displacement ellipsoids are drawn at the 50% probability level; hydrogen atoms are omitted for clarity. Selected bond lengths (Å), bond angles (°), and torsion angles (°): I1–C1 = 2.08(3), I2–C2 = 2.10(3), C16–C17 = 1.36(3); I1–C1–C2 = 122(2), I1–C1–C22 = 117.1(19), C2–C1–C22 = 121(3), I2–C2–C1 = 124(2), I2–C2–C3 = 117(2), C1–C2–C3 = 118(2), H16–C16–C17 = 119.5; I1–C1–C2–I2 = 13(5), C18–C19–C20–C21 = –25(6).

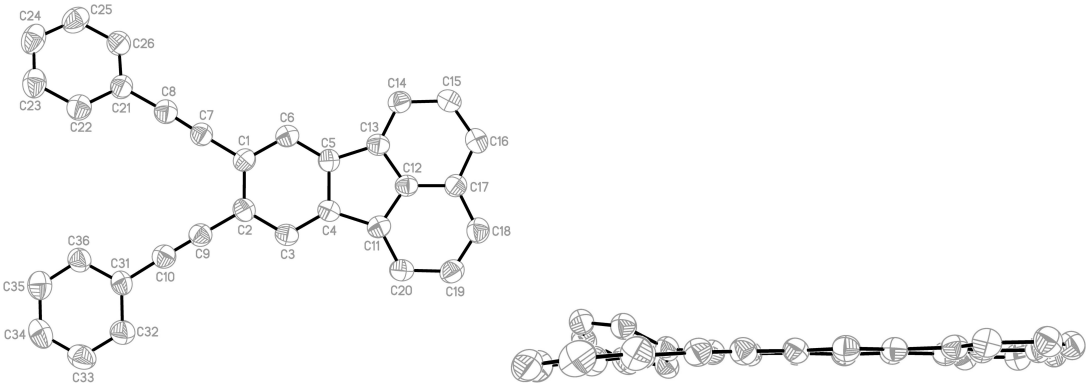

Figure S49 (CCDC 2007118): Molecular structure of $\mathbf{7^{CCPh}}$ in the solid state. Displacement ellipsoids are drawn at the 50% probability level; hydrogen atoms are omitted for clarity. Selected bond lengths (Å), bond angles (°), and torsion angles (°): C1–C7 = 1.423(4), C7–C8 = 1.199(4), C2–C9 = 1.431(4), C9–C10 = 1.202(4); C1–C7–C8 = 177.3(3), C2–C9–C10 = 179.2(3), C11–C12–C13 = 11.6(3); C7–C1–C2–C9 = 2.7(4).

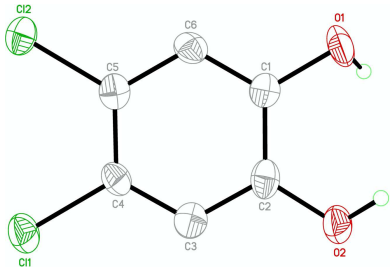

Figure S50 (CCDC 2007119): Molecular structure of 4,5-dichlorocatechol^{A} in the solid state. Displacement ellipsoids are drawn at the 50% probability level. Selected bond lengths (Å), bond angles (°), and torsion angles (°): Cl1–C4 = 1.728(9), Cl2–C5 = 1.728(9), O1–C1 = 1.385(11), O2–C2 = 1.366(12); Cl1–C4–C3 = 120.5(8), Cl1–C4–C5 = 119.3(7), C3–C4–C5 = 120.2(8), Cl2–C5–C4 = 121.8(7), Cl2–C5–C6 = 119.6(8), C4–C5–C6 = 118.6(8), O1–C1–C2 = 119.9(8), O1–C1–C6 = 119.9(9), C2–C1–C6 = 120.1(9), O2–C2–C1 = 122.4(8), O2–C2–C3 = 118.8(9), C1–C2–C3 = 118.8(9); Cl1–C4–C5–Cl2 = 0.4(11), O1–C1–C2–O2 = –3.7(14).

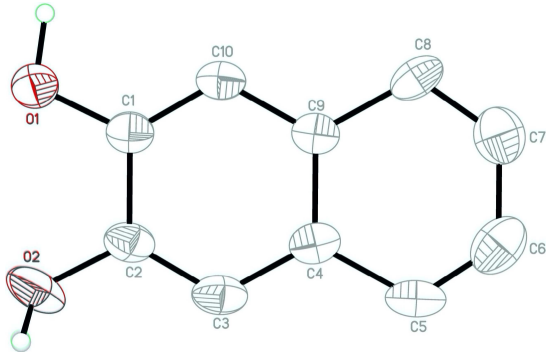

Figure S51 (CCDC 2007120): Molecular structure of $\mathbf{1}^{\mathbf{OH}}_{\mathbf{A}}$ in the solid state. Displacement ellipsoids are drawn at the 50% probability level. Selected bond lengths (Å), bond angles (°), and torsion angles (°): O1–C1 = 1.369(3), O2–C2 = 1.364(3); O1–C1–C2 = 115.7(2), O1–C1–C10 = 124.1(2), C2–C1–C10 = 120.2(2), O2–C2–C1 = 117.5(2), O2–C2–C3 = 122.4(2), C1–C2–C3 = 120.1(2); O1–C1–C2–O2 = 0.2(3).

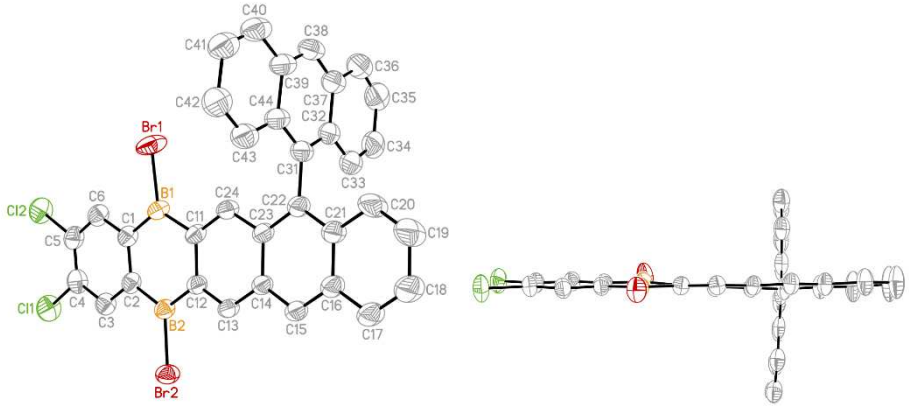

Figure S52 (CCDC 2007121): Molecular structure of **4**^{BBr} in the solid state. Displacement ellipsoids are drawn at the 50% probability level; hydrogen atoms are omitted for clarity. Selected bond lengths (Å), bond angles (°), and torsion angles (°): Br1–B1 = 1.929(4), Cl2–C5 = 1.732(3), B1–C11 = 1.547(4), C22–C31 = 1.505(4); C11–B1–C1 = 122.1(3), C11–B1–Br1 = 119.9(2), C23–C22–C31 = 121.0(3), C21–C22–C31 = 119.4(3); Br1–B1–C1–C6 = 2.5(4), C23–C22–C31–C44 = 93.9(4), C21–C22–C31–C44 = –86.4(4).

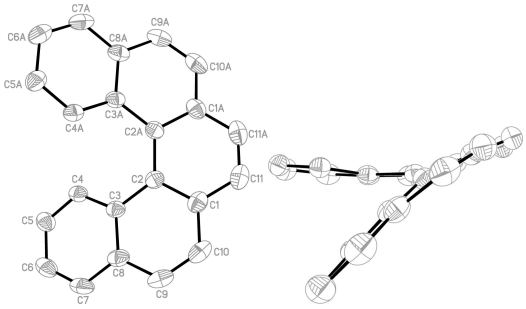

Figure S53 (CCDC 2007122): Molecular structure of [5]helicene in the solid state. Displacement ellipsoids are drawn at the 50% probability level; hydrogen atoms are omitted for clarity. Selected bond lengths (Å), bond angles (°), and torsion angles (°): C4–C5 = 1.371(2); C(4)–C(5)–H(5) = 119.6; C3–C2–C2A–C3A = 32.3(3).

Symmetry transformation used to generate equivalent atoms: –x+1, y, –z+$\frac{1}{2}$.

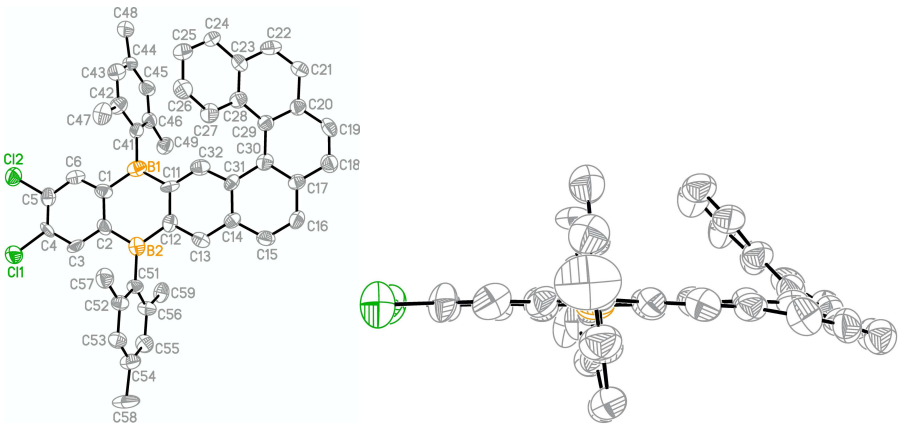

Figure S54 (CCDC 2007123): Molecular structure of **8**^{BMes} in the solid state. Displacement ellipsoids are drawn at the 50% probability level; hydrogen atoms are omitted for clarity. Selected bond lengths (Å), bond angles (°), and torsion angles (°): B1–C41 = 1.553(12), B1–C11 = 1.555(13), B1–C1 = 1.601(14), Cl2–C5 = 1.768(9), C26–C27 = 1.367(11); C41–B1–C11 = 122.5(10), C27–C26–H26 = 120.0; C28–C29–C30–C31 = 29.2(15).

Table S3: Selected crystallographic data for 1,2-dichloro-4,5-diiodobenzene–**4^{I}**.

compound	1,2-dichloro-4,5-diiodobenzene	**3^{I}**	**4^{I}**
CCDC	CCDC 2007111	CCDC 2007112	CCDC 2007113
formula	$C_6H_2Cl_2I_2$	$C_{27}H_{17}Cl_3I_2$	$C_{28}H_{16}I_2$
M_r	398.78	701.56	606.21
T (K)	173(2)	173(2)	173(2)
radiation, λ (Å)	0.71073	0.71073	0.71073
crystal system	Triclinic	Monoclinic	Orthorhombic
space group	$P\,\bar{1}$	$P\,2_1/c$	*Pbca*
a [Å]	4.1228(3)	16.1596(5)	13.8238(7)
b [Å]	14.9556(9)	13.7549(6)	8.3204(4)
c [Å]	14.9733(10)	11.3277(3)	37.384(2)
α [°]	87.575(5)	90	90
β [°]	82.440(5)	91.143(2)	90
γ [°]	82.169(5)	90	90
V [Å^3]	906.40(11)	2517.35(15)	4299.9(4)
Z	4	4	8
D_{calcd} (g cm^{-3})	2.922	1.851	1.873
μ (mm^{-1})	7.452	2.831	2.938
F(000)	712	1344	2320
crystal size (mm)	0.080 × 0.060 × 0.050	0.080 × 0.050 × 0.030	0.260 × 0.230 × 0.080
Θ [°]	2.745 to 25.904	3.407 to 27.605	1.832 to 25.626
h	–5 to 5	–21 to 21	–16 to 16
k	–18 to 18	–17 to 17	–10 to 10
l	–18 to 18	–12 to 14	–45 to 38
reflections collected	10063	37657	14117
independent reflections	3477	5807	4017
R_{int}	0.0197	0.0519	0.0337
data/restraints/parameters	3477/0/182	5807/0/289	4017/0/271
R_1, wR_2 (I > 2σ(I))	0.0247, 0.0637	0.0524, 0.0868	0.0504, 0.1068
R_1, wR_2 (all data)	0.0274, 0.0647	0.0657, 0.0906	0.0603, 0.1110
Goodness-of-fit an F^2	1.026	1.244	1.185
largest diff. peak and hole (e Å^{-3})	1.105 and –0.808	1.192 and –1.047	0.788 and –0.844

Table S4: Selected crystallographic data for **5ᴵ–7ᴵ**.

compound	**5ᴵ**	**6ᴵ**	**7ᴵ**
CCDC	CCDC 2007114	CCDC 2007115	CCDC 2007116
formula	$C_{20}H_{10}I_2$	$C_{13}H_8I_2$	$C_{16}H_8I_2$
M_r	504.08	417.99	454.02
T (K)	173(2)	173(2)	173(2)
radiation, λ (Å)	0.71073	0.71073	0.71073
crystal system	Monoclinic	Monoclinic	Orthorhombic
space group	$P\,2_1$	$P\,2_1/c$	*Pbca*
a [Å]	4.5337(3)	12.0564(10)	12.7112(4)
b [Å]	21.5636(9)	11.6647(7)	8.5379(4)
c [Å]	8.0111(5)	8.4160(8)	24.7869(8)
α [°]	90	90	90
β [°]	104.536(5)	99.777(7)	90
γ [°]	90	90	90
V [Å^3]	758.12(8)	1166.39(16)	2690.05(17)
Z	2	4	8
D_{calcd} (g cm^{-3})	2.208	2.380	2.242
μ (mm^{-1})	4.141	5.355	4.654
F(000)	472	768	1680
crystal size (mm)	0.130 × 0.020 × 0.020	0.070 × 0.060 × 0.030	0.190 × 0.090 × 0.020
Θ [°]	2.627 to 25.897	3.668 to 31.188	2.295 to 25.961
h	–5 to 5	–17 to 17	–15 to 15
k	–26 to 23	–16 to 16	–10 to 10
l	–9 to 9	–12 to 12	–30 to 26
reflections collected	10900	3735	26565
independent reflections	2860	3735	2615
R_{int}	0.0344		0.0358
data/restraints/parameters	2860/1/199	3735/0/137	2615/0/164
R_1, wR_2 (I > 2σ(I))	0.0388, 0.0942	0.0414, 0.1090	0.0302, 0.0788
R_1, wR_2 (all data)	0.0417, 0.0965	0.0455, 0.1114	0.0344, 0.0808
Goodness-of-fit an F^2	1.057	1.073	1.164
largest diff. peak and hole (e Å^{-3})	0.473 and –0.892	2.065 and –2.034	0.971 and –0.503

Table S5: Selected crystallographic data for **8^{I}** and **7^{CCPh}**.

compound	**8^{I}**	**7^{CCPh}**
CCDC	CCDC 2007117	CCDC 2007118
formula	$C_{22}H_{12}I_2$	$C_{32}H_{18}$
M_r	530.12	402.46
T (K)	173(2)	173(2)
radiation, λ (Å)	0.71073	0.71073
crystal system	Monoclinic	Monoclinic
space group	*Pn*	$P2_1/n$
a [Å]	10.9058(5)	13.4695(10)
b [Å]	15.7784(7)	3.8986(2)
c [Å]	20.6207(10)	40.028(3)
α [°]	90	90
β [°]	100.423(4)	97.504(6)
γ [°]	90	90
V [Å^3]	3489.8(3)	2084.0(2)
Z	8	4
D_{calcd} (g cm^{-3})	2.018	1.283
μ (mm^{-1})	3.604	0.073
F(000)	2000	840
crystal size (mm)	0.090 × 0.020 × 0.020	0.230 × 0.130 × 0.020
Θ [°]	3.205 to 25.773	1.544 to 25.027
h	–13 to 13	–16 to 16
k	–19 to 19	–4 to 4
l	–25 to 25	–47 to 47
reflections collected	30194	18819
independent reflections	30194	3698
R_{int}		0.0924
data/restraints/parameters	30194/962/866	3698/0/290
R_1, wR_2 (I > 2σ(I))	0.0900, 0.1699	0.0620, 0.1390
R_1, wR_2 (all data)	0.1418, 0.1951	0.1351, 0.1821
Goodness-of-fit an F^2	1.277	1.005
largest diff. peak and hole (e Å^{-3})	2.731 and –1.959	0.245 and –0.243

Table S6: Selected crystallographic data for 4,5-dichlorocatechol and **1^{OH}**

compound	4,5-dichlorocatechol	**1^{OH}**
CCDC	CCDC 2007119	CCDC 2007120
formula	$C_6H_4Cl_2O_2$	$C_{10}H_8O_2$
M_r	178.99	160.16
T (K)	173(2)	173(2)
radiation, λ (Å)	0.71073	0.71073
crystal system	Triclinic	Triclinic
space group	*P*–1	*P*–1
a [Å]	7.4468(17)	5.7771(6)
b [Å]	12.345(2)	8.2249(9)
c [Å]	12.404(3)	16.3023(19)
α [°]	118.559(15)	75.747(9)
β [°]	94.057(18)	84.933(9)
γ [°]	92.365(17)	87.404(9)
V [Å^3]	995.4(4)	747.62(15)
Z	6	4
D_{calcd} (g cm^{-3})	1.792	1.423
μ (mm^{-1})	0.900	0.099
F(000)	540	336
crystal size (mm)	0.110 × 0.030 × 0.020	0.170 × 0.160 × 0.030
Θ [°]	3.327 to 25.972	3.542 to 25.025
h	–9 to 9	–6 to 6
k	–15 to 15	–9 to 9
l	–14 to 15	–19 to 19
reflections collected	11610	7875
independent reflections	11610	2618
R_{int}		0.0425
data/restraints/parameters	11610/6/290	2618/0/241
R_1, wR_2 (I > 2σ(I))	0.0779, 0.1743	0.0639, 0.1689
R_1, wR_2 (all data)	0.1350, 0.1941	0.0787, 0.1789
Goodness-of-fit an F^2	0.966	1.043
largest diff. peak and hole (*e* Å^{-3})	0.626 and –0.508	0.393 and –0.264

Table S7: Selected crystallographic data for **4**^{BBr} – **8**^{BMes}.

compound	**4**^{BBr}	[5]helicene	**8**^{BMes}
CCDC	CCDC 2007121	CCDC 2007122	CCDC 2007123
formula	$C_{34}H_{18}B_2Br_2Cl_2$	$C_{22}H_{14}$	$C_{46}H_{36}B_2Cl_2$
M_r	678.82	278.33	681.27
T (K)	173(2)	173(2)	173(2)
radiation, λ (Å)	0.71073	0.71073	0.71073
crystal system	Monoclinic	Orthorhombic	Triclinic
space group	*C* 2/*c*	*Pbcn*	*P* –1
a [Å]	27.4413(12)	20.307(3)	8.2050(14)
b [Å]	14.4197(4)	8.9772(10)	9.7845(17)
c [Å]	15.7830(7)	7.7556(9)	22.778(4)
α [°]	90	90	101.999(15)
β [°]	118.344(3)	90	92.852(14)
γ [°]	90	90	90.177(14)
V [Å^3]	5496.5(4)	1413.8(3)	1786.3(6)
Z	8	4	2
D_{calcd} (g cm^{-3})	1.641	1.308	1.267
μ (mm^{-1})	3.169	0.074	0.215
F(000)	2688	584	712
crystal size (mm)	0.220 × 0.180 × 0.090	0.170 × 0.130 × 0.040	0.170 × 0.140 × 0.080
Θ [°]	2.456 to 26.370	3.614 to 25.701	1.830 to 26.252
h	–33 to 34	–24 to 20	–10 to 10
k	–18 to 18	–10 to 10	–12 to 12
l	–19 to 19	–9 to 8	–28 to 28
reflections collected	28675	4047	17343
independent reflections	5598	1324	17343
R_{int}	0.0659	0.0365	
data/restraints/parameters	5598/0/361	1324/0/100	17343/0/458
R_1, wR_2 (I > 2σ(I))	0.0468, 0.1145	0.0411, 0.0913	0.0854, 0.1584
R_1, wR_2 (all data)	0.0583, 0.1215	0.0631, 0.0979	0.2390, 0.1794
Goodness-of-fit an F^2	1.061	0.967	1.031
largest diff. peak and hole (*e* Å^{-3})	0.625 and –0.482	0.136 and –0.131	0.389 and –0.383

11. Reagents, conditions, and overall yields for the literature known syntheses of 1^{Br} and 2^{Br}

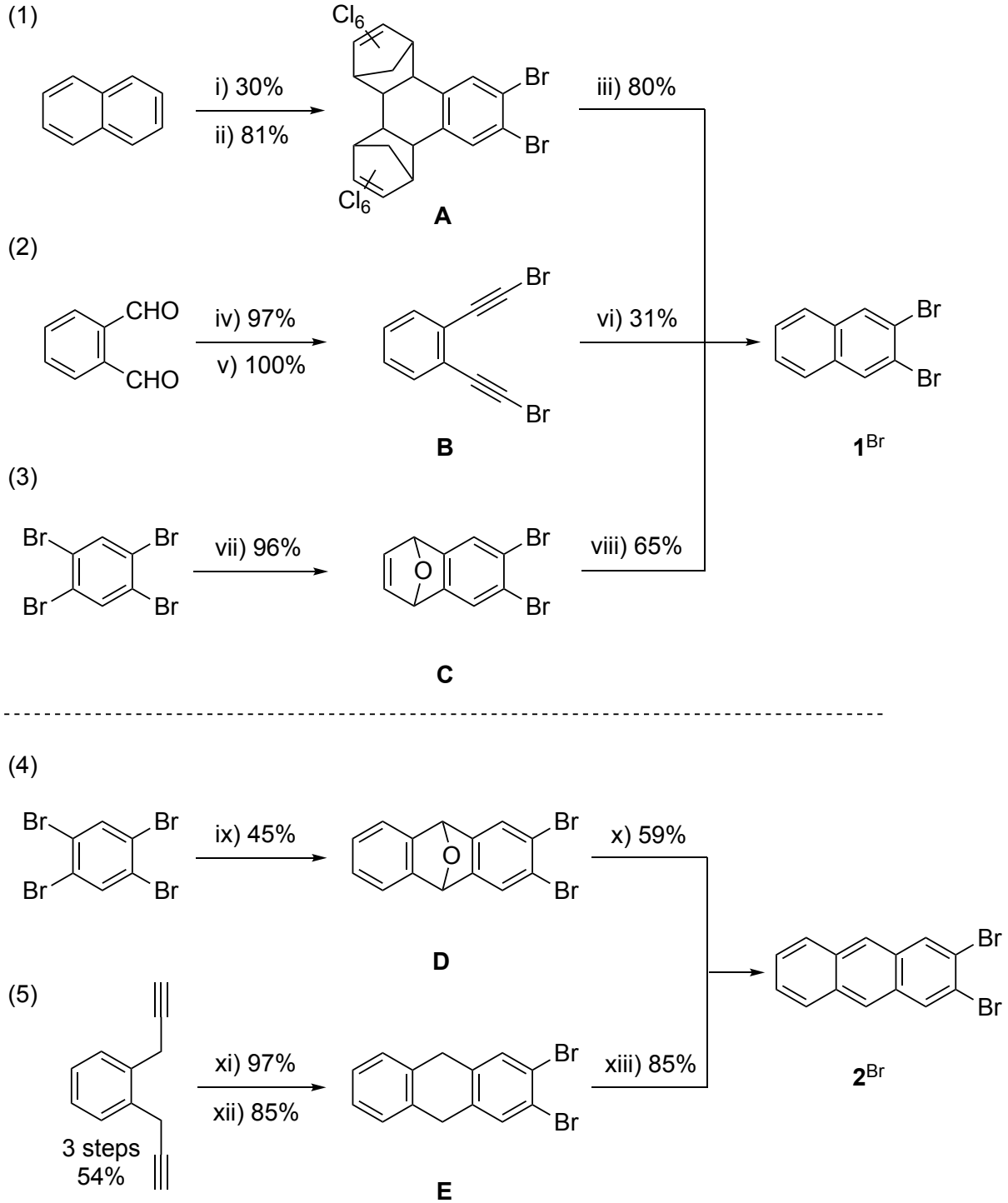

Scheme S1: Syntheses of 2,3-dibromonaphthalene $\mathbf{1^{Br}}$ and 2,3-dibromonanthracene $\mathbf{2^{Br}}$. Reagents and conditions. (1) i) hexachlorocyclopentadien (HCCPD), 160 °C, 120 h. ii) Br_2, Fe, tetrachloroethane, reflux, 3 h. iii) continuous high-vacuum distillation, 220 °C.[S21,S22] (2) iv) CBr_4, PPh_3, DCM, 0 °C, 2h. v) KO*t*Bu, H_2O, THF, –78 °C, 5 min.[S23] vi) γ-terpinene, *o*-dichlorobenzene, 180 °C, 2h.[S24] (3) vii) furan, *n*BuLi, toluene, –25 °C, 3h to rt, 12h. viii) Zn/$TiCl_4$, THF, reflux, 18 h.[S15] (4) ix) isobenzofuran (synthesized in 3 steps as an intermediate, starting from phthalide, (67% yield for the first 2 steps)), MeLi, Et_2O, reflux, 18 h. x) Zn/$TiCl_4$, THF, 65 °C, 18 h.[S25] (5) xi) bis(trimethylsilyl)acetylene, [$CoCp(CO)_2$], hν, 5 h. xii) NBS, CH_3CN, rt, 16 h. xiii) DDQ, toluene, reflux, 4 h.[S10]

12. References

[S1] A. Lorbach, C. Reus, M. Bolte, H.-W. Lerner, M. Wagner, *Adv. Synth. Catal.* **2010**, *352*, 3443–3449.
[S2] A. John, M. Bolte, H.-W. Lerner, M. Wagner, *Angew. Chemie Int. Ed.* **2017**, *56*, 5588–5592.
[S3] S. Goretta, C. Tasciotti, S. Mathieu, M. Smet, W. Maes, Y. M. Chabre, W. Dehaen, R. Giasson, J.-M. Raimundo, C. R. Henry, C. Barth, M. Gingras, *Org. Lett.* **2009**, *11*, 3846–3849.
[S4] K. Suzuki, A. Kobayashi, S. Kaneko, K. Takehira, T. Yoshihara, H. Ishida, Y. Shiina, S. Oishi, S. Tobita, *Phys. Chem. Chem. Phys.* **2009**, *11*, 9850–9860.
[S5] A. M. Brouwer, *Pure Appl. Chem.* **2011**, *83*, 2213–2228.
[S6] T. S. Ahn, R. O. Al-Kaysi, A. M. Müller, K. M. Wentz, C. J. Bardeen, *Rev. Sci. Instrum.* **2007**, *78*, 2005–2008.
[S7] B. C. Berris, G. H. Hovakeemian, Y. H. Lai, H. Mestdagh, K. P. C. Vollhardt, *J. Am. Chem. Soc.* **1985**, *107*, 5670–5687.
[S8] F. Mo, J. M. Yan, D. Qiu, F. Li, Y. Zhang, J. Wang, *Angew. Chemie Int. Ed.* **2010**, *49*, 2028–2032.
[S9] D. Rodríguez-Lojo, A. Cobas, D. Peña, D. Pérez, E. Guitián, *Org. Lett.* **2012**, *14*, 1363–1365.
[S10] H. Hoffmann, D. Mukanov, M. Ganschow, F. Rominger, J. Freudenberg, U. H. F. Bunz, *J. Org. Chem.* **2019**, *84*, 9826–9834.
[S11] L. Niu, H. Yang, Y. Jiang, H. Fu, *Adv. Synth. Catal.* **2013**, *355*, 3625–3632.
[S12] L. Niu, H. Zhang, H. Yang, H. Fu, *Synlett* **2014**, *25*, 995–1000.
[S13] J. Cvengroš, D. Stolz, A. Togni, *Synthesis* **2009**, *2009*, 2818–2824.
[S14] J. Urban, A. Dlabač, M. Valchář, M. Protiva, *Collect. Czechoslov. Chem. Commun.* **1984**, *49*, 992–1001.
[S15] S. Kirschner, J.-M. Mewes, M. Bolte, H.-W. Lerner, A. Dreuw, M. Wagner, *Chem. Eur. J.* **2017**, *23*, 5104–5116.
[S16] D.-S. Chen, J.-M. Huang, *Synlett* **2013**, *24*, 499–501.
[S17] V. Mamane, P. Hannen, A. Fürstner, *Chem. Eur. J.* **2004**, *10*, 4556–4575.
[S18] Stoe & Cie, *X-AREA*. *Diffractometer control program system*. Stoe & Cie, Darmstadt, Germany, 2002**.**
[S19] G. M. Sheldrick, *Acta Crystallogr. Sect. A Found. Crystallogr.* **2007**, *64*, 112–122.
[S20] V. K. Bel'skii, E. V. Kharchenko, A. N. Sobolev, V. E. Zavodnik, N. A. Kolomiets, G. S. Prober, L. P. Oleksenko, *Russ. J. Struct. Chem.* **1990**, *31*, 116–121.
[S21] A. A. Danish, M. Silverman, Y. A. Tajima, *J. Am. Chem. Soc.* **1954**, *76*, 6144–6150.
[S22] T. K. Wood, W. E. Piers, B. A. Keay, M. Parvez, *Chem. Eur. J.* **2010**, *16*, 12199–12206.
[S23] M. L. G. Borst, R. E. Bulo, D. J. Gibney, Y. Alem, F. J. J. de Kanter, A. W. Ehlers, M. Schakel, M. Lutz, A. L. Spek, K. Lammertsma, *J. Am. Chem. Soc.* **2005**, *127*, 16985–16999.
[S24] M. Białkowska, W. Chaładaj, I. Deperasińska, A. Drzewiecka-Antonik, A. E. Koziol, A. Makarewicz, B. Kozankiewicz, *RSC Adv.* **2017**, *7*, 2780–2788.
[S25] T. Geiger, A. Haupt, C. Maichle-Mössmer, C. Schrenk, A. Schnepf, H. F. Bettinger, *J. Org. Chem.* **2019**, *84*, 10120–10135.